

THESIS ON NATURAL AND EXACT SCIENCES B79

Doubly charged Higgs boson decays  
and implications on neutrino physics

MARIO KADASTIK

TALLINN UNIVERSITY OF TECHNOLOGY

Faculty of Science

Department of Physics

**Dissertation was accepted for the defence of the degree of Doctor of Philosophy  
in Natural Sciences on August 27, 2008**

**Supervisors:**

Ph.D Martti Raidal, National Institute of Chemical and Biophysics

Prof. Rein-Karl Loide, Department of Physics, Faculty of Science, TUT.

**Opponents:**

Dr. Oxana Smirnova, Lund University, Sweden

Dr. Margus Saal, Tartu University, Estonia

**Defense of the thesis:** October 14, 2008

**Declaration:** Hereby I declare that this doctoral thesis, my original investigation and achievement, submitted for the doctoral degree at Tallinn University of Technology has not been submitted for any degree.

Mario Kadastik

Copyright: Mario Kadastik, 2008

ISSN 1406-4723

ISBN 978-9985-59-853-5

LOODUS JA TÄPPISTEADUSED B79

Kahekordse laenguga Higgsi bosoni  
lagunemiste analüüs ja selle mõju  
neutriinofüüsikale

MARIO KADASTIK



## List of publications

This thesis is based on the following papers, which have been referred to in the text as Article I till Article III.

- I. Hektor, A., Kadastik, M., Müntel, M., Raidal, M., Rebane, L., 2007. “Testing neutrino masses in little Higgs models via discovery of doubly charged Higgs at LHC”, Nucl.Phys.B787:198-210,2007
- II. The CMS Collaboration, 2006. “CMS technical design report, volume II: Physics performance”, J.Phys.G34:995-1579,2007  
Authors contribution is section 12.2.2, "Search for final states with  $\tau$  leptons" on pages 1378-1382.
- III. Kadastik, M., Raidal, M., Rebane, L.,2008. “Direct determination of neutrino mass parameters at future colliders”, Phys.Rev.D77:115023, 2008

## CONTENTS

1. Introduction	7
2. List of acronyms	8
3. Principles of high energy particle physics	9
3.1. Study of fundamental interactions through particle collisions	9
3.2. Current and future colliders and the physics outlook	10
4. Overview of the Standard Model	12
4.1. The current status of the model	16
4.2. Model predictions regarding new particles	16
5. Introduction to modern neutrino physics	16
5.1. Oscillation and mixing of the flavor and mass states	16
5.2. Neutrinoless double-beta decay	19
5.3. Extensions to the Standard Model to account for massive neutrinos	20
6. The scalar triplet of Higgs bosons and neutrinos	21
6.1. The model	21
6.2. Phenomenology of $\Phi^{\pm\pm}$ in HEP collider experiments	22
6.3. Searching for $\Phi^{\pm\pm}$ in upcoming experiments	30
7. Measuring neutrino parameters in HEP collider experiments	34
7.1. Branching ratios as an indirect measurement of neutrino parameters	34
7.2. Determination of the neutrino mass hierarchy and the lightest neutrino mass	35
7.3. Probing for Majorana phases	36
7.4. Probing the mixing angle $\theta_{13}$ and CP violation	37
7.5. Possibilities on measuring the vacuum expectation value of the scalar triplet	38
8. Conclusion	40
References	41
ARTICLE I	45
ARTICLE II	61
ARTICLE III	85
Abstract	104
Resümee	105

---

## 1. INTRODUCTION

In this thesis we cover the research done on a particular extension of the Standard Model (SM), the scalar triplet of Higgs bosons. With the introduction of the scalar triplet to the SM, the current neutrino mass problem can be solved and we look for the experimental signatures that can lead to the discovery of the scalar triplet components as well as the concrete decay mechanisms. In addition we discuss the possible implications from the decay statistics to neutrino physics through the relationship between the Yukawa coupling of the scalar triplet and the neutrino mass matrix. It can be shown that the connection does indeed give us valuable information. It can be used to predict the results of collider experiments by estimating the collider signatures. Once the particle is found the same relation and the information obtained in the collider can be used to estimate the actual unknown neutrino parameters.

This thesis is organized as follows. In the beginning a short introduction to the concepts of high energy physics (HEP) is given in Section 3 followed by a more detailed explanation of the Standard Model on the aspects required for this thesis in Section 4. We then give an introduction to the neutrino physics and its problems in Section 5 as well as possible solutions. In Section 6 we go into more details of the Type-II seesaw and introduce the scalar triplet and its phenomenology. We also go into more details on how to predict the branching ratios using neutrino data in the same section as well as searches for the scalar triplet in the current and upcoming experiments. As a last section, the Section 7 covers the reverse process of estimating neutrino parameters based on the already found scalar triplet decay statistics after which we conclude the thesis.

The author would like to thank James Letts, Kristjan Kannike and Andi Hektor for useful comments and proofreading and his lovely wife, dogs, cats and other animals for standing by him and supporting him during the work on this thesis.

---

## 2. LIST OF ACRONYMS

- ALICE - A Large Ion Collider Experiment. A detector at the LHC accelerator.
- ATLAS - A Toroidal LHC ApparatuS. A detector at the LHC accelerator.
- BR - Branching Ratio.
- CDF - Collider Detector at Fermilab. A detector at the Tevatron accelerator.
- CERN - Conseil Européen pour la Recherche Nucléaire. European nuclear research center.
- CMS - Compact Muon Solenoid. A detector at the LHC accelerator.
- CP - Charge and Parity symmetry.
- DELPHI - DEtector with Lepton, Photon and Hadron Identification.
- EWSB - ElectroWeak Symmetry Breaking.
- GeV - Giga electron-Volt.
- HEP - High Energy Physics.
- IGEX - International Germanium EXperiment.
- ILC - International Linear Collider.
- LFV - Lepton Flavor Violation.
- LHC - Large Hadron Collider.
- LHCb - Large Hadron Collider beauty experiment at the LHC accelerator.
- LEP - Large Electron Positron collider.
- OPAL - Omni-Purpose experiment At LEP.
- PETRA - Positron Elektron Tandem Ringbeschleuniger Anlager (positron electron cyclotron machine).
- PMNS - Pontecorvo-Maki-Nakagawa-Sakata mixing matrix.
- SM - Standard Model.
- VEV - Vacuum Expectation Value.

---

### 3. PRINCIPLES OF HIGH ENERGY PARTICLE PHYSICS

**3.1. Study of fundamental interactions through particle collisions.** We know that the electromagnetic and weak force can be joined to a new force called the electroweak force. We also know that we can extend the same mechanisms to some extent and we can include the strong interaction to form a general model of fundamental interactions called the Standard Model [1]. However the theoretical model explains that such unifications happen at energies way beyond that which we have in our usual room temperature regions or what we can obtain from simple experiments in the laboratory. The theories also predict that our universe contains a multitude of objects which at times are so short lived that we have no easy way of observing them. We know from evidence of radioactive decay, experiments with light and so on that certain particles are related to each other through different interactions, which seem to be mediated by different forces. If we describe the model in mathematical terms through symmetries and gauge fields adhering to these symmetry groups, then we get a number of new fields that we do not observe in the ordinary day-to-day life. To understand how correct our predictions are we need to create laboratory conditions where we can on a regular basis create these particles/fields and study their properties. Only through understanding the relations between the actual world and our mathematical models can we understand how close to the truth we are and from there extend our knowledge to predict new phenomena.

To do so requires the search and precise measurements of a multitude of particles that are not visible ordinarily as well as not created in a simple way. The only way we can create them on a regular basis is to build particle accelerators, which in essence are high energy concentration machines. Through acceleration of particles to very high energies and then collisions of such energetic particles can we get a glimpse of the state of the universe as it is at high energies. The reason we require the energies to be high is due to the fact that a number of these new phenomena are carried by particles with a very large self energy and in normal conditions they cannot exist. To give an example of the latest discoveries in this field would be the discovery of the top quark in 1995 at Tevatron [2, 3] or the discovery of the  $W$  [4] and  $Z$  [5] particles in the middle of the 1980-s. The energy that these particles operate at is in the region of 100 – 200 GeV which if we were to convert this energy to temperature (where the average energy of the particles would be in the order that we describe) would mean an average temperature of ca  $10^{15}$ K. The temperature of the Sun for comparison is the

---

order of  $10^7\text{K}$  [6] and is an extremely cool place in comparison. The only time such particles were freely produced and seen in abundance was at a very early stage of the universe when the average temperature was on the same order. A particle collision is built on the principle that during the collision the two particles, which are colliding, interact and as they have an abundance of energy besides their rest-mass then this energy can during the interaction be used to create new particles as long as the particles have direct interactions with the colliding particles. As some of these particles have a very large mass in comparison to the particles we observe every day, then they can only be produced if the excess energy in the collision is higher than the mass of the particles to be created.

Through building particle accelerators we can hence take a glimpse at an universe in an early phase, understand the particle content of it and from there deduce the fundamental interactions that govern our universe. Through such understanding comes new knowledge and that new knowledge converts over time to new technologies. As a good example the work on electromagnetism and the discovery of electron have lead us to a highly technical society where electronics is so common that life without it would be unthinkable. Yet a bit more than a century ago we couldn't even utilize electricity. It was only a few decades ago when majority of the technology around us was still based on simple mechanics, but which is being replaced every day by electronics. The understanding of radioactivity has lead to a number of breakthroughs in medical research as well as understanding materials and providing higher quality components to manufacturing through ways to observe the internal structure of components. The understanding of radioactivity and strong interactions has also lead to the use of nuclear energy without what our society probably couldn't exist in the current energy utilizing way it does to date. Who knows which doors will be opened with the further understanding of the fundamental interactions and possible discoveries of new interactions.

**3.2. Current and future colliders and the physics outlook.** A small overview of the recently closed Large Electron Positron collider (LEP) [7] experiment is in order, before a more detailed overview of the experiments currently in operation can be given. The LEP experiment was an electron-positron collider which reached by the end of its life centre-of-mass energies of around 210 GeV allowing it to perform precision measurements of the electroweak carrier bosons and to-date it has provided the best measurements on them [8]. LEP was an electron-positron collider, which means it belongs to the class of colliders capable

---

of precision measurements. In an electron-positron collider the initial state at the time of collision is known in all dimensions and the energy distribution can be estimated very well. In addition as the electron and positron annihilate and the resulting new physics comes from the annihilation energy, then the experimental signatures are extremely clean with a very low multiplicity of particles. This allows in addition to searches of new physics also very high precision measurements of a number of physical phenomena. As an example we make use later on of the measurements of the decay widths of the  $Z$  boson to estimate the number of neutrino generations in our universe. Such measurements are only possible in very high purity samples which can only be obtained from electron-positron or similar colliders<sup>1</sup>.

We now turn our attention to the experiments currently in operation. For over 20 years Fermilab has been operating a proton anti-proton collider called the Tevatron [10]. Although the initial startup didn't go very smoothly, the accelerator with the two main detectors of D0 and CDF has made at least one discovery and a number of additional measurements and has been performing well over the past few years. The highlight of Tevatron is most certainly the discovery of the top quark in 1995 which had been anticipated for a very long time and which was not seen in LEP due to kinematic constraints (the mass of the top-quark is approximately 175 GeV and the main production channel is production of a top and anti-top). Since LEP did not find the currently most sought after Higgs boson (for details on the boson see section 4), the search has continued at the Tevatron collider. To date the particle has not been observed, however the mass reach has been extended by the Tevatron experiments on multiple occasions and in recent publications they are close to excluding the Higgs boson in some mass regions. The current operations of Tevatron were planned to be stopped at the time of the Large Hadron Collider (LHC) [11] startup around the beginning of this century, however as the LHC project was delayed on a number of occasions, the Tevatron has been extended to increase its statistics and hopefully provide already some evidence of physics beyond the SM by the startup of LHC. As it is now known that LHC will start this year (2008), then the 2009 is at this time considered the last year of Tevatron running as the LHC experiment will pass the statistical amount as well as the energy frontier already in the first full year of operations.

---

<sup>1</sup>Under similar colliders we mean lepton colliders, which at this moment means electron-positron machines. However potential muon-antimuon machines have been under discussion if the muon cooling problems are solved [9].

---

The LHC is the newest particle accelerator to be built. It is built in the same tunnel as the original LEP experiment at the border of Switzerland and France. It is a proton-proton collider with a centre-of-mass energy of 14 TeV. However, like in the Tevatron experiment the actual energy between the colliding particles is smaller due to the use of protons because proton is not an elementary particle, but a composite object with a very complex inner structure. Depending on the collision process the effective collision energies can be as low as 1 TeV to all the way around 10 – 12 TeV. Due to this uncertainty as well as an initial state uncertainty (the kinematic distribution between the different partons inside proton is unknown) the machine is mostly a discovery machine and not that much a high-precision machine. It has four main experiments: CMS [12], ATLAS [13], LHCb [14] and ALICE [15] with the first two being general purpose experiments and the final two being built for very specific studies. The LHCb concentrates on the b-quark physics and the CP violation studies while ALICE is designed for the heavy ion running phase of LHC to study the quark-gluon plasma effects.

In case the LHC makes a certain discovery of new particles and the need arises to perform precision measurements of such particles, then a possible new particle accelerator, which has been labelled as the International Linear Collider (ILC) [16], could be built. The ILC would be a linear collider as opposed to the cyclotrons covered above. Due to new developments in accelerator techniques the collider could reach as high centre-of-mass energies as 500 GeV to 1 TeV using electrons and positrons as the colliding particles. The ILC is currently still in the design phase and a number of speculations say that its building decision depends on the results of the first years of LHC running.

#### 4. OVERVIEW OF THE STANDARD MODEL

The Standard Model of particle interactions [1] is one of the most formidable theories of 20th century. This theory describes the weak, electromagnetic and strong interactions. The central idea of the Standard Model is that all the interactions are based on local gauge symmetry. The gauge bosons which mediate interactions correspond to the generators of the symmetry group. These bosons interact with fermions of the model. The fermion content is constructed in order to reproduce experimental data. There are three generations of leptons and quarks in the Standard Model. The former particles feel only the electroweak interactions while the latter also know the strong interaction. In addition, the minimal model contains one scalar

---

doublet which interacts with fermions via Yukawa interactions and induces the spontaneous symmetry breaking which gives masses to all the particles in the model.

The Standard Model is based on the local gauge group

$$SU(3)_c \times SU_L(2) \times U_Y(1),$$

where  $SU(3)_c$  is responsible for strong interactions and  $SU_L(2) \times U_Y(1)$  for the electroweak interactions. In what follows, only the gauge group  $SU_L(2) \times U_Y(1)$  plays a role and all the quantum numbers for the fields are given for that group only.

There are four gauge fields in the electroweak sector of the model. They correspond to the generators of the gauge group. The fields corresponding to the non-abelian  $SU(2)$  group are denoted by  $A = \{A_1, A_2, A_3\}$  and the one for the abelian  $U(1)$  symmetry by  $B$ . The physical particles are linear combinations of these fields, two of them are charged ( $W^\pm$ ) and two are neutral ( $Z^0$  and the photon  $\gamma$ ).

The leptonic fermion content of the model is constructed as follows. In the theory the left-handed fields for neutrinos and charged leptons,  $\nu_L$  and  $\ell_L$ , respectively, form an  $SU(2)_L$  doublet while the right-handed field for charged leptons,  $\ell_R$ , is a singlet,

$$L = \begin{pmatrix} \nu_L \\ \ell_L \end{pmatrix} \sim (2, -1), \quad \ell_R \sim (1, -2).$$

The fields  $\ell_L$  and  $\ell_R$  form one Dirac fermion with the Dirac mass for each generation of charged leptons. The right-handed neutrino ( $\nu_R$ ) is not required for the theory to be consistent and, therefore, neutrinos are exactly massless in this model. The hypercharge quantum numbers of the fields come from the charge formula:

$$Q = \mathbf{T}_3 + \frac{Y}{2},$$

where  $Y$  is the hypercharge, the quantum number of  $U(1)$  group, and  $T_3$  is the third component of the  $SU(2)$  generators. The left handed leptons form a doublet to allow them to emit  $W^\pm$  bosons and hence account for experimental evidence for left handed weak currents. There has not been any experimental evidence for right-handed weak currents and hence no right-handed doublet [17].

---

In addition to the lepton doublet and singlet the theory also contains an  $SU(2)$  doublet of scalar fields,

$$\varphi = \begin{pmatrix} \varphi^+ \\ \varphi^0 \end{pmatrix} \sim (2, 1).$$

This is required for electroweak symmetry breaking (EWSB) and for generating the Dirac masses for the fermions.

The parts of the Standard Model Lagrangian relevant for our studies can be written as

$$\mathcal{L} = \mathcal{L}_{\text{int}} - V,$$

where

$$\mathcal{L}_{\text{int}} = -\frac{1}{4}\mathbf{G}_{\mu\nu}\mathbf{G}^{\mu\nu} - \frac{1}{4}F_{\mu\nu}F^{\mu\nu} + i\bar{L}\hat{D}L + i\bar{\ell}_R\hat{D}\ell_R + (f\bar{L}\ell_R\varphi + h.c.), \quad (1)$$

and the potential  $V$  is

$$V = \frac{1}{2}m^2|\varphi|^2 + \frac{1}{4}\lambda|\varphi|^4. \quad (2)$$

Above,  $D_\mu$  denotes the covariant derivative

$$D_\mu = \partial_\mu - ig\mathbf{T} \cdot \mathbf{A}_\mu - ig'\frac{1}{2}YB_\mu,$$

where

$$\hat{D} = D_\mu\gamma^\mu.$$

The field strengths of the gauge fields are

$$G_{\mu\nu} = \partial_\mu A_\nu - \partial_\nu A_\mu - ig[A_\mu A_\nu - A_\nu A_\mu] = \mathbf{G}_{\mu\nu}\mathbf{T},$$

where

$$A_\mu = \mathbf{A}_\mu \cdot \mathbf{T}; \quad F_{\mu\nu} = \partial_\mu B_\nu - \partial_\nu B_\mu.$$

For isoscalar fields  $\mathbf{T}$  vanishes, for isospinor fields ( $\varphi$  and  $L$ )  $\mathbf{T} = \frac{1}{2}\tau$ .

The meaning of the terms in the Lagrangian (1) is the following. The first two terms  $\frac{1}{4}\mathbf{G}_{\mu\nu}\mathbf{G}^{\mu\nu}$  and  $\frac{1}{4}F_{\mu\nu}F^{\mu\nu}$  give kinetic terms and self interactions of the gauge bosons. The terms  $i\bar{L}\hat{D}L$  and  $i\bar{\ell}_R\hat{D}\ell_R$  describe both the free motion of the fermions and their interaction with the gauge fields. The last terms in eq. (1) are called Yukawa interaction terms. They describe the Higgs boson interactions with fermions with the strength determined by the interaction constant  $f$ .

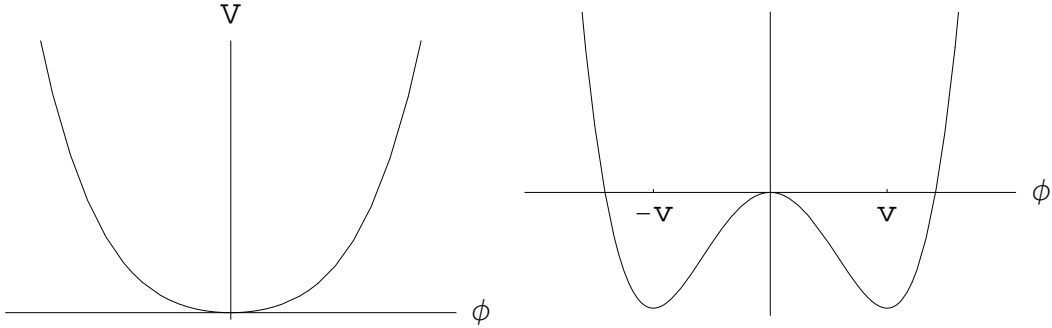


FIGURE 1. On the left: scalar Field Potential for  $\mu^2 > 0$  and on the right for  $\mu^2 < 0$

Let us consider the potential  $V$  in eq. (2). It depends on the variable  $\mu^2$  which can be interpreted as a mass parameter. If  $\mu^2 > 0$ , then the potential behaves as seen on the left side of Figure 1 with a single minimum at  $\varphi = 0$ . If, however,  $\mu^2 < 0$  ( $\mu$  is imaginary), then the potential behaves as seen on the right hand side of Figure 1 having two minima at  $\pm\langle\varphi^0\rangle$  where

$$\langle\varphi^0\rangle \equiv v = \sqrt{\frac{-\mu^2}{\lambda}}. \quad (3)$$

As the minima of the potential define the physical vacuum, the system falls from the vacuum  $\langle\varphi^0\rangle = 0$  to a new vacuum  $\langle\varphi^0\rangle = v$ . This is called the spontaneous electroweak symmetry breaking. It introduces a shift in the Higgs field, namely  $\varphi^0 \rightarrow \varphi^0 + v$ . Substituting this shift into the Yukawa terms in eq. (1) we obtain terms like

$$f\bar{\ell}_L\ell_Rv + h.c = m_\ell\bar{\ell}_L\ell_R + h.c., \quad (4)$$

which is nothing but the Dirac mass term for fermions with the mass

$$m_L = fv. \quad (5)$$

Since there is no  $\nu_R$  field, this mechanism does not work for neutrinos which remain exactly massless.

The Standard Model is a gauge theory which means that the forces between particles are modeled through coupling of fermions to bosons which mediate the force. The physical bosons in the SM which mediate the forces are:

- photons – mediate the electromagnetic interaction and as the boson is massless its range is infinite. It is one of orthogonal superpositions of fields  $A_3$  and  $B$ .

- 
- $W$  and  $Z$  bosons – mediate weak interaction which is finite due to large mass of the bosons (80.4 GeV for  $W^\pm$  boson [18] and 91.2 GeV for  $Z^0$  boson [19]).  $W^\pm$  are two orthogonal superpositions of fields  $A_1$  and  $A_2$ .  $Z^0$  boson is another orthogonal superposition of fields  $A_3$  and  $B$ .
  - gluons – mediate the strong force. They possess colour charges (red, green, blue) and mediate strong interaction. There are a total of eight gluons.
  - Higgs boson – introduces spontaneous symmetry breaking which results in particles having inertial mass.

4.1. **The current status of the model.** The model has only been confirmed since its first introduction, but still one element of the model has not been experimentally observed – the Higgs boson. In addition the model requires neutrinos to be massless, but the latest measurements indicate that between the three flavors of neutrinos there do exist mass differences [20, 21, 22], which in turn implies that at least two of the neutrinos must have a non-zero mass. To account for that discrepancy the theory has to be extended.

4.2. **Model predictions regarding new particles.** The model predicted three new field carrier bosons:  $W$ ,  $Z$  and Higgs boson. For the  $W$  and  $Z$  bosons the theory gives an exact relation for their mass regarding one of the model’s parameters – the Weinberg angle. Once one of the bosons was found at CERN in 1983 [4] the mass of the other particle was predicted and later found within experimental measurement errors [5]. Since then a lot of these parameters have been remeasured with higher precision and it has all been in agreement with the theory, the only missing piece is the Higgs boson whose mass is not related to any other parameter in the model.

## 5. INTRODUCTION TO MODERN NEUTRINO PHYSICS

5.1. **Oscillation and mixing of the flavor and mass states.** In SM there are three flavors of leptons. This implies also three flavors of neutrinos interacting through the weak interaction. Due to their coupling to the  $W$  and  $Z$  boson it is possible to indirectly measure the number of neutrino generations from the partial width of the  $Z$  boson. The latest results on this measurement are from the combined LEP results [23] with

$$N_\nu = 2.9841 \pm 0.0083.$$

---

Besides the three generations that we know from the electroweak interaction we could also have a few generations, which are not interacting through the three SM interactions and only interact through gravity. Such additional neutrinos are called sterile neutrinos [24]. However in this thesis we only consider the three known generations of neutrinos and leave the extension to include sterile neutrinos for the future.

Thanks to many neutrino oscillation experiments which have been running in the past decade that involve solar, atmospheric, accelerator and reactor neutrinos it is now known that even when a neutrino is produced in a well defined flavor eigenstate, it can during the passage of a macroscopic distance be detected in a different eigenstate. The simplest explanation is that the flavor and mass eigenstates differ and that neutrinos have a non-zero mass with at least slight differences between the mass states. This difference in essence means that neutrinos mix. To define this mixing in mathematical terms we need to define the relationship between the flavor and mass eigenstates and the mixing matrix that connects them [25].

The neutrino mass matrix can be diagonalized by the unitary leptonic mixing matrix  $U$ ,

$$m_\nu = U^* m_\nu^D U^\dagger, \quad (6)$$

where the diagonalized neutrino mass matrix  $m_\nu^D$  is given by

$$m_\nu^D = \begin{pmatrix} m_1 & 0 & 0 \\ 0 & m_2 & 0 \\ 0 & 0 & m_3 \end{pmatrix}.$$

Here  $m_1$ ,  $m_2$  and  $m_3$  represent the masses of neutrino mass eigenstates  $\nu_1$ ,  $\nu_2$  and  $\nu_3$ . The masses of  $\nu_1$  and  $\nu_2$  differ by  $\Delta m_{\text{sol}}^2 = 7.92(1 \pm 0.09) \times 10^{-5} \text{ eV}^2$  measured by solar oscillation experiments [26] and  $m_1 < m_2$ . The third eigenstate  $\nu_3$  is separated from the first two by splitting  $\Delta m_{\text{atm}}^2 = 2.6(1_{-0.15}^{+0.14}) \times 10^{-3} \text{ eV}^2$  [27] and can be heavier or lighter than the solar pair. The two possibilities are called normal and inverted spectrum, respectively and an illustration to that effect can be found on Figure 2. The third possibility – nearly degenerate masses – appears when the lowest neutrino mass is large compared to the measured mass differences and  $m_1 \approx m_2 \approx m_3$ . Cosmology implies that neutrinos are lighter than about 0.2 eV [28].

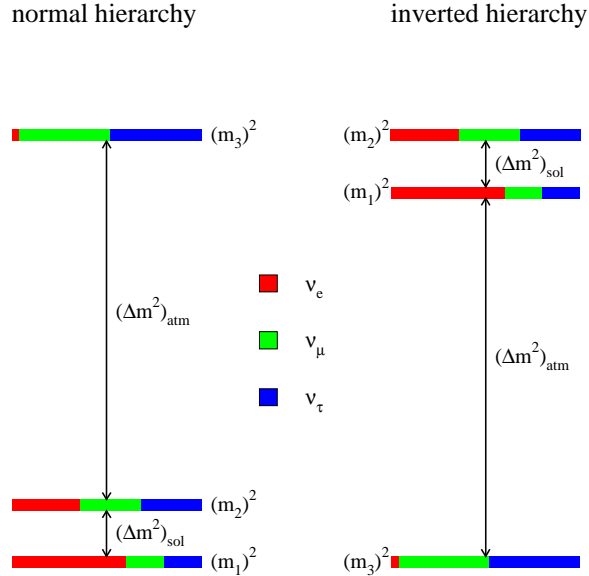


FIGURE 2. Cartoon of the two distinct neutrino-mass hierarchies that fit all of the current neutrino data, for fixed values of all mixing angles and mass-squared differences. The color coding (shading) indices the fraction  $|U_{\alpha i}|^2$  of each distinct flavor  $\nu_\alpha$ ,  $\alpha = e, \mu, \tau$  contained in each mass eigenstate  $\nu_i$ ,  $i = 1, 2, 3$ . For example,  $|U_{e2}|^2$  is equal to the fraction of the  $(m_2)^2$  “bar” that is painted red (shading labeled as ‘ $\nu_e$ ’). Illustration courtesy of [29].

Since we have assumed that there are only three Majorana neutrinos,  $U$  is a  $3 \times 3$  mixing matrix that depends on three mixing angles and three phases and can be parameterized as

$$U = \begin{pmatrix} 1 & 0 & 0 \\ 0 & c_{23} & s_{23} \\ 0 & -s_{23} & c_{23} \end{pmatrix} \begin{pmatrix} c_{13} & 0 & s_{13}e^{-i\delta} \\ 0 & 1 & 0 \\ -s_{13}e^{i\delta} & 0 & c_{13} \end{pmatrix} \begin{pmatrix} c_{12} & s_{12} & 0 \\ -s_{12} & c_{12} & 0 \\ 0 & 0 & 1 \end{pmatrix} \begin{pmatrix} e^{i\alpha_1} & 0 & 0 \\ 0 & e^{i\alpha_2} & 0 \\ 0 & 0 & 1 \end{pmatrix}, \quad (7)$$

where  $c_{ij} \equiv \cos \theta_{ij}$ ,  $s_{ij} \equiv \sin \theta_{ij}$  and  $\theta_{ij}$  denote the mixing angles. The quantities  $\delta$ ,  $\alpha_1$  and  $\alpha_2$  are CP violating phases. This matrix is also known as the PMNS matrix [30, 31].  $\delta$  is the Dirac phase and characterizes CP violation regardless of the character of neutrinos Majorana phases  $\alpha_1$  and  $\alpha_2$  are physical only if neutrinos are Majorana particles. If the neutrinos were Dirac fermions, both Majorana phases could be absorbed by appropriately redefining the neutrino fields, and the only observable CP violation parameter would be the Dirac phase

---

$\delta$ . Also note that  $\delta$  appears in the mixing matrix only as  $\sin \theta_{13} e^{i\delta}$  – so the influence of  $\delta$  crucially depends on the value of  $\theta_{13}$  and has physical consequences only if  $\theta_{13}$  is non-zero.

The mixing matrix contains six independent parameters: three mixing angles ( $\theta_{13}$ ,  $\theta_{23}$  and  $\theta_{12}$ ) and three phases ( $\alpha_1$ ,  $\alpha_2$  and  $\delta$ ). Mixing angles are known from the global fit to neutrino oscillation data and are given by ( $2\sigma$  errors) [26, 27]

$$\sin^2 \theta_{12} = 0.314(1_{-0.15}^{+0.18}), \quad \sin^2 \theta_{23} = 0.45(1_{-0.20}^{+0.35}), \quad \sin^2 \theta_{13} = 0.8_{-0.8}^{+2.3} \times 10^{-2}. \quad (8)$$

Up to now no experiment has been able to determine the values of phases so that

$$\delta, \alpha_1, \alpha_2 \in [0, 2\pi], \quad (9)$$

remain unconstrained.

**5.2. Neutrinoless double-beta decay.** The  $\beta$ -decay studies are sensitive to neutrino masses regardless of whether the neutrinos are Dirac or Majorana particles. An additional sensitive probe of the neutrino masses is a study of neutrinoless double beta decay, the nuclear process

$$2X_m^n \rightarrow 2Y_{m+1}^n + 2e^- + 0\bar{\nu}_e. \quad (10)$$

The decay rate is potentially measurable only if neutrino is a Majorana fermion. Also,  $m_{ee} = \sum_i U_i^2 m_{ei}$  should be large enough [32, 33] and/or there should exist any new lepton number violating interactions [34, 35]. The present best upper bounds on double  $\beta$ -decay lifetimes come from the Heidelberg-Moscow [36] and the IGEX [37] experiments. The combined upper limit [38] is

$$m_{\beta\beta} \leq 0.9 \text{ eV}. \quad (11)$$

However, if  $m_{\beta\beta}$  is very small and there are new lepton number violating interactions then neutrinoless double beta decay will measure the strength of the new interactions rather than neutrino mass. For example, doubly charged Higgs fields or R-parity violating interactions can strongly influence the value of  $m_{\beta\beta}$ . Thus, we must be very careful to interpret a nonzero signal in double  $\beta$ -decay experiments. The positive results do not automatically mean that a direct measurement of neutrino mass has been made. To distinguish between the neutrino mass effect or a reflection of new interactions we have to supplement double  $\beta$ -decay results with collider searches for these new interactions. In a later chapter we will show how the results from neutrinoless double beta decay can be combined with collider results to give additional information on the neutrino sector.

---

**5.3. Extensions to the Standard Model to account for massive neutrinos.** For a short overview on the neutrino mass generation mechanisms we will now concentrate on the three minimal models. Those are the right-handed singlet neutrinos, scalar triplet and heavy vector-like fermions. The models all together are called Seesaw models of types I-III.

5.3.1. *Massive right-handed neutrinos or the type-I seesaw mechanism.* In the simplest case of Type-I seesaw [39, 40, 41, 42, 43] we introduce mass mixing with two 2-spinors for the right-handed heavy neutrinos to the SM. The mass matrix can be represented as:

$$M_{ij} = \begin{pmatrix} m_1 & m_3 \\ m_3 & m_2 \end{pmatrix}. \quad (12)$$

From the Fermi-Dirac statistics the mass matrix  $M_{ij}$  has to be symmetric as we can interchange the fermion fields in the mass term. We can diagonalize the symmetric matrix using an orthogonal matrix, which gives us:

$$M_{diag} = OMO^T = \begin{pmatrix} m_+ & 0 \\ 0 & m_- \end{pmatrix}, \quad (13)$$

where O is an orthogonal diagonalizing matrix. If we now look at a few special cases:

- Dirac mass. If we assume  $m_1 = m_2 = 0$  and  $m_3 \neq 0$ , then the eigenvalues will be  $\pm m_3$  and we get in the Lagrangian the Dirac mass terms. Thus we can consider a pure Dirac neutrino to be a composition of two massive Majorana neutrinos with equal mass.
- Pseudo-Dirac mass. If we have  $m_1 \sim m_2 \ll m_3$  then this state is called pseudo-Dirac. The neutrino is Majorana, but there is only a slight variation from the Dirac case. The mass is now  $\pm m + \delta$  where  $\delta \ll m$ . In this case the two 2-spinors are maximally mixed which is strongly supported by the experimental atmospheric neutrino data.
- Majorana mass. In case  $m_1 = 0$  and  $m_3 \ll m_2$  the eigenvalues become:

$$m_\nu \equiv m_- \simeq -\frac{m_3^2}{m_2}, \quad (14)$$

$$M_\nu \equiv m_+ \simeq m_2. \quad (15)$$

It is known as the seesaw mechanism and the source of that name is clear. If  $M_\nu$  is getting bigger then  $m_\nu$  is getting smaller and vice versa.

That last case explains also why right-handed neutrinos can be very heavy and have not been discovered yet by experiments as well as the smallness of the neutrino masses.

---

5.3.2. *Scalar triplet or the type-II seesaw mechanism.* In the case of the Type-II seesaw [44, 45, 46, 47, 48] the SM content is extended only by the addition of a SU(2) triplet of scalar fields with the hypercharge 2. This model with its interactions and predictions is further discussed in detail later on in section 6. To give a short overview, the scalar triplet is represented as:

$$(\Phi^{\pm\pm}, \Phi^\pm, \Phi^0). \quad (16)$$

The mass term for the neutrinos comes after the EWSB and can be written as

$$m_\nu = -2\lambda_\Phi v^2 \frac{\mu_\Phi}{M_\Phi^2}. \quad (17)$$

This is again a typical seesaw term. The smallness of neutrino masses can either come from the smallness of the  $\mu_\Phi$  parameter or the largeness of the scalar triplet mass.

5.3.3. *Massive fermions or the type-III seesaw mechanism.* The last possible scenario that we consider is the type III seesaw [49, 50], which is an extension of the SM with a SU(2) triplet fermions with zero hypercharge. The triplet is denoted as

$$\vec{\Sigma} \equiv (\Sigma^1, \Sigma^2, \Sigma^3).$$

The eigenstates of electric charge are:

$$\Sigma^\pm \equiv \frac{1}{\sqrt{2}} (\Sigma^1 \mp i\Sigma^2), \quad \Sigma^0 \equiv \Sigma^3.$$

The fermion triplet is an adjoint representation of the SU(2) gauge group, thus the Majorana mass term is automatically gauge invariant. After the EWSB the respective terms in the Lagrangian induce Majorana masses on the SM left handed neutrino fields through the exchange of  $\vec{\Sigma}$  fermions. The term generating neutrino masses is

$$m_\nu = -\frac{v^2}{2} \lambda_\Sigma^T M_\Sigma^{-1} \lambda_\Sigma. \quad (18)$$

## 6. THE SCALAR TRIPLET OF HIGGS BOSONS AND NEUTRINOS

6.1. **The model.** In this work we assume that the SM particle spectrum is extended by a scalar multiplet  $\Phi$  with the  $SU(2)_L \times U(1)_Y$  quantum numbers  $\Phi \sim (3, 2)$  as already introduced in the Type-II seesaw model in equation (16).

The Lagrangian describing the doubly charged Higgs boson interaction with leptons is given by [51]:

$$\mathcal{L} = \mathcal{L}_{\text{lepton}} + \mathcal{L}_\varphi,$$

---

where

$$\mathcal{L}_{\text{lepton}} = (Y_{\Phi})_{ij}[\Phi^0\nu_i\nu_j + \Phi^{\pm}\frac{\nu_i\ell_j^{\mp} + \ell_i^{\mp}\nu_j}{\sqrt{2}} + \Phi^{\pm\pm}\ell_i^{\mp}\ell_j^{\mp}] + h.c.,$$

and

$$\mathcal{L}_{\varphi} = \mu\Phi^0\varphi^0\varphi^0 + \mu\sqrt{2}\Phi^{-}\varphi^0\varphi^{+} + \mu\Phi^{--}\varphi^{+}\varphi^{+} + h.c.$$

The matrix  $(Y_{\Phi})_{ij}$  is the Yukawa coupling matrix of the new Higgs bosons to the lepton generations  $i, j = 1, 2, 3$ .

A direct connection can be made from doubly charged Higgs boson to neutrino masses:

$$(\mathcal{M}_{\nu})_{ij} = (Y_{\Phi})_{ij}v_l, \tag{19}$$

where  $v_l$  is the vacuum expectation value (VEV) of  $\Phi^0$  given by [51]

$$v_l \simeq \frac{\mu v^2}{m_{\Phi}^2}.$$

Because only left-handed neutrinos are involved, this mechanism generates Majorana masses for the neutrinos, which breaks the lepton number by two units,  $\Delta L = 2$ . This is in contrast with the Dirac masses, which conserve lepton number.

Introduction of the scalar triplet introduces three new particles: the neutral, single charged and doubly charged Higgs bosons. Of these only the doubly charged Higgs boson is a stand-alone new particle, the other two Higgs bosons are in a mixed state with the SM Higgs bosons.

## 6.2. Phenomenology of $\Phi^{\pm\pm}$ in HEP collider experiments.

6.2.1. *Generation mechanisms for  $\Phi^{\pm\pm}$ .* There are two major methods of producing  $\Phi^{\pm\pm}$  in collider experiments. The concrete Feynman diagrams for the production vary depending on the experimental setup (either the collider is a lepton collider like LEP or future ILC or the collider is based on hadrons e.g. LHC).

In hadron based colliders like LHC or Tevatron there are three possible methods to produce the doubly charged Higgs bosons. The respective diagrams can be seen on Figure 3. The only diagram of these that does not depend on any unknown coupling constant is the pair-production Drell-Yan diagram. The cross section of this process is easily calculable and only depends on the mass of the doubly charged Higgs boson. The  $WW$  fusion process depends on the vacuum expectation value of the scalar triplet, which is unknown at this time and can only be estimated from precision measurements of the  $\rho$  variable and other indirect sources. In most cases the VEV is assumed to be extremely small, which in turn means that the

single production through  $WW$  fusion cross section is negligible. The third and last diagram depends on the Yukawa coupling of the  $\Phi^{\pm\pm}$  boson and the respective leptons. This coupling is also not known, however the primary process of electron-positron scattering has a very large cross section, which could compensate for the low coupling. However this particular diagram has not been calculated yet and hence its effects have not been estimated by the experiments.

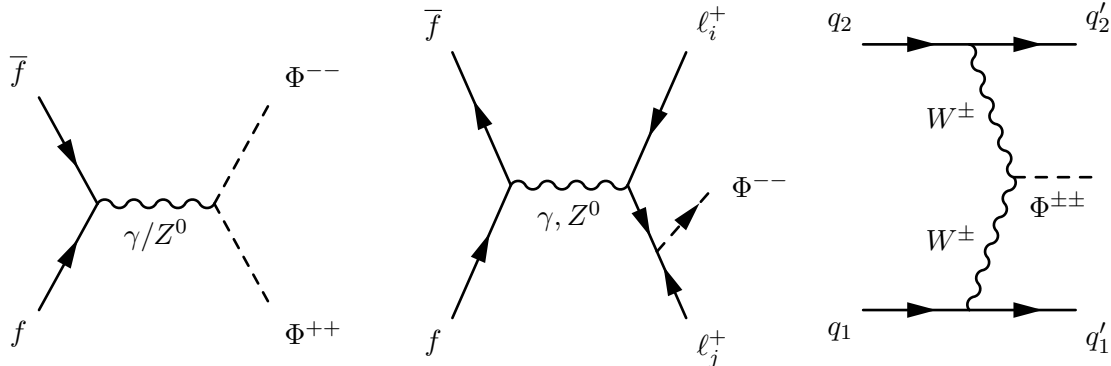


FIGURE 3.  $\Phi^{\pm\pm}$  generation diagrams. From left to right: Drell-Yan pair production, Drell-Yan lepton production with radiative  $\Phi^{\pm\pm}$  emission,  $WW$  fusion.

For lepton colliders like LEP and the future ILC experiments there are in addition to the Drell-Yan diagrams from Figure 3 also a number of diagrams due to the direct coupling of leptons to the  $\Phi^{\pm\pm}$  boson. The diagrams have been depicted on Figure 4.

In addition to the above mentioned generation processes, there is also a resonance process where a fusion of two same charged leptons would produce a  $\Phi^{\pm\pm}$  boson. In the model another similar vertex is allowed, namely the fusion of a single charged Higgs boson from the scalar triplet and a  $W$  to form the doubly charged component. However most literature excludes such a vertex due to kinematic constraints as it is natural to assume that the scalar triplet mass does not vary by much. For such a vertex to exist the following condition has to be met:

$$m(\Phi^{\pm\pm}) - m(\Phi^{\pm}) \geq m(W) \approx 80 \text{ GeV}.$$

The vertices of such processes can be seen on Figure 5.

6.2.2. *Decays of the  $\Phi^{\pm\pm}$ .* The doubly charged Higgs boson has couplings to charged leptons,  $W$  boson and other components of the scalar triplet. From this we can deduce that depending on kinematic limits the possible decays of it involve either to two same charge leptons, a pair of same charge  $W$  bosons or a pair of same charge charged Higgs boson and a  $W$ . The latter

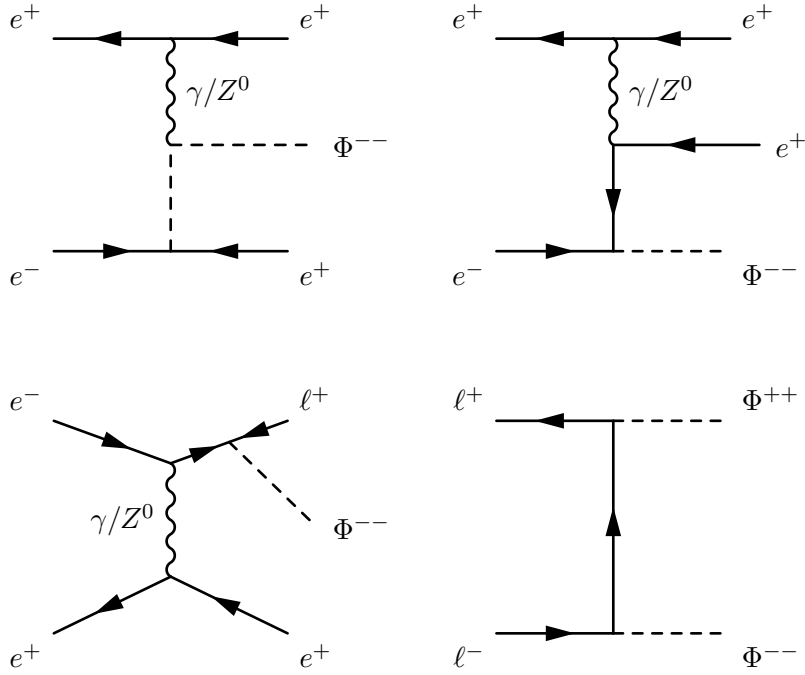


FIGURE 4.  $\Phi^{\pm\pm}$  generation diagrams. First three diagrams depict the same basic process, the only difference being the point at which an electron radiates a  $\Phi^{\pm\pm}$  boson. The fourth one depicts a pair production in case of lepton colliders (the cross section is smaller due to two vertices with  $\Phi^{\pm\pm}$  and hence the respective coupling squared).

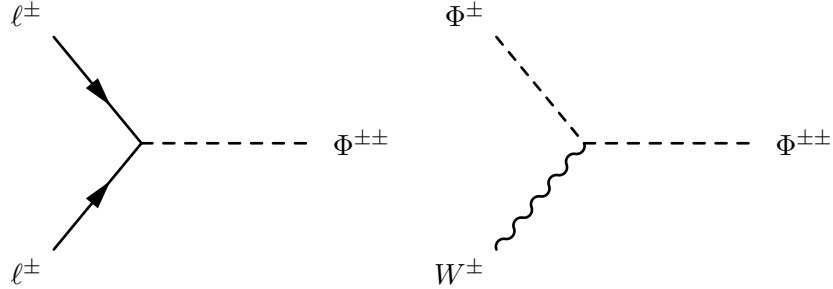


FIGURE 5. Vertices of same charge lepton fusion and single charged Higgs fusion

two are only possible in case the mass of the  $\Phi^{\pm\pm}$  boson is at least the sum of the decay products e.g. for the decay to  $W$ -s to happen the mass of the  $\Phi^{\pm\pm}$  must be at least 160 GeV. In this thesis we will neglect<sup>2</sup> the final state with  $\Phi^\pm$ .

The decay widths for the different decays are:

<sup>2</sup>We assume the masses of  $\Phi^{\pm\pm}$  and  $\Phi^\pm$  are close enough to kinematically exclude this decay.

---


$$\Gamma_{ij} \equiv \Gamma(\Phi^{\pm\pm} \rightarrow \ell_i^\pm \ell_j^\pm) = \begin{cases} \frac{1}{8\pi} |(Y_\Phi)_{ii}|^2 m_{\Phi^{\pm\pm}} & i = j, \\ \frac{1}{4\pi} |(Y_\Phi)_{ij}|^2 m_{\Phi^{\pm\pm}} & i \neq j, \end{cases} \quad (20)$$

$$\Gamma_{WW} \equiv \Gamma(\Phi^{\pm\pm} \rightarrow W^\pm W^\pm) \quad (21)$$

$$= \frac{2v_\Phi^2 m_{\Phi^{\pm\pm}} m_{W^\pm}^2}{\pi v_0^4} \left( \frac{3m_{W^\pm}^2}{m_{\Phi^{\pm\pm}}^2} + \frac{m_{\Phi^{\pm\pm}}^2}{4m_{W^\pm}^2} - 1 \right) \left( 1 - \frac{4m_{W^\pm}^2}{m_{\Phi^{\pm\pm}}^2} \right)^{1/2} \quad (22)$$

$$= kv_\Phi^2. \quad (23)$$

The total decay width is

$$\Gamma_{\text{tot}} = \sum \Gamma_{ij} + \Gamma_{WW}. \quad (24)$$

The branching ratios of the  $\Phi^{\pm\pm}$  can now be expressed as:

$$\text{BR}(\Phi^{\pm\pm} \rightarrow \ell_i^\pm \ell_j^\pm) = \frac{\Gamma_{ij}}{\Gamma_{\text{tot}}}, \quad (25)$$

$$\text{BR}(\Phi^{\pm\pm} \rightarrow W^\pm W^\pm) = \frac{\Gamma_{WW}}{\Gamma_{\text{tot}}}. \quad (26)$$

The relationship between these two different channels depends strictly on the vacuum expectation value and mass of the scalar triplet. The currently allowed values of the VEV are between 1 eV and 1 GeV. The lower bound coming from naturalness of the neutrino masses and the upper from the tree level  $\rho$  parameter. The whole region of that allowed space can be divided into three interesting regions. Until around  $10^{-5}$  GeV the leptonic decays dominate absolutely. In the region between  $10^{-5}$  GeV and  $10^{-3}$  GeV there is a smooth transition from leptonic decays to  $WW$  and in case the VEV is higher than  $10^{-3}$  GeV the  $WW$  dominates in the decays. The concrete relationship can be seen on Figure 6.

*6.2.3. Current limits on the mass of the  $\Phi^{\pm\pm}$  from previous and current experiments.* The doubly charged Higgs boson has been searched for in a variety of experiments. Some of the earliest searches originate from 1989 where a lower limit on the mass was set to around 20–22 GeV from the PETRA experiment [52]. The most complete search to date has been performed by the various LEP experiments. The combined lower limit on mass of the  $\Phi^{\pm\pm}$  is around 100 GeV. For concrete searches see Table 1.

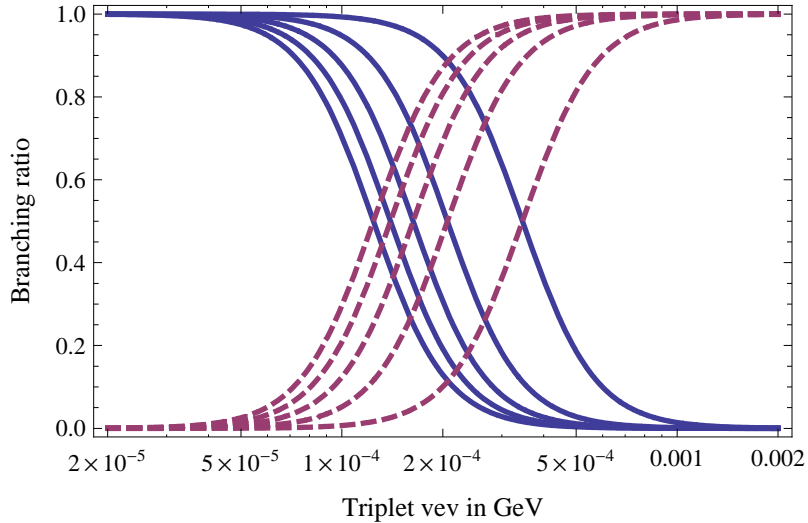


FIGURE 6. Running of branching ratios depending on the vacuum expectation value of the scalar triplet. The blue (solid) lines representing leptonic decays and the red ones (dashed) the decay to the  $WW$  channel. The different combinations show relation to the  $\Phi^{\pm\pm}$  mass (lower mass means higher VEV for transition)

TABLE 1. Summary of searches for  $\Phi^{\pm\pm}$  at the LEP experiments.

Experiment	Mass limit	Final states	Comments
OPAL [53]	98.5 GeV	All, no mixing	Although all channels have been searched, the pair of $\Phi^{\pm\pm}$ has to decay to the same final state.
DELPHI [54]	97.3 GeV	$\tau\tau\tau\tau$	A very impure channel and in almost every possible neutrino configuration a very low branching ratio configuration
L3 [55]	95.5 – 100.2 GeV	All, no mixing	Same search strategy and limitations as OPAL search

As can be seen there is still room for improvement as only a subspace of the possible final states has been searched. With all six final states considered in concrete configurations the worst case configuration is when all branching ratios are exactly 1/6 and such a configuration

---

or at least a very close one is allowed by the neutrino parameters. Due to that the actual upper limit at around 100 GeV could be over-estimated as the cross section times branching ratio squared, which is used to estimate the mass limits, can be six times higher than estimated and hence point towards lower mass. This creates a problem as the future experiments might no longer cover the region of masses below 100 GeV, which could lead to missing the  $\Phi^{\pm\pm}$  boson altogether due to the crowded region of dilepton invariant mass final states in the 80 – 100 GeV region from  $Z$  boson contamination.

The latest results on searches for  $\Phi^{\pm\pm}$  come from the Tevatron experiments. However unlike the LEP experiments, there is to this date no single search performed, which would have covered all channels simultaneously. The LEP searches were limited mostly by centre-of-mass energy as at  $\sqrt{s} = 209$  GeV it is not possible to create pair-produced  $\Phi^{\pm\pm}$  at higher energies than around 100 – 105 GeV and the single production channels are all dependent on the unknown Yukawa couplings of the scalar triplet. At Tevatron on the other hand it is possible to extend this reach towards higher masses, but to do so requires a thorough study in all available final states. It is acceptable to ignore the  $WW$  channel until the mass of 160 GeV as it is kinematically excluded and the lepton channels dominate independent of the VEV value. A brief summary on what has been searched and to what extent can be seen in Table 2.

TABLE 2. Summary of searches for  $\Phi^{\pm\pm}$  at the Tevatron experiments.

Experiment	Mass limit	Final states	Comments
D0 [56]	150 GeV	$\mu\mu\mu\mu$	Only muons in final state, no other channel has been searched at D0.
CDF [57]	115 – 136 GeV	$ee, e\mu$ and $\mu\mu$	Search for a single $\Phi^{\pm\pm}$ in the final state, all limits set assuming branching to only that final state.
CDF [58]	114 GeV	$e\tau e\tau, \mu\tau\mu\tau$	First search in Tevatron with LFV decays. Complements previous searches.

Out of all the possible final states the only ones searched for are cases where the pair produced  $\Phi^{\pm\pm}$  bosons decay to the same final state (or only one is searched) and only  $ee, e\mu,$

---

$e\tau$ ,  $\mu\mu$  and  $\mu\tau$  have been searched. No search has been performed in the  $\tau\tau$  final state, neither have there been searches with different final states simultaneously. To give a simple example, it is possible to find a parameter set according to the currently allowed neutrino parameters which results in only  $ee$  and  $\mu\tau$  final states for the  $\Phi^{\pm\pm}$ . Such a configuration would only show partially in  $ee$  and  $\mu\tau\mu\tau$  which would only make up a fraction of the total production. However a detailed analysis of possible final state configurations and corrections to the mass limit estimations is beyond the scope of this thesis and is reserved for the future. What can be concluded however is that the current estimates on  $\Phi^{\pm\pm}$  mass above around 110 GeV and higher should be taken cautiously and the region below the LEP exclusion should be probed at every new search to avoid missing the  $\Phi^{\pm\pm}$ .

6.2.4. *Estimates on the branching ratios of  $\Phi^{\pm\pm}$  from neutrino data.* The branching ratios of the  $\Phi^{\pm\pm}$  depend on three parameters. The mass of the  $\Phi^{\pm\pm}$ , the VEV and the Yukawa coupling matrix. Depending on the mass of the  $\Phi^{\pm\pm}$  the  $WW$  channel might be kinematically excluded and as can be seen from Figure 6 the mass also moves the point where leptonic and  $WW$  decays swap dominance. The VEV defines the relative strength of the  $WW$  channel in case the mass of  $\Phi^{\pm\pm}$  permits it kinematically. Below 160 GeV the only allowed decay channels are into a pair of same charge leptons and hence this is fully governed by the Yukawa coupling matrix. As there is no indirect way to estimate the VEV beyond the  $\rho$  parameter which sets an upper limit at around 1 GeV and as there is no upper bound on the mass, then the only estimation that can be done is for the leptonic channels and their relative distribution amongst themselves.

The connection between the leptonic final states branching ratios and the neutrino parameters can easily be seen from the equations (19), (20) and (25). In our estimations we assume 100% branching to leptons. This is the case below 160 GeV and in case the VEV is very small. However as the leptonic and weak interactions are fully independent one can consider the leptonic part as self contained and the relations from neutrino data still hold. If there is in addition the  $WW$  decay channel, then one just has to rescale the leptonic branching ratios with the total leptonic branching ratio.

As already shown, the leptonic branching ratios are directly related to the neutrino parameters. In essence, the six leptonic branching ratios are all functions of eight neutrino parameters:

$$\text{BR}_{ij} = f_k(m_0, \text{sign}(\Delta m_{\text{atm}}), \theta_{13}, \theta_{23}, \theta_{12}, \delta, \alpha_1, \alpha_2), \quad (27)$$

As two of the mixing angles  $\theta_{23}$  and  $\theta_{12}$  have been determined with quite good precision, then this can also be seen in the  $\Phi^{\pm\pm}$  branchings as varying these two parameters within their allowed region does only minor changes to the final branching ratios. The third mixing angle and the Dirac phase  $\delta$  have some contributions in specific scenarios, but are not major modifiers. There are three major players in determining the branchings are the mass of the lightest neutrino, the hierarchy and the majorana phases. If we for now leave the third mixing angle and the CP violation phases aside and study the effects of mass and hierarchy, then one can clearly see from Figure 7 that at low mass regions the two hierarchies contribute differently to the branching ratios of  $\Phi^{\pm\pm}$ .

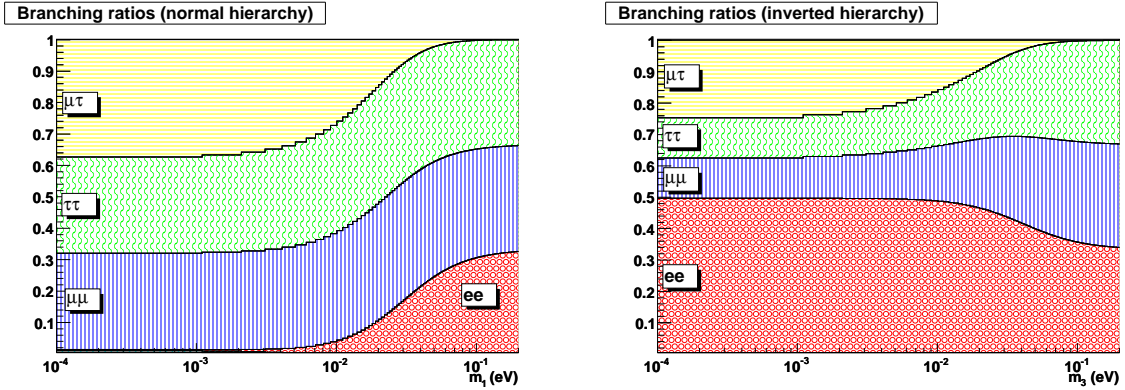


FIGURE 7. Distribution of the  $\Phi^{\pm\pm}$  leptonic branching ratios as a function of the lightest neutrino mass. The left (right) panel corresponds to the normal (inverted) mass hierarchy. For nearly degenerate masses the two possibilities imply almost the same result.

In case of the normal hierarchy the final states are almost equal fractions of  $\mu\mu$ ,  $\mu\tau$  and  $\tau\tau$  final states. In case of inverted hierarchy the  $\mu$  and  $\tau$  final states have about the same distribution amongst themselves, however the  $ee$  final state dominates at above 50%. So in case of normal hierarchy we would expect an experimental signature dominated by muons and taus, in case of inverse hierarchy we should expect a strong  $ee$  final state with some muon and tau final states and in case of a degenerate state of masses we can expect the three diagonal elements to dominate. In case one introduces also the three CP phases (and the third mixing), then the branching ratio plots get even more interesting introducing the  $e\mu$  and  $e\tau$  channels

in a wide variety of configurations and in most cases increasing the off-diagonal contributions. A variety of expected scenarios can be seen on Figures 8 and 9.

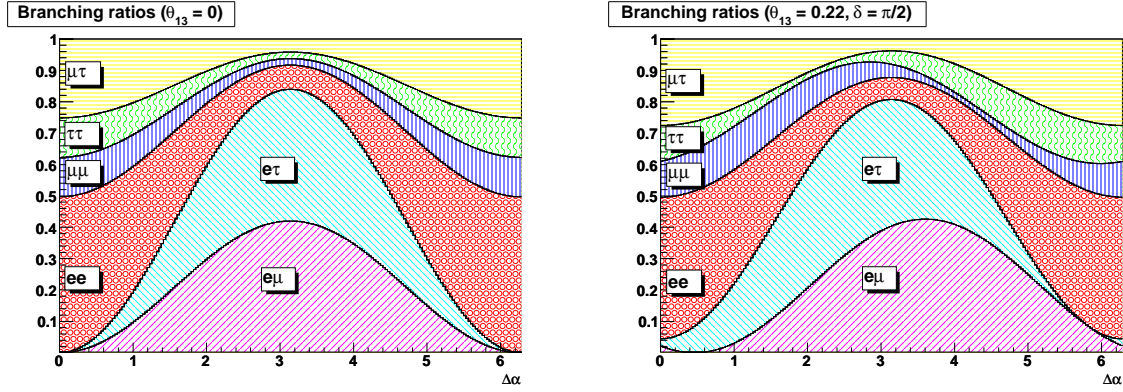


FIGURE 8. Distribution of the  $\Phi^{\pm\pm}$  branching ratios for inverted hierarchy as a function of  $\Delta\alpha$  for  $\theta_{13} = 0$  (left panel), and  $\theta_{13} = 0.22$ ,  $\delta = \pi/2$  (right panel). The asymmetry of the latter plot signals non-vanishing CP-violation.

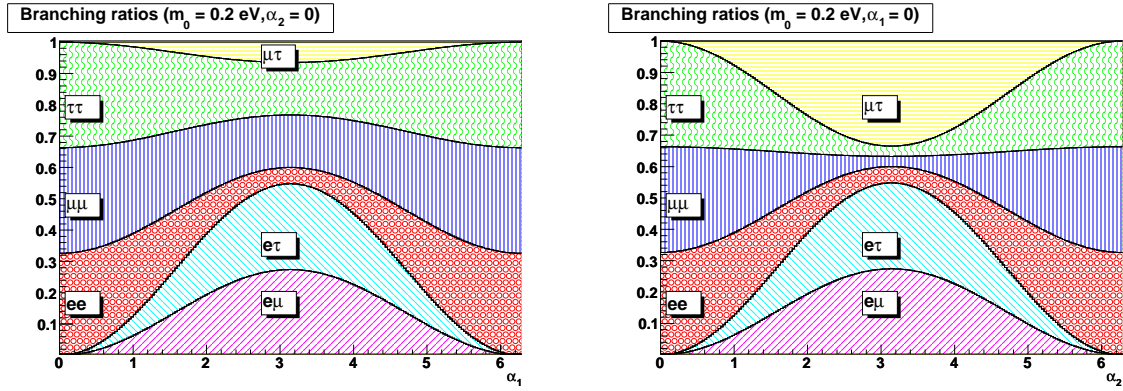


FIGURE 9. Distributions of the  $\Phi^{\pm\pm}$  branching ratios for non-zero  $\Delta\alpha$ . The left figure presents the case for fixed  $\alpha_2 = 0$ , and the right figure for fixed  $\alpha_1 = 0$ . Both figures are for inverted hierarchy.

### 6.3. Searching for $\Phi^{\pm\pm}$ in upcoming experiments.

6.3.1. *Signal and background processes.* The main production method, which has been analyzed for the LHC is the Drell-Yan pair production which can be seen as the leftmost diagram on Figure 3. The cross section of that process is independent of the unknown couplings and is only dependent on the mass of  $\Phi^{\pm\pm}$ . The final state signature of such a process would be

four charged leptons (assuming a vanishing VEV), which is already a good elimination of SM backgrounds. The decay chains for processes which can give a similar final state are shown on Figures 10 and 11. The actual generation diagrams are not shown as there is a number of them and not relevant to this work.

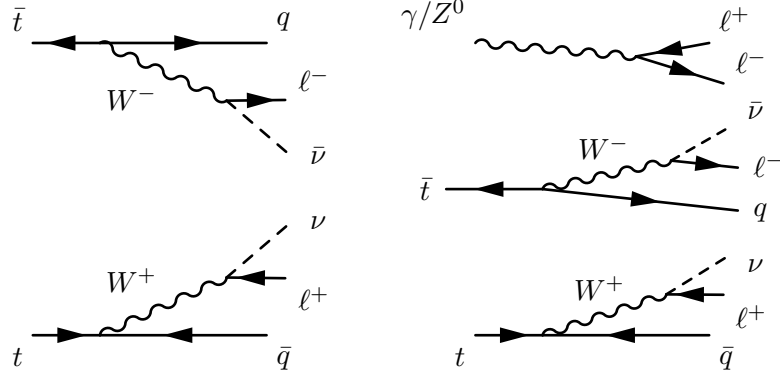


FIGURE 10. Background processes from the Standard Model contributing to the four lepton final state originating from top quarks. The b quarks are at times mis-identified as  $\tau$ -jets. On left the process  $t\bar{t} \rightarrow q\bar{q}\ell^+\ell^-\nu\bar{\nu}$  and on the right  $t\bar{t}Z^0 \rightarrow q\bar{q}2\ell^+2\ell^-\nu\bar{\nu}$

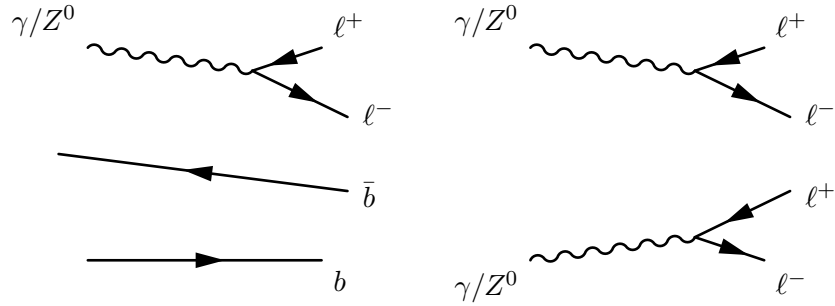


FIGURE 11. Background processes from the Standard Model contributing to the four lepton final state from Z bosons. The b quarks are at times mis-identified as  $\tau$ -jets. On left the process  $Z^0 b\bar{b} \rightarrow \ell^+\ell^- b\bar{b}$  and on the right  $Z^0 Z^0 \rightarrow 2\ell^+2\ell^-$

As a comparison of the signal and background production rates the relevant cross sections<sup>3</sup> to four lepton final states are shown in Table 3. The most similar process of  $ZZ \rightarrow 4\ell$  which contribute to background and which tend to be irreducible is luckily also of small cross section.

<sup>3</sup>Signal cross sections from [59].

TABLE 3. Cross sections and expected number of events at different luminosities

Process	$\sigma$ in fb	$N_{\text{events}} @ 10 fb^{-1}$	$N_{\text{events}} @ 50 fb^{-1}$	$N_{\text{events}} @ 100 fb^{-1}$
$\Phi^{\pm\pm} @ 100 \text{ GeV}$	1000	$10^4$	$5 \times 10^4$	$10^5$
$\Phi^{\pm\pm} @ 200 \text{ GeV}$	94	940	$4.7 \times 10^3$	$9.4 \times 10^3$
$\Phi^{\pm\pm} @ 300 \text{ GeV}$	19.6	196	980	1960
$\Phi^{\pm\pm} @ 400 \text{ GeV}$	5.9	59	295	590
$\Phi^{\pm\pm} @ 500 \text{ GeV}$	2.2	22	110	220
$\Phi^{\pm\pm} @ 600 \text{ GeV}$	0.9	9	45	90
$t\bar{t}$	$88.4 \times 10^3$	$8.8 \times 10^5$	$4.4 \times 10^6$	$8.8 \times 10^6$
$Z^0 b\bar{b}$	$26.2 \times 10^3$	$2.6 \times 10^5$	$1.3 \times 10^6$	$2.6 \times 10^6$
$t\bar{t}Z^0$	650	$6.5 \times 10^3$	$3.3 \times 10^4$	$6.5 \times 10^4$
$Z^0 Z^0$	212	$2.1 \times 10^3$	$1.1 \times 10^4$	$2.1 \times 10^4$

As can be seen from the table, the signal production is only comparable to the background in the mass region of 100 – 200 GeV. Above that the signal production cross section falls rapidly and the amount of produced events is not comparable to that of the background events. To still be able to find the signal amongst the background a number of discriminators have to be found. To this date most of the analysis concentrate on the normal hierarchy of neutrinos and hence look for mostly muons and taus in the final state. In theory the addition of electrons would not introduce new backgrounds and should be straightforward. However such a full analysis is yet to be performed at any hadron machine currently in operation or planned to.

6.3.2. *Discrimination of signal from background.* To discriminate between the signal and the background in case of muon and tau final states one has to understand the kinematics of the different processes. The main contribution to background from processes  $t\bar{t}$  and  $Zb\bar{b}$  comes from the misidentification of the b quark jets<sup>4</sup> as hadronic tau jets. A good discrimination of b and tau jets can eliminate a very large percentage of these processes as without the b quark jets the other leptons in these processes don't add up to a four lepton final state. To best discriminate tau jets from other quark jets one can use the simpleness of the hadronic tau decay. The jet produced in a hadronic tau decay is very narrow and has very few charged

<sup>4</sup>A top quark decays to a b quark and a W boson 99.8% of the times [60].

---

tracks (approximately 60% of the times one charged track, 35% of the times three charged tracks [60]). Also the lifetime of tau can be used as the lifetime of the tau lepton in comparison to the b quark can be a discriminating factor.

As the doubly charged Higgs boson is quite heavy and the leptons it decays into are light, then one very distinct signature kinematics-wise is that the leptons coming from a  $\Phi^{\pm\pm}$  decay tend to be extremely energetic and boosted towards the transverse plane while the decay products from the  $Z$  and  $W$  decays tend to be softer. The discriminating parameter used to separate based on this is the transverse momentum. The usual cut range is around 30 – 50 GeV with an additional optional cut on a scalar sum of all four leptons, which provides even better separation for leptons coming from the signal and those coming from electroweak carrier bosons.

As three of the four background processes include the  $Z$  boson, then a veto on the invariant mass of different charge leptons in the  $Z$  mass peak region provide also excellent  $Z$  rejection and even though one of the  $Z$  bosons in the  $ZZ \rightarrow 4\ell$  process is likely off-shell the rejection of the  $Z$  boson, which is on-shell provides an excellent rejection for events containing  $Z$  bosons.

As a final discriminator between signal and background events one can use the structure of the generation process and place a requirement on the mass difference between the invariant masses of the same charge lepton pairs. As two  $\Phi^{\pm\pm}$  are produced in every event, then their mass should be the same. As there are some inefficiencies in reconstruction and as the shape of the mass peak depends on the Yukawa coupling then this cut cannot be too strong, but a cut within 20% should eliminate majority of the background processes which have survived the previous requirements as there is no physical relationship behind same charge lepton pairs in the background events and hence their mass distribution is mostly random.

The studies performed so far have been based on Monte Carlo (MC) mechanisms, where events are generated with predetermined initial state and after the collision the collision products decay through their decay chains. The methodology and numerical models used have been previously verified to be in good agreement with the actual experiments in both the estimated actual cross section as well as the event kinematics. The MC software mostly used in current HEP experiments is PYTHIA [61] although a few others have been used for particular background processes to provide for best accuracy. For a detailed study on the search criteria and methodologies please refer to the two attached articles. Article I describes a general purpose Monte Carlo search at the LHC for final states with muons and taus and

---

has an average efficiency in the 30 – 40% region for the signal samples and a background acceptance of less than  $\approx 0.1\%$  in the signal region. In Article II a specific signature of muons and taus is studied at the CMS detector with the objective in mind to eliminate the background 100%. The respective cuts do eliminate the background completely and leave the signal efficiency in the 3-9% region. However as no background is estimated, then already a few events passing all the cuts would indicate the presence of a  $\Phi^{\pm\pm}$ .

## 7. MEASURING NEUTRINO PARAMETERS IN HEP COLLIDER EXPERIMENTS

There are various ways to measure the different neutrino parameters. One can measure the  $ee$  channel coupling and the effective mass from neutrinoless double beta decay. One can measure the mixing angles and mass differences from the oscillation experiments. In addition there is a way to estimate the upper bound on the neutrino mass from the cosmological models and a few experiments to measure the Dirac CP phase  $\delta$ . However the coupling matrix in general and the Majorana phases are something that cannot that easily be measured through these experiments. If the new scalar triplet that we have introduced indeed generates the masses for neutrinos, then almost all of the neutrino parameters can be measured from the results of a HEP experiment upon discovery of the doubly charged Higgs boson.

**7.1. Branching ratios as an indirect measurement of neutrino parameters.** As already described previously in the Section 6.2.4, there is a concrete relationship between the branching ratios of a  $\Phi^{\pm\pm}$  boson and the neutrino parameters. However we used these relations to estimate the branching ratios assuming certain settings of the neutrino parameters. Now in case the boson is actually found in any of the currently running or future experiments, it is important to know if the same measured branching ratios can be used to give some additional information about the neutrino sector that cannot be measured elsewhere or to give better results than obtained elsewhere.

The branching ratio equations (27) account for six equations. There are however eight parameters in the neutrino sector:  $\theta_{12}, \theta_{13}, \theta_{23}, \delta, \alpha_1, \alpha_2, \text{sign}(\Delta m_{12}), m_0$ . In addition as we do not know the other possible branching ratios of the  $\Phi^{\pm\pm}$  to W-s or  $\Phi^\pm$  then we cannot use the branching ratios directly as the formulas contain the  $\Gamma_{\text{tot}}$  variable which contains also the decay widths of these unknown decays. However by using relations between the branching ratios we can eliminate the denominator of equation (25) and hence be independent of the other branching ratios. However doing so reduces us to five equations and eight parameters.

---

So to be able to solve this system we need to fix three of the parameters and luckily for us the mixing angles of the neutrinos have been measured with very good precision and fixing them to some concrete set should not provide a strong bias. Also, in case the mixing angles are remeasured with higher precision we only have to insert the new numbers and the final math remains the same. A good estimate from a number of theories and in good agreement with the current experimental best fits is the tribimaximal mixing model [62]:

$$\sin^2 \theta_{12} = \frac{1}{3}, \quad \sin^2 \theta_{23} = \frac{1}{2}, \quad \sin^2 \theta_{13} = 0. \quad (28)$$

Having fixed the mixing angles according to equation (28), we end up with four independent equations for branching ratios, since  $\text{BR}_{e\mu} = \text{BR}_{e\tau}$  and  $\text{BR}_{\mu\mu} = \text{BR}_{\tau\tau}$ . If a measurement would show that these branching ratios are not equal, this is a clear indication that the tri-bi-maximal model has to be modified. As we are using the relations between branching ratios for the calculations, the number of independent equations is reduced to three. Such equation system can be solved with respect to three unknown parameters: the lowest neutrino mass  $m_0$  and Majorana phases  $\alpha_1$  and  $\alpha_2$ . We show how the mass of the lowest neutrino mass eigenstate, neutrino mass hierarchy and the difference of two Majorana phases  $|\Delta\alpha|$  can be uniquely determined from the relation (25). Unique solutions for  $\alpha_1$  and  $\alpha_2$  are not determined by the  $\Phi^{\pm\pm}$  branching ratios, and two sets of degenerate solutions are found.

## 7.2. Determination of the neutrino mass hierarchy and the lightest neutrino mass.

Through combining the  $\mu\mu, \mu\tau, ee$  and  $e\mu$  channel branching ratios we can define a characteristic dimensionless constant:

$$C_1 \equiv \frac{2\text{BR}_{\mu\mu} + \text{BR}_{\mu\tau} - \text{BR}_{ee}}{\text{BR}_{ee} + \text{BR}_{e\mu}} = \frac{-m_1^2 + m_2^2 + 3m_3^2}{2m_1^2 + m_2^2}. \quad (29)$$

The mass hierarchy can be easily determined by simply measuring the value of  $C_1$  that is independent of the values of  $\alpha_1$  and  $\alpha_2$ . It can be found that  $C_1$  uniquely determines the mass hierarchy as follows:

- $C_1 > 1$  – normal mass hierarchy,
- $C_1 < 1$  – inverted mass hierarchy,
- $C_1 \approx 1$  – degenerate masses.

Once the hierarchy is known we can solve the equation for the lowest neutrino mass by inserting the respective mass differences  $\Delta m_{\text{sol}}^2$  and  $\Delta m_{\text{atm}}^2$ . For the concrete results see equations 15 and 16 in attached Article III.

---

**7.3. Probing for Majorana phases.** Once the neutrino mass hierarchy and lightest neutrino mass have been determined they can be then used in turn to solve the remaining equations systems for the Majorana phases. To do so we start with solving for the difference in the phases ( $\Delta\alpha$ ). This is best done using just the  $e\mu$  and  $ee$  channels, but can be done using other channels too:

$$C_2 \equiv \frac{\text{BR}_{e\mu}}{\text{BR}_{ee}} = \frac{2(m_1^2 + m_2^2 - 2m_1m_2 \cos \Delta\alpha)}{4m_1^2 + m_2^2 + 4m_1m_2 \cos \Delta\alpha}. \quad (30)$$

This equation can now be solved for the difference in phases depending on the hierarchy. The concrete formulas can be again seen in equations 18 and 19 in Article III. The only thing we would like to draw attention to is that if one looks at the simplified form of the solution for inverted hierarchy<sup>5</sup> one can see that the equation for  $\Delta\alpha$  is independent of the lightest neutrino mass and can hence also be used for the degenerate state. In case of normal hierarchy we need to also use the lightest neutrino mass to determine the difference in the phases.

As the cosine is an even function, then the solution will be unique but with an uncertainty on the sign. This means that once we start to solve the equations for the Majorana phases separately we have to make an assumption which of them is larger and as this leads to different solutions, then we will have two separate undistinguishable results of which one is correct.

A few special scenarios exist that can be probed separately and allow precise determination of the parameters. A few of them are listed here:

- Normal mass hierarchy with lowest neutrino mass exactly zero. In this case the branching ratios are independent of the Majorana phase  $\alpha_1$  and  $\alpha_2$  can be determined precisely.
- Inverted hierarchy with lowest neutrino mass exactly zero. In this case the branching ratios are independent of absolute values of the phases and we can determine the difference ( $\Delta\alpha$ ) only.
- In case of nearly degenerate masses we have  $m_1 \approx m_2 \approx m_3 = m$  and the branching ratios become independent of the mass  $m$ .

The effect of non-zero Majorana phase in case of normal hierarchy and very low mass of the lightest neutrino can be seen on the left hand side of Figure 12. As can be seen the effects are really small. The  $\mu\tau$  channel is enhanced, but in general the effects are minor. In case of

---

<sup>5</sup>Equation (20) in Article III.

the inverse hierarchy however the the effects are much more dominant as seen on Figures 8 and 9.

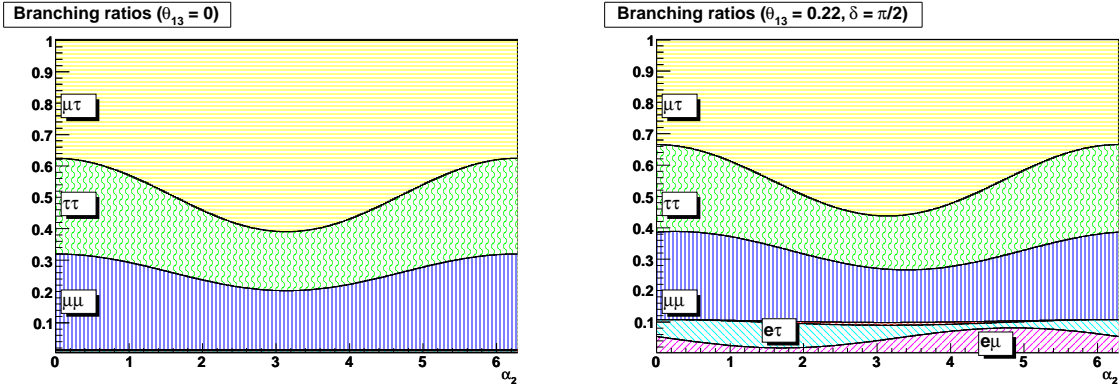


FIGURE 12. Distributions of the branching ratios as a function of  $\alpha_2$ . The left panel corresponds to  $\theta_{13} = 0$  with the  $ee$ ,  $e\mu$  and  $e\tau$  channels giving nearly negligible contributions. When  $\theta_{13}$  is non-zero (the right panel), small branching ratios to  $e\mu$  and  $e\tau$  channels can be measured. Non-zero  $\delta$  in the right panel causes the slight asymmetry with respect to  $\alpha_2 = \pi$ . Both diagrams represent the normal hierarchy.

**7.4. Probing the mixing angle  $\theta_{13}$  and CP violation.** As stated above the simplification that we have done to come to the above mentioned conclusions has been the adaptation of the tribimaximal mixing model. However that model explicitly states that the mixing angle  $\theta_{13}$  is zero which effectively neutralizes the Dirac CP phase. In case however that the actual physical world has a non-zero mixing angle  $\theta_{13}$  and the effects of the CP phase indeed have direct effects on the  $\Phi^{\pm\pm}$  decays, then we should also study the impact of this. As stated one of the obvious results of the tribimaximal mixing was that

$$\text{BR}_{e\mu} = \text{BR}_{e\tau}, \quad (31)$$

$$\text{BR}_{\mu\mu} = \text{BR}_{\tau\tau}. \quad (32)$$

If there is mixing between first and third mass state, then these relations no longer hold. This is our possibility to test our assumptions based on the experimental results. However it must be noted that to be able to determine that these relations do not hold a substantial amount of statistics is necessary as the branching to  $e\mu$  and  $e\tau$  channels should be orders of

---

magnitude smaller than to the other channels. If however such a discrepancy is found, then the results we have obtained until now have to be reviewed. It can be however noted that even when we can no longer assume that the full tribimaximal mixing holds, the methodology to achieve the results remains the same. The introduction of  $\theta_{13}$  and  $\delta$  would provide only small corrections to the already found solutions due to their smallness, but the general structure would still hold. As an example for the lowest neutrino mass we can still find the solution as before, the formula for the dimensionless constant  $C_1$  changes slightly and requires measurements of more branching ratios than before. The modified formula as listed in equation 27 in Article III is:

$$C'_1 \equiv \frac{2\text{BR}_{\mu\mu} + 2\text{BR}_{\tau\tau} + 2\text{BR}_{\mu\tau} - 2\text{BR}_{ee}}{2\text{BR}_{ee} + \text{BR}_{e\mu} + \text{BR}_{e\tau}} = \frac{-m_1^2 + m_2^2 + 3m_3^2}{2m_1^2 + m_2^2} + \mathcal{O}(\sin^2 \theta_{13}). \quad (33)$$

Similarly the determination of the other results has similar formulas with slight corrections and the formulas usually become slightly more complex involving more branching ratios. Considering the pureness of the LHC machine we can assume that the best case scenario will be using the simple formulas to determine the first estimates on the neutrino parameters.

### 7.5. Possibilities on measuring the vacuum expectation value of the scalar triplet.

So far we have been working with the leptonic channels. To understand the scalar triplet better we would also need to measure the vacuum expectation value of it.

Let us first assume that  $v_\Phi$  is large enough to imply, according to eq. (23), observable fraction of the decays  $\Phi^{\pm\pm} \rightarrow W^+W^+$ , and the collider experiments are sensitive enough to measure not just the branching fractions but also the partial widths of the bosons in the scalar triplet, namely  $\Gamma_{ij}$  and  $\Gamma_{WW}$ . The latter may not be possible at LHC but could be possible at ILC experiments [63]. In such a case one gets from eq. (20) and eq. (23),

$$\frac{\text{BR}_{ll}}{\text{BR}_{WW}} = \frac{\Gamma_{ll}}{\Gamma_{WW}} = \frac{\Gamma_{ll}}{kv_\Phi^2} \Rightarrow v_\Phi = \sqrt{\frac{\Gamma_{ll}\text{BR}_{WW}}{k\text{BR}_{ll}}} = \sqrt{\frac{\Gamma_{\text{tot}}\text{BR}_{WW}}{k}}, \quad (34)$$

and the determination of  $v_\Phi$  from collider experiments is possible.

If the collider experiments are not able to measure the partial widths, one needs additional information on the neutrino mass matrix.

7.5.1. *Combined data from  $0\nu\beta\beta$  and collider experiments.* Assuming that the branching ratio to  $WW$  channel is measured at any accelerator experiment and  $|(m_\nu)_{ee}|$  is probed from  $0\nu\beta\beta$

---

experiment one gets

$$\frac{\text{BR}_{ee}}{\text{BR}_{WW}} = \frac{\Gamma_{ee}}{\Gamma_{WW}} = \frac{1}{32\pi} \frac{|(m_\nu)_{ee}|^2 m_{\Phi^{\pm\pm}}}{k v_\Phi^4}. \quad (35)$$

Now  $v_\Phi$  can be directly found as

$$v_\Phi = \left( \frac{|(m_\nu)_{ee}|^2 m_{\Phi^{\pm\pm}} \text{BR}_{WW}}{32\pi k \text{BR}_{ee}} \right)^{\frac{1}{4}}. \quad (36)$$

7.5.2. *Direct measurement of couplings and  $W^\pm W^\pm$  channel in a lepton collider.* Finally, if  $v_\Phi$  is too small to imply observable  $\Phi^{\pm\pm} \rightarrow WW$  decay rates at colliders, one has to rely entirely on leptonic data. If one of the leptonic Yukawa couplings is directly measured in the accelerator experiments and  $|(m_\nu)_{ee}|$  is probed from the  $0\nu\beta\beta$  experiments, one is able to derive the VEV from data. As the simplest example, when  $\Gamma_{ee}$  is measured, perhaps from the resonance at  $e^-e^-$  collider [64], the VEV can be directly found from

$$\Gamma_{ee} = \frac{|(m_\nu)_{ee}|^2 m_{\Phi^{\pm\pm}}}{32\pi v_\Phi^2} \Rightarrow v_\Phi = \sqrt{\frac{|(m_\nu)_{ee}|^2 m_{\Phi^{\pm\pm}}}{32\pi \Gamma_{ee}}}. \quad (37)$$

As shown, direct measurement of the VEV is possible. However it does require additional information which cannot be obtained from the LHC alone. Should the  $0\nu\beta\beta$  yield positive results or some of the scalar triplet Yukawa coupling be measured at ILC, we can also give estimates on the magnitude of the VEV of the scalar triplet.

---

## 8. CONCLUSION

As has been shown, the scalar triplet model is a very simple and promising extension to the Standard Model. It provides the full explanation of the neutrino masses that have been observed and provides also a very pure and simple experimental signature that shows promise in detecting it already in the upcoming LHC or possible future ILC experiments. We have shown the possible signatures that can occur based on the currently allowed parameter space of the neutrino sector and have also shown the possible ways to search for the doubly charged component of the scalar triplet.

Once found the actual statistics of the  $\Phi^{\pm\pm}$  can be used to predict the currently undetermined parameters in the neutrino sector. The simplest of which are the determination of the mass hierarchy, the mass of the lightest neutrino and if good enough precision is available, then also the Majorana phases and possibly with very good precision also estimates on the validity of the tribimaximal mixing model through estimations on the  $\theta_{13}$  mixing angle. In addition if the decay width of the leptonic channels and the WW final state can be measured or in addition using the neutrinoless double beta decay results we can also estimate the last unknown parameter of the model the vacuum expectation value of the scalar triplet.

The search algorithms for searching the  $\Phi^{\pm\pm}$  at future colliders in Section 6.3 as well as the analysis of the branching ratios covered in Section 7 which allow us to measure almost all of the unknown parameters of the neutrino sector and which are further elaborated in the attached three articles are the original work of the author.

---

## REFERENCES

- [1] S. Weinberg, “A Model Of Leptons,” *Phys. Rev. Lett.* **19** (1967) 1264.  
A. Salam, p. 367 of *Elementary Particle Theory*, ed. N. Svartholm (Almqvist and Wilksells, Stockholm, 1969)  
S. L. Glashow, *Nucl. Phys.* **20**, 57 (1961)
- [2] S. Abachi *et al.* [D0 Collaboration], “Observation of the top quark,” *Phys. Rev. Lett.* **74** (1995) 2632 [arXiv:hep-ex/9503003].
- [3] F. Abe *et al.* [CDF Collaboration], “Observation of top quark production in  $\bar{p}p$  collisions,” *Phys. Rev. Lett.* **74** (1995) 2626 [arXiv:hep-ex/9503002].
- [4] G. Arnison *et al.* [UA1 Collaboration], “Observation Of The Muonic Decay Of The Charged Intermediate Vector Boson,” *Phys. Lett. B* **134** (1984) 469.
- [5] K. Borer, B. Hahn, H. Hanni, P. Mani, J. Schacher, F. Stocker and W. Zeller [UA2 COLLABORATION Collaboration], “Observation Of The Neutral Boson Z0 Of The Weak Interaction,”
- [6] J. N. Bahcall, “The Be-7 Solar Neutrino Line: A Reflection Of The Central Temperature Distribution Of The Sun,” *Phys. Rev. D* **49** (1994) 3923 [arXiv:astro-ph/9401024].
- [7] The LEP study groups, “LEP design report. 1. The LEP injector chain,” “Lep Design Report: Vol. 2. The Lep Main Ring,”
- [8] A. Venturi [ALEPH, DELPHI, L3, OPAL Collaborations], “New (almost final) W mass and width results from LEP,” *Prepared for 20th Rencontres de Physique de La Vallee d’Aoste: Results and Perspective in Particle Physics, La Thuile, Aosta Valley, Italy, 5-12 Mar 2006*
- [9] C. M. Ankenbrandt *et al.*, “Status of muon collider research and development and future plans,” *Phys. Rev. ST Accel. Beams* **2** (1999) 081001 [arXiv:physics/9901022].
- [10] R. R. Wilson, “The Tevatron,” *Phys. Today* **30N10** (1977) 23.
- [11] L. Evans and P. Bryant, “LHC Machine,” *JINST* **3** (2008) S08001.
- [12] S. Chatrchyan *et al.* [The CMS Collaboration], “The CMS experiment at the CERN LHC,” *JINST* **3** (2008) S08004.
- [13] G. Aad *et al.* [The ATLAS Collaboration], “The ATLAS experiment at the CERN Large Hadron Collider,” *JINST* **3** (2008) S08003.
- [14] A. A. Alves *et al.* [LHCb Collaboration], “The Lhcb Detector At The Lhc,” *JINST* **3** (2008) S08005.
- [15] K. Aamodt *et al.* [ALICE Collaboration], “The Alice Experiment At The Cern Lhc,” *JINST* **3** (2008) S08002
- [16] J. Brau *et al.*, “International Linear Collider reference design report. 1: Executive summary. 2: Physics at the ILC. 3: Accelerator. 4: Detectors,”
- [17] H. Ejiri *et al.*, “Limits on the Majorana neutrino mass and right-handed weak currents by neutrinoless double beta decay of Mo-100,” *Phys. Rev. C* **63** (2001) 065501.
- [18] V. M. Abazov *et al.* [D0 Collaboration], “Improved W boson mass measurement with the D0 detector,” *Phys. Rev. D* **66** (2002) 012001 [arXiv:hep-ex/0204014].

- 
- [19] P. Achard *et al.* [L3 Collaborations], “Measurement of the Z-boson mass using  $e^+ e^- \rightarrow Z$  gamma events at centre-of-mass energies above the Z pole,” *Phys. Lett. B* **585** (2004) 42 [arXiv:hep-ex/0402001].
- [20] Y. Fukuda *et al.* [Super-Kamiokande Collaboration], “Evidence for oscillation of atmospheric neutrinos,” *Phys. Rev. Lett.* **81** (1998) 1562 [arXiv:hep-ex/9807003].
- [21] S. Fukuda *et al.* [Super-Kamiokande Collaboration], “Determination of solar neutrino oscillation parameters using 1496 days of Super-Kamiokande-I data,” *Phys. Lett. B* **539**, 179 (2002) [arXiv:hep-ex/0205075].
- [22] Q. R. Ahmad *et al.* [SNO Collaboration], “Direct evidence for neutrino flavor transformation from neutral-current interactions in the Sudbury Neutrino Observatory,” *Phys. Rev. Lett.* **89** (2002) 011301 [arXiv:nucl-ex/0204008].
- [23] J. Lee-Franzini, F. Bossi and P. Franzini, “Lepton and photon interactions at high energies. Proceedings, 20th International Symposium, LP 2001, Rome, Italy, July 23-28, 2001,” *Prepared for 20th International Symposium on Lepton and Photon Interactions at High Energies (LP 01), Rome, Italy, 23-28 Jul 2001*
- [24] A. Strumia and F. Vissani, “Neutrino masses and mixings and.,” arXiv:hep-ph/0606054.
- [25] R. N. Mohapatra *et al.*, “Theory of neutrinos: A white paper,” *Rept. Prog. Phys.* **70** (2007) 1757 [arXiv:hep-ph/0510213].
- [26] G. L. Fogli *et al.*, “Observables sensitive to absolute neutrino masses: A reappraisal after WMAP-3y and first MINOS results,” *Phys. Rev. D* **75** (2007) 053001 [arXiv:hep-ph/0608060].
- [27] G. L. Fogli, E. Lisi, A. Marrone, A. Palazzo and A. M. Rotunno, “Global analysis of neutrino masses and mixing,” *Prog. Part. Nucl. Phys.* **57** (2006) 71.
- [28] J. Lesgourgues and S. Pastor, “Massive neutrinos and cosmology,” *Phys. Rept.* **429**, 307 (2006) [arXiv:astro-ph/0603494].
- [29] A. de Gouvea, “Neutrino physics,” arXiv:hep-ph/0411274.
- [30] Z. Maki, M. Nakagawa and S. Sakata, “Remarks on the unified model of elementary particles,” *Prog. Theor. Phys.* **28** (1962) 870.
- [31] B. Pontecorvo, “Neutrino experiments and the question of leptonic-charge conservation,” *Sov. Phys. JETP* **26**, 984 (1968) [*Zh. Eksp. Teor. Fiz.* **53**, 1717 (1967)].
- [32] S. M. Bilenky and S. T. Petcov, “Massive Neutrinos and Neutrino Oscillations,” *Rev. Mod. Phys.* **59** (1987) 671 [Erratum-*ibid.* **61** (1989) ERRAT,60,575-575.1988) 169.1989 ERRAT,60,575].
- [33] A. Morales and J. Morales, “The neutrinoless double beta decay: The case for germanium detectors,” *Nucl. Phys. Proc. Suppl.* **114** (2003) 141 [arXiv:hep-ph/0211332].
- [34] R. N. Mohapatra and J. D. Vergados, “New contribution to neutrinoless double beta decay in gauge models,” *Phys. Rev. Lett.* **47**, 1713 (1981).
- [35] B. Brahmachari and E. Ma, “Neutrinoless double beta decay with negligible neutrino mass,” *Phys. Lett. B* **536**, 259 (2002) [arXiv:hep-ph/0202262].
- [36] H. V. Klapdor-Kleingrothaus *et al.*, “Latest results from the Heidelberg-Moscow double-beta-decay experiment,” *Eur. Phys. J. A* **12**, 147 (2001) [arXiv:hep-ph/0103062].

- 
- [37] C. E. Aalseth *et al.* [IGEX Collaboration], “The IGEX Ge-76 neutrinoless double-beta decay experiment: Prospects for next generation experiments,” *Phys. Rev. D* **65**, 092007 (2002) [arXiv:hep-ex/0202026].
- [38] G. L. Fogli, E. Lisi, A. Marrone, A. Melchiorri, A. Palazzo, P. Serra and J. Silk, “Observables sensitive to absolute neutrino masses: Constraints and correlations from world neutrino data,” *Phys. Rev. D* **70**, 113003 (2004) [arXiv:hep-ph/0408045].
- [39] P. Minkowski, “ $\mu \rightarrow e \gamma$  At A Rate Of One Out Of 1-Billion Muon Decays?,” *Phys. Lett. B* **67** (1977) 421.
- [40] T. Yanagida, “Horizontal gauge symmetry and masses of neutrinos,” *In Proceedings of the Workshop on the Baryon Number of the Universe and Unified Theories, Tsukuba, Japan, 13-14 Feb 1979*
- [41] M. Gell-Mann, P. Ramond and R. Slansky, Complex Spinors And Unified Theories, in *Supergravity*, P. van Nieuwenhuizen and D.Z. Freedman (eds.), North Holland Publ. Co., 1979.
- [42] S. L. Glashow, “The Future Of Elementary Particle Physics,” *NATO Adv. Study Inst. Ser. B Phys.* **59**, 687 (1979).
- [43] R. N. Mohapatra and G. Senjanovic, “Neutrino mass and spontaneous parity nonconservation,” *Phys. Rev. Lett.* **44**, 912 (1980).
- [44] M. Magg and C. Wetterich, “Neutrino Mass Problem And Gauge Hierarchy,” *Phys. Lett. B* **94**, 61 (1980).
- [45] J. Schechter and J. W. F. Valle, “Neutrino Masses In  $SU(2) \times U(1)$  Theories,” *Phys. Rev. D* **22**, 2227 (1980).
- [46] G. Lazarides, Q. Shafi and C. Wetterich, “Proton Lifetime And Fermion Masses In An  $SO(10)$  Model,” *Nucl. Phys. B* **181**, 287 (1981).
- [47] R. N. Mohapatra and G. Senjanovic, “Neutrino Masses And Mixings In Gauge Models With Spontaneous Parity Violation,” *Phys. Rev. D* **23**, 165 (1981).
- [48] G. B. Gelmini and M. Roncadelli, “Left-Handed Neutrino Mass Scale And Spontaneously Broken Lepton Number,” *Phys. Lett. B* **99**, 411 (1981).
- [49] R. Foot, H. Lew, X. G. He and G. C. Joshi, “SEESAW NEUTRINO MASSES INDUCED BY A TRIPLET OF LEPTONS,” *Z. Phys. C* **44**, 441 (1989).
- [50] E. Ma, “Pathways to naturally small neutrino masses,” *Phys. Rev. Lett.* **81**, 1171 (1998) [arXiv:hep-ph/9805219].
- [51] E. Ma, M. Raidal, U. Sarkar, “Verifiable model of neutrino masses from large extra dimensions,” *Phys. Rev. Lett.* 85:3769-3772,2000.
- [52] M. L. Swartz, “Limits On Doubly Charged Higgs Bosons And Lepton Flavor Violation,” *Phys. Rev. D* **40** (1989) 1521.
- [53] G. Abbiendi *et al.* [OPAL Collaboration], “Search for doubly charged Higgs bosons with the OPAL detector at LEP,” *Phys. Lett. B* **526**, 221 (2002) [arXiv:hep-ex/0111059].
- [54] J. Abdallah *et al.* [DELPHI Collaboration], “Search for doubly charged Higgs bosons at LEP2,” *Phys. Lett. B* **552**, 127 (2003) [arXiv:hep-ex/0303026].

- 
- [55] P. Achard *et al.* [L3 Collaboration], “Search for doubly charged Higgs bosons at LEP,” *Phys. Lett. B* **576**, 18 (2003) [arXiv:hep-ex/0309076].
- [56] V. M. Abazov *et al.* [D0 Collaboration], “Search for pair production of doubly-charged Higgs bosons in the  $H^{++}H^{--}$  to  $\mu^+\mu^+\mu^-\mu^-$  final state at D0,” arXiv:0803.1534 [hep-ex].
- [57] D. E. Acosta *et al.* [CDF Collaboration], “Search for doubly-charged Higgs bosons decaying to dileptons in  $p\bar{p}$  collisions at  $\sqrt{s} = 1.96$  TeV,” *Phys. Rev. Lett.* **93**, 221802 (2004) [arXiv:hep-ex/0406073].
- [58] T. Aaltonen [CDF Collaboration], “Search For Doubly Charged Higgs Bosons With Lepton-Flavour-Violating Decays Involving Tau Leptons,”
- [59] M. Muhlleitner and M. Spira, “A note on doubly-charged Higgs pair production at hadron colliders,” *Phys. Rev. D* **68** (2003) 117701 [arXiv:hep-ph/0305288].
- [60] C. Amsler *et al.* [Particle Data Group], “Review of particle physics,” *Phys. Lett. B* **667** (2008) 1.
- [61] T. Sjostrand, P. Eden, C. Friberg, L. Lonnblad, G. Miu, S. Mrenna and E. Norrbin, “High-energy-physics event generation with PYTHIA 6.1,” *Comput. Phys. Commun.* **135** (2001) 238 [arXiv:hep-ph/0010017].
- [62] P. F. Harrison, D. H. Perkins and W. G. Scott, “A redetermination of the neutrino mass-squared difference in tri-maximal mixing with terrestrial matter effects,” *Phys. Lett. B* **458**, 79 (1999) [arXiv:hep-ph/9904297].
- [63] G. Barenboim, K. Huitu, J. Maalampi and M. Raidal, “Constraints on doubly charged Higgs interactions at linear collider,” *Phys. Lett. B* **394** (1997) 132 [arXiv:hep-ph/9611362].
- [64] M. Raidal, “Lower bounds on bilepton processes at e- e- and mu- mu- colliders,” *Phys. Rev. D* **57**, 2013 (1998) [arXiv:hep-ph/9706279].

---

ARTICLE I

---

Hektor, A., Kadastik, M., Müntel, M., Raidal, M., Rebane, L., 2007. Testing neutrino masses in little Higgs models via discovery of doubly charged Higgs at LHC, Nucl.Phys.B787:198-210,2007.

Copyright (2007), with permission from Elsevier.

# Testing neutrino masses in little Higgs models via discovery of doubly charged Higgs at LHC

A. Hektor, M. Kadastik, M. Müntel, M. Raidal, L. Rebane\*

*National Institute of Chemical Physics and Biophysics, Ravala 10, Tallinn 10143, Estonia*

Received 7 June 2007; accepted 18 July 2007

Available online 27 July 2007

---

## Abstract

We have investigated the possibility of direct tests of little Higgs models incorporating triplet Higgs neutrino mass mechanism at LHC experiments. We have performed Monte Carlo studies of Drell–Yan pair production of doubly charged Higgs boson  $\Phi^{++}$  followed by its leptonic decays whose branching ratios are fixed from the neutrino oscillation data. We propose appropriate selection rules for the four-lepton signal, including reconstructed taus, which are optimized for the discovery of  $\Phi^{++}$  with the lowest LHC luminosity. As the Standard Model background can be effectively eliminated, an important aspect of our study is the correct statistical treatment of the LHC discovery potential. Adding detection efficiencies and measurement errors to the Monte Carlo analyses,  $\Phi^{++}$  can be discovered up to the mass 250 GeV in the first year of LHC, and 700 GeV mass is reachable for the integrated luminosity  $L = 30 \text{ fb}^{-1}$ .

© 2007 Elsevier B.V. All rights reserved.

---

## 1. Introduction

The main motivation of the Large Hadron Collider (LHC) experiment is to reveal the secrets of electroweak symmetry breaking. If the light Standard Model (SM) Higgs boson  $H$  will be discovered, the question arises what stabilizes its mass against the Planck scale quadratically divergent radiative corrections. The canonical answer to this question is supersymmetry, predicting a very rich phenomenology of sparticles in the future collider experiments.

Alternatively, the light SM Higgs boson may signal some strong dynamics at high scale  $\Lambda \sim 4\pi f$ , where  $f$  is the decay constant of the new strongly interacting theory [1]. The most

---

\* Corresponding author.

*E-mail address:* [liis.rebane@cern.ch](mailto:liis.rebane@cern.ch) (L. Rebane).

interesting class of models in such a scheme are the little Higgs models [2–4]. In those models the SM Higgs boson is a pseudo Goldstone mode of a broken global symmetry and remains much lighter than the other modes of the model, thus solving the little hierarchy problem and postponing the solution to the fundamental hierarchy problem to the scale  $\Lambda$ . Those models are also very interesting from collider physics point of view since they predict the existence of new particles, such as a new set of heavy gauge bosons  $W_H, Z_H$ , a vectorlike heavy quark pair  $T, \bar{T}$  with charge  $2/3$ , and triplet Higgs bosons  $\Phi$ . If the new particle masses are  $\mathcal{O}(1)$  TeV, direct tests of the models are possible at LHC [5–7].

An important open issue to address in the context of little Higgs models is the origin of non-zero neutrino masses [8–12]. The neutrino mass mechanism which naturally occurs in those models is the triplet Higgs mechanism [13,14] (sometimes called type II seesaw) which employs a scalar with the  $SU(2)_L \times U(1)_Y$  quantum numbers  $\Phi \sim (3, 2)$ . The existence of such a multiplet in some versions of the little Higgs models is a direct consequence of global symmetry breaking which makes the SM Higgs light. For example, in the minimal littlest Higgs model [15], the triplet Higgs with non-zero hypercharge arises from the breaking of global  $SU(5)$  down to  $SO(5)$  symmetry as one of the Goldstone bosons. Its mass  $M_\Phi \sim g_s f$ , where  $g_s < 4\pi$  is a model dependent coupling constant in the weak coupling regime [1], is therefore predicted to be below the cut-off scale  $\Lambda$ , and could be within the mass reach of LHC. Although the triplet mass scale is  $\mathcal{O}(1)$  TeV, the observed neutrino masses can be obtained naturally. Firstly, non-observation of rare decays  $\mu \rightarrow eee, \mu \rightarrow e\gamma, \tau \rightarrow \ell\ell\ell$ , where  $\ell = e, \mu$ , implies that the triplet Higgs boson Yukawa couplings  $Y_{ij}$  must be small, thus suppressing also the neutrino masses. Secondly, the vacuum expectation value (vev) of the neutral component of triplet  $v_\Phi$  contributes at tree level to the SM oblique corrections, and is therefore severely constrained by precision data. There exist additional mechanisms which can explain the smallness of  $v_\Phi$  in little Higgs models. Since the smallness of  $v_\Phi$  is the most natural explanation of the smallness of neutrino masses in the little Higgs models, we assume this to be the case in this work.

The aim of this paper is to study the possibility of direct tests of little Higgs models and neutrino mass mechanisms at LHC experiments via pair productions and subsequent decays of triplet Higgs boson. We study the Drell–Yan pair production of doubly charged component of the triplet [16–21]

$$pp \rightarrow \Phi^{++} \Phi^{--}, \quad (1)$$

followed by the leptonic decays. Notice that (i) the production cross section does not depend on any unknown model parameter but the mass of  $\Phi^{++}$ ; (ii) smallness of  $v_\Phi$  in this scenario, following from the smallness of neutrino masses, implies that the decays  $\Phi^{++} \rightarrow W^+ W^+$  are negligible, and we neglect this channel in the following analyses; (iii) the  $\Phi^{++}$  leptonic decay branching fractions do not depend on the size of the Yukawa couplings but only on their ratios which are known from neutrino oscillation experiments. In the triplet model the normally hierarchical light neutrino masses predict  $\text{BR}(\Phi^{++} \rightarrow \mu^+ \mu^+) \approx \text{BR}(\Phi^{++} \rightarrow \tau^+ \tau^+) \approx \text{BR}(\Phi^{++} \rightarrow \mu^+ \tau^+) \approx 1/3$ . Therefore this scenario is predictive and testable at LHC experiments.

The production process (1) has been studied before in various theory papers. In this work we first carry out a pure Monte Carlo study of the signal and background processes in the environment of LHC detectors. After that we improve our analyses by adding particle reconstruction efficiencies and Gaussian distortion functions for particle momentas and  $E_T^{\text{miss}}$ . Those mimic the detector inefficiency effects at the Monte Carlo level. We believe that those effects help us to estimate the realistic mass reach of the LHC detectors to the process under study.

In our study the new results are the following. For the signal reconstruction we use new criteria, such as equality of invariant masses of positively and negatively charged leptons together with total  $\Sigma p_T$  cut for all leptons, which allows us to achieve better reconstruction efficiencies compared to the standard cuts. We also reconstruct tau lepton final states with more than one  $\tau$ , which has not done before in this context. As all the SM background can be eliminated in the case of this process, correct statistical analyses of the results in the limit of no background is an important aspect of our study. For the discovery criteria we have used the Log-Likelihood Ratio (LLR) statistical method to demand  $5\sigma$  discovery potential to be bigger than 95% ( $1 - \text{CL}_{s+b} > 0.95$ ). Our results are optimized for the discovery of process (1) with the lowest possible LHC luminosity. The pure Monte Carlo study shows that  $\Phi^{++}$  up to the mass 300 GeV is reachable in the first year of LHC ( $L = 1 \text{ fb}^{-1}$ ) and  $\Phi^{++}$  up to the mass 800 GeV is reachable for the luminosity  $L = 30 \text{ fb}^{-1}$ . Including the Gaussian measurement errors in the Monte Carlo the corresponding mass reaches become 250 GeV and 700 GeV, respectively. The errors of our estimates of the required luminosity for discovery depend strongly on the size of statistical Monte Carlo sample of the background processes.

The paper is organized as follows. In Section 2 we present the collider phenomenology of triplet Higgs boson and relate collider observables to neutrino mass measurements. In Section 3 we discuss the Monte Carlo produced signal and background processes. In Section 4 we present the details of reconstruction and analysis procedure and results. Detector effects are discussed in Section 5. Finally we conclude in Section 6.

## 2. Neutrino masses and collider phenomenology

In this work we consider little Higgs scenarios in which, due to the breaking of global symmetry protecting the SM Higgs boson mass, the spectrum of the model contains also a pseudo Goldstone boson with the  $SU(2)_L \times U(1)_Y$  quantum numbers  $\Phi \sim (3, 2)$  [15,22]. Although  $\Phi$  is predicted to be heavier than the SM Higgs boson, the little Higgs philosophy implies that its mass could be  $\mathcal{O}(1)$  TeV [1]. Due to the specific quantum numbers the triplet Higgs boson couples only to the left-chiral lepton doublets  $L_i \sim (2, -1)$ ,  $i = e, \mu, \tau$ , via the Yukawa interactions given by

$$L = i\bar{L}_i^c \tau_2 Y^{ij} (\tau \cdot \Phi) L_j + \text{h.c.}, \quad (2)$$

where  $Y_{ij}$  are the Majorana Yukawa couplings. The interactions (2) induce lepton flavour violating decays of charged leptons which have not been observed. The most stringent constraint on the Yukawa couplings comes from the upper limit on the tree-level decay  $\mu \rightarrow eee$  and is<sup>1</sup>  $Y_{ee} Y_{e\mu} < 3 \times 10^{-5} (\text{M}/\text{TeV})^2$  [18,23]. Experimental bounds on the tau Yukawa couplings are much less stringent. In our collider studies we take  $Y_{\tau\tau} = 0.01$  and rescale other Yukawa couplings accordingly. In particular, hierarchical light neutrino masses imply  $Y_{ee}, Y_{e\mu} \ll Y_{\tau\tau}$  consistently with the direct experimental bounds.

According to Eq. (2), the neutral component of the triplet Higgs boson  $\Phi^0$  couples to the left-handed neutrinos with the same strength as  $\Phi^{++}$  couples to the charged leptons. If  $\Phi^0$  acquires a vev  $v_\Phi$ , non-zero Majorana masses are generated for the left-handed neutrinos [13,14]. Non-zero neutrino masses and mixing is presently the only experimentally verified signal of new physics

<sup>1</sup> In little Higgs models with  $T$ -parity there exist additional sources of flavour violation from the mirror fermion sector [24,25].

beyond the SM. In the triplet neutrino mass mechanism the neutrino masses are given by

$$(m_\nu)_{ij} = Y_{ij} v_\phi. \quad (3)$$

We assume that the smallness of neutrino masses is explained by the smallness of  $v_\phi$ . In a realistic scenario massless Majoron, the Goldstone boson of broken lepton number, must be avoided. This is achieved by an explicit coupling of  $\Phi$  to the SM Higgs doublet  $H$  via  $\mu\Phi^0 H^0 H^0$  [14], where  $\mu$  has a dimension of mass. If  $\mu \sim M_\phi$ , in the concept of seesaw [26] the smallness of neutrino masses is attributed to the very high scale of triplet mass  $M_\phi$  because  $v_\phi = \mu v^2 / M_\phi^2$ , where  $v = 174$  GeV. However, in the little Higgs models the triplet mass scale  $\mathcal{O}(1)$  TeV alone cannot suppress  $v_\phi$ . Therefore in this model  $\mu \ll M_\phi$ , which can be achieved, for example, via shining of explicit lepton number violation from extra dimensions as shown in Refs. [27,28], or if the triplet is related to the Dark Energy of the Universe [29,30]. Models with additional (approximate)  $T$ -parity [22] make the smallness of  $v_\phi$  technically natural. However, if the  $T$ -parity is exact,  $v_\phi$  must vanish. In this work we do not consider the naturalness criteria and assume that the above described neutrino mass scenario is realized in nature. In that case  $Y v_\phi \sim \mathcal{O}(0.1)$  eV while the Yukawa couplings  $Y$  can be on the order of charged lepton Yukawa couplings of the SM. As a result, the branching ratio of the decay  $\Phi \rightarrow WW$  is negligible. We also remind that  $v_\phi$  contributes to the SM oblique corrections, and the precision data fit  $\hat{T} < 2 \times 10^{-4}$  [31] sets an upper bound  $v_\phi \leq 1.2$  GeV on that parameter.

Notice the particularly simple connection between the flavour structure of light neutrinos and the Yukawa couplings of the triplet via Eq. (3). Therefore, independently of the overall size of the Yukawa couplings, one can predict the leptonic branching ratios of the triplet from neutrino oscillations. For the normally hierarchical light neutrino masses neutrino data implies negligible  $\Phi$  branching fractions to electrons and  $\text{BR}(\Phi^{++} \rightarrow \mu^+ \mu^+) \approx \text{BR}(\Phi^{++} \rightarrow \tau^+ \tau^+) \approx \text{BR}(\Phi^{++} \rightarrow \mu^+ \tau^+) \approx 1/3$ . Those are the final state signatures predicted by the triplet neutrino mass mechanism for collider experiments.

At LHC  $\Phi^{++}$  can be produced singly and in pairs. The cross section of the single  $\Phi^{++}$  production via the  $WW$  fusion process [18]  $qq \rightarrow q'q'\Phi^{++}$  scales as  $\sim v_\phi^2$ . In the context of the littlest Higgs model this process, followed by the decays  $\Phi^{++} \rightarrow W^+W^+$ , was studied in Refs. [5,7,32]. The detailed ATLAS simulation of this channel shows [32] that in order to observe an 1 TeV  $\Phi^{++}$ , one must have  $v_\phi > 29$  GeV. This is in conflict with the precision physics bound  $v_\phi \leq 1.2$  GeV as well as with the neutrino data. Therefore the  $WW$  fusion channel is not experimentally promising for the discovery of doubly charged Higgs.

On the other hand, the Drell–Yan pair production process  $pp \rightarrow \Phi^{++}\Phi^{--}$  is not suppressed by any small coupling and its cross section is known up to next to leading order [19] (possible additional contributions from new physics such as  $Z_H$  are strongly suppressed and we neglect those effects here). Followed by the lepton number violating decays  $\Phi^{\pm\pm} \rightarrow \ell^\pm \ell^\pm$ , this process allows to reconstruct  $\Phi^{\pm\pm}$  invariant mass from the same charged leptons rendering the SM background to be very small in the signal region. If one also assumes, as we do in this work, that neutrino masses come from the triplet Higgs interactions, one fixes the  $\Phi^{\pm\pm}$  leptonic branching ratios. This allows to test the triplet neutrino mass model at LHC.

### 3. Monte Carlo simulation of the signal and backgrounds

The production of the doubly-charged Higgs is implemented in the PYTHIA Monte Carlo generator [33]. The final and initial state interactions and hadronization have been taken into account. We have used the CTEQ5L parton distribution functions.

Table 1

Cross-sections, numbers of Monte Carlo generated events and the corresponding integrated luminosities of the generated events. For the signal events we have taken the branching ratios  $\text{BR}(\Phi^{\pm\pm} \rightarrow \mu^{\pm}\mu^{\pm}) = \text{BR}(\Phi^{\pm\pm} \rightarrow \mu^{\pm}\tau^{\pm}) = \text{BR}(\Phi^{\pm\pm} \rightarrow \tau^{\pm}\tau^{\pm}) = 1/3$

Process	Total $\sigma$ (fb)	$N$ of events generated	Corresponding luminosity (fb $^{-1}$ )
Signal			
$M_{\Phi} = 200$ GeV	7.78E+01	1.00E+05	1.28E+03
$M_{\Phi} = 500$ GeV	1.99E+00	1.00E+05	5.03E+04
$M_{\Phi} = 1000$ GeV	5.58E-02	1.00E+05	1.79E+06
Background			
$pp \rightarrow t\bar{t} \rightarrow 4\ell$	8.84E+04	2.55E+07	2.88E+02
$pp \rightarrow t\bar{t} Z$	6.50E+02	1.50E+05	2.3E+02
$pp \rightarrow ZZ$	2.12E+02	1.00E+05	4.72E+02

In the following analysis the normal hierarchy of neutrino masses and a very small value of the lowest neutrino mass is assumed. Such a model predicts that Higgs decay into electrons can be neglected and that there are three dominant decay channels for  $\Phi^{++}$  with approximately equal branching ratios:

- $\Phi^{\pm\pm} \rightarrow \mu^{\pm}\mu^{\pm}$ ,
- $\Phi^{\pm\pm} \rightarrow \mu^{\pm}\tau^{\pm}$ ,
- $\Phi^{\pm\pm} \rightarrow \tau^{\pm}\tau^{\pm}$ .

We have studied only pair production of doubly charged Higgs due to the reasons pointed out above.  $\Phi^{\pm\pm}$  pair decay products can combine to five different  $\tau$  and  $\mu$  combinations:  $4\mu$ ,  $3\mu 1\tau$ ,  $2\mu 2\tau$ ,  $1\mu 3\tau$  and  $4\tau$ . Before reaching the detector,  $\tau$  decays into an  $e$ ,  $\mu$  or a hadronic jet (marked as  $j$  below) with branching ratios of 0.18, 0.17 and 0.65, respectively [34].  $\tau$  hadronic jets and  $\mu$ 's are well visible and reconstructible in detector. The reconstruction of an energetic  $\tau$  from electron decay is sensitive to detector effects, involving sophisticated background processes [35]. In the current analyses we will neglect this channel, which will cause 31% loss of the total signal. Such loss is still sufficiently low and can be considered acceptable. Table 1 gives the cross sections and the Monte Carlo generated event numbers in our study.

The signatures of  $\Phi$  decay are very clean due to (i) high transfer momentum of the decay products, (ii) lepton number violation and (iii) pair production of  $\Phi$ . The Standard Model particles are lighter than  $\Phi$ , so the background  $\mu$ 's and  $\tau$ 's must have smaller transverse energy and they do not produce an invariant mass peak in  $\mu^+\mu^+$ ,  $\mu^+\tau^+$ ,  $\tau^+\tau^+$ , final states. The present lower bound for the invariant mass of  $\Phi$  is set by Tevatron to  $M_{\Phi} \geq 136$  GeV [36,37]. In our study, four-lepton background processes with reasonable cross sections and high  $p_T$  leptons arise from three Standard Model processes

- $pp \rightarrow t\bar{t}$ ,
- $pp \rightarrow t\bar{t} Z$ ,
- $pp \rightarrow ZZ$ .

PYTHIA was used to generate  $t\bar{t}$  and  $ZZ$  background ( $t\bar{t}$  is forced to decay to  $WWb\bar{b}$  and  $W$  leptonically). The CTEQ5L parton distribution functions were used. CompHEP was used to

generate the  $Zt\bar{t}$  background via its PYTHIA interface [38,39]. All the datasets were generated in Baltic Grid. In addition to background processes shown in Table 1, some other four-lepton background processes exist involving  $b$ -quarks in the final state (for example,  $pp \rightarrow b\bar{b}$ ). As such processes are very soft, it is possible to use the effective tagging methods [40] and totally eliminate this soft background [41]. Also, we do not consider possible background processes from the physics beyond the Standard Model.

#### 4. Reconstruction and analysis of the Monte Carlo data

To study the feasibility of detecting the signal over background, we have to work with five possible reconstruction channels according to the following final states.

- $\Phi^{++}\Phi^{--} \rightarrow 4\mu$ : The cleanest and most simple channel.
- $\Phi^{++}\Phi^{--} \rightarrow 3\mu 1\tau$ : The channel is easily reconstructable using an assumption that the neutrino originating from the  $\tau$  decay is collinear with  $\tau$ -jet and gives majority to the missing transverse energy ( $E_T^{\text{miss}}$ ).
- $\Phi^{++}\Phi^{--} \rightarrow 2\mu 2\tau$ : The signature can be reconstructed using the same assumptions for both  $\tau$ -neutrinos. The whole  $E_T^{\text{miss}}$  vector has to be used here, while in the previous channel only one component was needed.
- $\Phi^{++}\Phi^{--} \rightarrow 1\mu 3\tau$ : The channel can be reconstructed theoretically relying on an additional requirement that the two Higgs bosons have equal invariant masses. However, the reconstruction is very sensitive to the experimental accuracy of  $E_T^{\text{miss}}$  determination.
- $\Phi^{++}\Phi^{--} \rightarrow 4\tau$ : The channel cannot be reconstructed (and triggered by the single muon trigger).

First, we apply general detector related cut-offs for the Monte Carlo generated data. Generated particles were reconstructed within the pseudorapidity region  $|\eta| < 2.4$  and with transverse momentum higher than 5 GeV. These are the natural restrictions of the CMS and ATLAS detectors at the LHC. Only the pseudorapidity region  $|\eta| < 2.4$  is reachable for the detector and only the events with  $p_T > 5$  GeV are typically triggered. These restrictions suppress mainly the soft Standard Model background. The efficiency of lepton reconstruction and charge identification rate are very high, we use the values 0.9 and 0.95, respectively [42].

The invariant mass of two like-sign  $\mu$ 's and/or  $\tau$ 's are calculated using equation:

$$(m_I^{\pm\pm})^2 = (p_1^\pm + p_2^\pm)^2, \quad (4)$$

where  $p_{1,2}$  is the  $\mu$  or  $\tau$  4-momentum. Since the like-sign signal of  $\mu$ 's or  $\tau$ 's originate from a doubly charged Higgs boson, the invariant mass peak measures the mass of doubly charged Higgs,  $m_I = M_\Phi$ .  $4\mu$  final state allows to obtain invariant masses directly from Eq. (4). In channels involving one or several  $\tau$ 's, which are registered as  $\tau$ -jets or secondary  $\mu$ 's (marked as  $\mu'$  below), the momenta of jets has to be corrected according to the equation system:

$$\mathbf{p}_\tau^i = k^i \mathbf{p}_{\text{jet}}^i, \quad (5)$$

$$\mathbf{p}_{T\text{miss}} = \sum_i \mathbf{p}_{T\nu}^i, \quad (6)$$

$$M_{\Phi^{++}} = M_{\Phi^{--}}, \quad (7)$$

Table 2

Probabilities of all possible decay chains for  $\Phi$  pairs in our scenario. “x” in the table marks  $\tau$  or, after  $\tau$  decay,  $\tau$ -jet. The reconstructed signatures are marked in bold, the remaining signatures were not reconstructed. After omitting the channels that include  $\tau \rightarrow e$  decay, 69% of the total signal is left. In total 64% of the signal has been reconstructed

Decay channel	After Higgs decay ( $x = \tau$ )	After $\tau$ decay ( $x = \text{jet}_\tau$ )				
		0 ( $\tau \rightarrow \mu'$ )	1 ( $\tau \rightarrow \mu'$ )	2 ( $\tau \rightarrow \mu'$ )	3 ( $\tau \rightarrow \mu'$ )	4 ( $\tau \rightarrow \mu'$ )
$2\Phi \rightarrow 4\mu$	0.1111	<b>0.1111</b>	<b>0.0377</b>	<b>0.0107</b>	0.0012	0.0001
$2\Phi \rightarrow 3\mu 1x$	0.2222	<b>0.1443</b>	<b>0.0736</b>	<b>0.0125</b>	0.0014	
$2\Phi \rightarrow 2\mu 2x$	0.3333	<b>0.1407</b>	<b>0.0478</b>	0.0054		
$2\Phi \rightarrow 1\mu 3x$	0.2222	<b>0.0610</b>	0.0207			
$2\Phi \rightarrow 4x$	0.1111	0.0198				
Sum	1.0	<b>0.64</b> + 0.05				

where  $i$  counts  $\tau$ 's,  $\mathbf{p}$  marks 3-momentum,  $\mathbf{p}_{T\nu}$  is the vector of transverse momentum of the produced neutrinos,  $\mathbf{p}_{T\text{miss}}$  is the vector of missing transverse momentum (measured by the detector) and  $k_i > 1$  are positive constants. Eq. (5) describes the standard approximation that the decay products of a heavily boosted  $\tau$  are collinear [42]. Eq. (6) assumes missing transverse energy only to be comprised of neutrinos from  $\tau$  decays. In general, it is not a high-handed simplification, because the other neutrinos in the event are much less energetic and the detector error of  $E_T^{\text{miss}}$  is order of magnitude smaller [43]. Using the first two formulas, it is possible to reconstruct up to two  $\tau$ 's per event. Additional requirement of Eq. (7) allows to reconstruct the third  $\tau$  per pair event, although very low measurement errors are needed.

A significant fraction of  $\tau$ 's (0.18) decay into  $\mu'$ 's that cannot be distinguished from primary  $\mu$ 's in the detector. Still, if reconstructed invariant masses of  $\Phi^{++}$  and  $\Phi^{--}$  are considerably different, we can suspect that one or several  $\mu$ 's originate from  $\tau$  decays. In such case we can again use Eqs. (5)–(7) to correct the 4-momenta of decay products. When only one secondary muon is present,  $E_T^{\text{miss}}$  points into the same direction as its  $p_T$ . Otherwise  $E_T^{\text{miss}}$  is a superposition of neutrino transverse momenta. Such correction tightens the invariant mass peak of the signal and does not produce any artificial background.

The occurrence probability of different reconstruction channels are presented in Table 2. The second column shows probabilities of Higgs decay to  $N$   $\mu$ 's and  $M$   $\tau$ 's. Next columns describe the final state after  $\tau$  decay to  $\mu'$ 's and/or jets. Different columns mark the number of secondary  $\mu$ 's and the rows designate  $\tau$ -jets in the detector recordings. The events having at least one  $\tau \rightarrow e$  in a final state are omitted in our analysis, as well as events with  $M > 3$  or  $N(\mu') > 2$ . The proportions of reconstructible signatures are marked in a bold-face. The table shows that 0–3 jet channels together with  $\mu$  correction are almost equally important and overall reconstructible channels comprise 64% of total events.

A clear signal extraction from the Standard Model background can be achieved using a set of selection rules imposed on a reconstructed event in the following order.

- S1: events with at least 2 positive and 2 negative muons or jets which have  $|\eta| < 2.4$  and  $p_T > 5$  GeV are selected.
- S2:  $\sum p_T$  (scalar) sum of 2 most energetic positive and negative  $\mu$ 's or  $\tau$ -jets has to be bigger than a certain value (depending on Higgs mass).
- S3:  $Z$ -tagging—if invariant mass of the pair of opposite charged  $\mu$ 's or  $\tau$ -jets is nearly equal to  $Z$  mass (85–95 GeV), then the particles are eliminated from the analysis.

- S4: as  $\Phi$ 's are produced in pairs, the reconstructed invariant masses (in one event) have to be equal. We have used the condition

$$0.8 < m_I^{++}/m_I^{--} < 1.2. \tag{8}$$

If the invariant masses satisfy the condition then we include them to the histogram, otherwise we suspect that some  $\mu$ 's may originate from  $\tau$  decay, and make an attempt to find corrections to their momenta according to the method described above.

The rule S1 is an elementary detector trigger. S2, performing scalar sum of  $p_T$ , is an untraditional cut. The advantage compared to the widely used  $p_T$  cut for a single particle is clearly visible from Fig. 1. The left panel shows that the maximum of Higgs line reaches clearly out of the background while on the right panel the maximum is deeply inside the background.

Z-tagging in S3 suppresses  $pp \rightarrow ZZ$  and  $pp \rightarrow t\bar{t}Z$  background. S4 is based on the equality of the invariant masses of like-signed  $\mu$ 's or  $\tau$ 's. Fig. 2 gives a clear picture of the behavior of signal and background for the S4 selection rule. Naturally, some freedom is needed due to the  $\Phi$

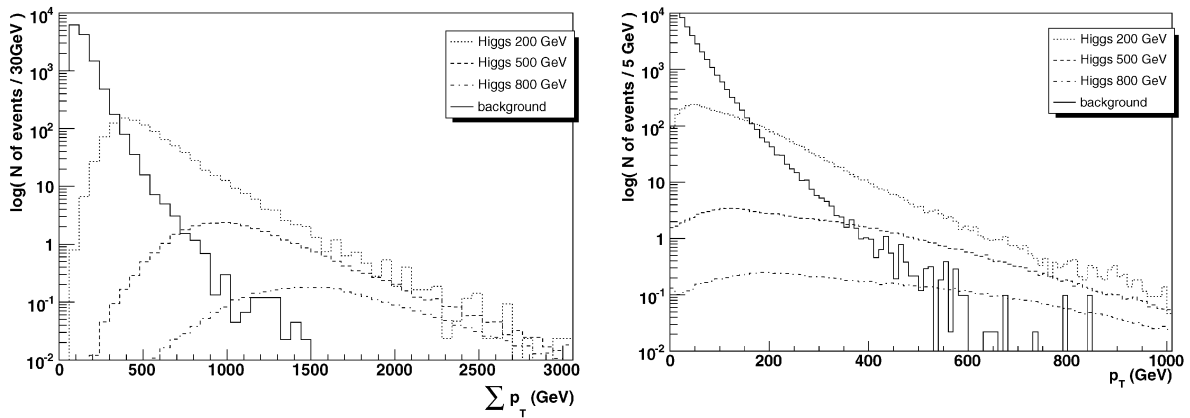


Fig. 1. The left panel shows the distribution of events according to scalar sum of 2 most energetic (highest  $p_T$ ) positively and 2 most energetic negatively charged muons or jets ( $\sum p_T$ ). The right panel shows the distribution of events considering traditional  $p_T$  cut for single particles. Both figures correspond to luminosity  $L = 30 \text{ fb}^{-1}$ .

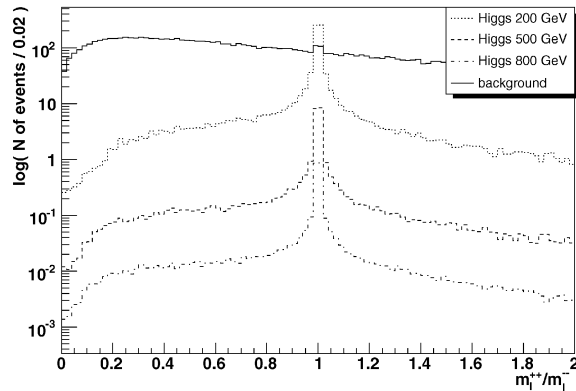


Fig. 2. Distribution of events according to the ratio of reconstructed invariant masses ( $m_{\Phi^{++}}/m_{\Phi^{--}}$ ) (no other cuts are applied). The figure corresponds to luminosity  $L = 30 \text{ fb}^{-1}$ .

Table 3

Optimal  $\sum p_T$  cut for different Higgs masses and the corresponding minimal discovery luminosities: the lower ( $L_{\min}$ ) corresponds to the generated background in our analyses and the higher ( $L_{\max}$ ) corresponds to 95% upper limit of the background error

Mass of $\Phi$ (GeV)	200	300	400	500	600	700	800	900	1000
Optimal $\sum p_T$ for S2 (GeV)	300	400	600	700	860	860	860	860	860
MC $L_{\min}$ ( $\text{fb}^{-1}$ )	0.25	0.93	2.0	3.6	8	17	34	62	120
MC $L_{\max}$ ( $\text{fb}^{-1}$ )	0.26	1.03	3.1	7.0	17	38	77	160	320

decay width and experimental errors of the detector. We require that the ratio  $m_I^{++}/m_I^{--}$  has to be in the region from 0.8 to 1.2.

While the selection rules S1, S3 and S4 are independent of the Higgs mass, the selection rule S2 ( $\sum p_T$  cut) has to be optimized for a certain Higgs mass value. The cut may be set to a very high value which eliminates all background events, but inevitable loss in signal may postpone the discovery of new physics at LHC. Thus it is natural to take the minimal discovery luminosity ( $L_{\min}$ ) as the optimization criteria. Looking for a cut value that enables to make a discovery with the lowest luminosity, we are dealing with small signal and background expectations by definition. Simple significance estimators cannot be exploited here. We have used the log-likelihood ratio (LLR) statistical method [44,45] to demand  $5\sigma$  discovery potential to be bigger than 95% ( $1 - \text{CL}_{s+b} > 0.95$ ) as for a discovery criteria. This is a rather strong requirement, because it allows to make a discovery (meaning the fluctuation of background may mimic the outcome of an experiment with probability less than  $2.9 \times 10^{-7}$  ( $5\sigma$ )) during the specified luminosity with a probability of 95% (if  $s + b$  hypothesis is correct). The widely used convention, that significance should exceed five, gives only 50% discovery potential in Gaussian limit and diminishes to very small values when background approaches zero.

The best value for S2 cut does depend on  $M_\Phi$  but is not too sensitive to it. Typically the  $\sum p_T$  can be assigned a value with a precision of 100 GeV while affecting the minimum luminosity by only a couple of percent. In the Table 3 the approximated middle point of this value is given. As the best S2 cut is very strong, it suppresses almost entirely the generated background (being combined with the other selection rules). For Higgs masses above 500 GeV the background is totally suppressed and the discovery potential criteria meets the requirement for 3 signal events (6 invariant masses). Nevertheless we cannot infer that the background is really zero in nature. To estimate the statistical error due to final number of generated background events we have found 95% upper limit of background according to Poisson statistics (Table 4, in brackets). Using this limit in LLR analysis we get much higher luminosities for discovery. Even a very small background expectancy ( $b = 0.01$ ) gives some possibility to have one ( $9.9 \times 10^{-3}$ ) or two ( $4.9 \times 10^{-5}$ ) background events in the experiment and these outcomes cannot be interpreted as discovery anymore. This phenomenon shifts the minimal required luminosity to much higher values denoted as  $L_{\max}$  in Table 3.

An example of invariant mass distribution after applying selection rules are shown in Fig. 3 for  $M_\Phi = 500$  GeV. A tabulated example is given for  $M_\Phi = 200, 500, 800$  GeV in Table 4 corresponding to the luminosity  $L = 30 \text{ fb}^{-1}$ . The strength of S2 cut is clearly visible: almost no decrease in signal while the number of the background events descends close to final minimum value. A peculiar behavior of S4—reducing the background, while also increasing the signal in its peak—is the effect of applying the  $\tau \rightarrow \mu'$  correction method described above.

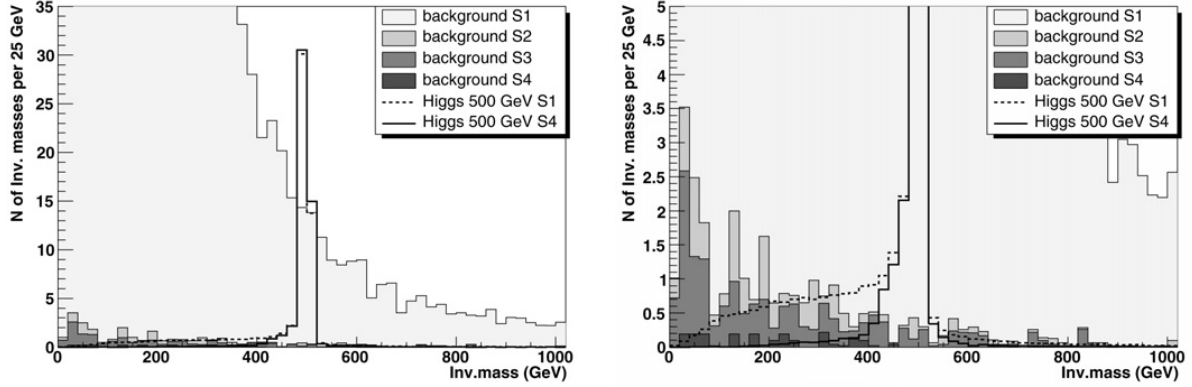


Fig. 3. Distribution of invariant masses after applying selection rules (S1–S4) for Higgs  $M_\phi = 500$  GeV and the Standard Model background ( $L = 30 \text{ fb}^{-1}$ ). The histogram in the right panel is a zoom of the left histogram to illustrate the effects of the selection rules S2–S4.

Table 4

Effectiveness of the selection rules for the background and signal. All event numbers in the table are normalized for  $L = 30 \text{ fb}^{-1}$ . The numbers in brackets mark errors at 95% confidence level for Poisson statistics. The signal increases after S4 due to the reconstructed  $\tau \rightarrow \mu'$  decays

Process	$N$ of invariant masses				
	$N$ of $\Phi$	S1	S2	S3	S4
Energy range 150–250 GeV					
$M_\phi = 200$ GeV	4670	1534	1488	1465	1539
$t\bar{t} \rightarrow 4\ell$	–	1222 (168)	172 (8.5)	134 (6.9)	17.6 (3.7)
$t\bar{t}Z$	–	21.3 (4.0)	15.5 (1.0)	6.3 (1.2)	2.2 (1.1)
$ZZ$	–	95.0 (12.0)	22.5 (0.7)	9.8 (0.5)	1.7 (0.2)
Energy range 375–625 GeV					
$M_\phi = 500$ GeV	119.2	48.4	47.5	46.8	49.5
$t\bar{t} \rightarrow 4\ell$	–	178 (28)	2.1 (0.9)	1.65 (0.87)	0.10 (0.35)
$t\bar{t}Z$	–	6.6 (1.7)	2.3 (1.0)	1.0 (1.0)	0.00 (0.1)
$ZZ$	–	9.4 (2.9)	1.4 (0.2)	0.68 (0.19)	0.08 (0.09)
Energy range 600–1000 GeV					
$M_\phi = 800$ GeV	11.67	5.05	5.00	4.92	5.21
$t\bar{t} \rightarrow 4\ell$	–	77 (12)	0.00 (0.22)	0.00 (0.22)	0.00 (0.07)
$t\bar{t}Z$	–	2.6 (1.2)	0.39 (0.4)	0.39 (0.4)	0.00 (0.1)
$ZZ$	–	2.5 (0.8)	0.34 (0.16)	0.17 (0.09)	0.00 (0.02)

## 5. Including measurement errors to Monte Carlo

In this section we make an attempt to estimate simplified detector effects at the level of Monte Carlo analyses. In order to do that we have added overall detection efficiencies for the Monte Carlo generated  $\mu$ 's and  $\tau$ -jets—0.98 and 0.6, respectively. Additionally, we applied Gaussian distortion functions to Monte Carlo produced data for  $\mu$ 's,  $\tau$ -jets and  $E_T^{\text{miss}}$  which were used to alter randomly those quantities in the analysis. Although the precision of  $\mu$  detection is sensitive to  $p_T$  of  $\mu$  and  $|\eta|$  we use the mean values for a rough estimation. We make the following assumptions based on [41–43].

Table 5

Optimal  $\sum p_T$  cuts and minimal discovery luminosities for different Higgs masses when the estimates of detector measurement errors are taken into account. Two boundaries for the minimal luminosity are given: the lower ( $L_{\min}$ ) corresponds to the generated background and the higher ( $L_{\max}$ ) corresponds to 95% upper limit of the background error

Mass of $\Phi$ (GeV)	200	300	400	500	600	700	800	900	1000
Optimal $\sum p_T$ for S2 (GeV)	300	400	600	700	860	860	860	860	860
Det Eff $L_{\min}$ ( $\text{fb}^{-1}$ )	0.526	1.20	3.0	6.6	15	30	60	111	200
Det Eff $L_{\max}$ ( $\text{fb}^{-1}$ )	0.546	2.19	6.5	16.6	39	86	190	420	900

Table 6

The importance of reconstruction channels at Monte Carlo level and considering detector efficiency effects

Decay channel	Percentage of the channel after reconstruction				
	$4\mu$	$3\mu 1j$	$2\mu 2j$	$1\mu 3j$	$\tau \rightarrow \mu$ correction
Monte Carlo	21	28	26	9	16
MC + efficiencies	38	25	12	1	24

The direction of muon ( $\tau$ -jet) is altered with the Gaussian distribution: mean  $\mu = 0.0005$  (0.031) and variance  $\sigma^2 = 0.003$  (0.017). The transverse momentum is altered according to the  $p_{T,\text{rec}}/p_{T,\text{Monte Carlo}}$  Gaussian distribution: mean  $\mu = 1$ . (0.897) and variance  $\sigma^2 = 0.03$  (0.089). Both components of missing transverse energy are altered independently according to the Gaussian distribution (mean  $\mu = 0$  GeV and variance  $\sigma^2 = 25$  GeV) by adding the piece to its Monte Carlo value.

The result of such a distortion is a decrease in both signal and background approximately by factor two (Table 5). As the background and the signal decrease proportionally, the luminosity needed for discovery roughly doubles. Remarkably the optimized S2 cut value does not change significantly. The proportion of the reconstruction channels in the total analysis has changed remarkably as shown in Table 6. The reason is clearly the small detection efficiency of  $\tau$ -jets. The  $1\mu 3j$  channel comprises only 1% of the total signal if the detector effects are considered, while in the pure Monte Carlo analysis it forms 9%. The additional possible detector effects make the  $\tau \rightarrow \mu$  correction even more relevant.

## 6. Conclusions and outlook

We have studied possible direct test of little Higgs scenarios which light particle spectrum includes a triplet scalar multiplet at LHC experiments. We have investigated the Drell–Yan pair production of the doubly charged Higgs boson and its subsequent leptonic decays. In addition to solving the little hierarchy problem, this scenario can also explain the origin of non-zero neutrino masses and mixing via the triplet Higgs neutrino mass mechanism. Simple connection between the observed neutrino mixing and triplet Yukawa couplings allows us to predict the leptonic branching ratios of the triplet. Thus the experimental signatures of the model do not depend on the size of the triplet Yukawa couplings allowing direct tests of this scenario at LHC.

In our analyses we have considered four  $\mu$  and/or  $\tau$  final states including up to 3 tau leptons. We propose four selection rules to achieve the optimized signal and background ratio. As the  $\Phi^{++}$  decays are lepton number violating, we have shown that the background can be practically eliminated. In such an unusual situation we have used the LLR statistical method to demand  $5\sigma$  discovery potential to be bigger than 95% ( $1 - \text{CL}_{s+b} > 0.95$ ) as the discovery criterion.

The results of optimized cut values are presented in Table 3. Considering the pure Monte Carlo study,  $\Phi^{++}$  up to the mass 300 GeV can be discovered in the first year of LHC ( $L = 1 \text{ fb}^{-1}$ ) and  $\Phi^{++}$  up to the mass 800 GeV can be discovered for the integrated luminosity  $L = 30 \text{ fb}^{-1}$ . Including particle reconstruction efficiencies as well as Gaussian distortion functions for the particle momentas and missing energy which mimic detector inefficiencies at Monte Carlo level, our results show that  $\Phi^{++}$  can be discovered up to the mass 250 GeV in the first year of LHC and 700 GeV mass is reachable for the integrated luminosity  $L = 30 \text{ fb}^{-1}$ .

For further studies of this scenario at LHC progress can be made both physics-wise as well as technically. Full simulations of the detector effects are needed which also include the electron, muon and tau final states. For better determination of statistical errors coming from the background studies bigger SM background datasets must be produced. This requires huge computing resources. If these goals can be achieved, the proposed phenomenology opens a new window to study the neutrino properties at colliders. In addition to the considerations in this paper, one can determine at LHC experiments the hierarchy (normal or inverse) of light neutrino mass spectrum, and to estimate the two Majorana phases which are not measurable in neutrino oscillation experiments [46].

## Acknowledgements

We thank the Estonian Science Foundation for the Grant No. 6140. The work described in this paper was also supported by the European Union through the FP6-2004-Infrastructures-6-contract No. 026715 project “BalticGrid”.

## References

- [1] G.F. Giudice, C. Grojean, A. Pomarol, R. Rattazzi, hep-ph/0703164.
- [2] N. Arkani-Hamed, A.G. Cohen, H. Georgi, Phys. Rev. Lett. 86 (2001) 4757, hep-th/0104005.
- [3] H.C. Cheng, C.T. Hill, S. Pokorski, J. Wang, Phys. Rev. D 64 (2001) 065007, hep-th/0104179.
- [4] N. Arkani-Hamed, A.G. Cohen, H. Georgi, Phys. Lett. B 513 (2001) 232, hep-ph/0105239.
- [5] T. Han, H.E. Logan, B. McElrath, L.T. Wang, Phys. Rev. D 67 (2003) 095004, hep-ph/0301040.
- [6] W. Kilian, J. Reuter, Phys. Rev. D 70 (2004) 015004, hep-ph/0311095.
- [7] T. Han, H.E. Logan, L.T. Wang, JHEP 0601 (2006) 099, hep-ph/0506313.
- [8] J. Lee, hep-ph/0504136.
- [9] T. Han, H. Logan, B. Mukhopadhyaya, R. Srikanth, Phys. Rev. D 72 (2005) 053007, hep-ph/0505260.
- [10] F. del Aguila, M. Masip, J.L. Padilla, Phys. Lett. B 627 (2005) 131, hep-ph/0506063.
- [11] S.R. Choudhury, N. Gaur, A. Goyal, Phys. Rev. D 72 (2005) 097702, hep-ph/0508146.
- [12] A. Abada, G. Bhattacharyya, M. Losada, Phys. Rev. D 73 (2006) 033006, hep-ph/0511275.
- [13] J. Schechter, J.W.F. Valle, Phys. Rev. D 22 (1980) 2227.
- [14] E. Ma, U. Sarkar, Phys. Rev. Lett. 80 (1998) 5716, hep-ph/9802445.
- [15] N. Arkani-Hamed, A.G. Cohen, E. Katz, A.E. Nelson, JHEP 0207 (2002) 034, hep-ph/0206021.
- [16] J.F. Gunion, C. Loomis, K.T. Pitts, in: the Proceedings of 1996 DPF/DPB Summer Study on New Directions for High-Energy Physics (Snowmass 96), Snowmass, Colorado, 25 June–12 July 1996, pp. LTH096, hep-ph/9610237.
- [17] J.F. Gunion, J. Grifols, A. Mendez, B. Kayser, F.I. Olness, Phys. Rev. D 40 (1989) 1546.
- [18] K. Huitu, J. Maalampi, A. Pietila, M. Raidal, Nucl. Phys. B 487 (1997) 27, hep-ph/9606311.
- [19] M. Muhlleitner, M. Spira, Phys. Rev. D 68 (2003) 117701, hep-ph/0305288.
- [20] A.G. Akeroyd, M. Aoki, Phys. Rev. D 72 (2005) 035011, hep-ph/0506176.
- [21] T. Rommerskirchen, T. Hebbeker, J. Phys. G 33 (2007) N47.
- [22] S. Chang, JHEP 0312 (2003) 057, hep-ph/0306034.
- [23] C.X. Yue, S. Zhao, hep-ph/0701017.
- [24] S.R. Choudhury, A.S. Cornell, A. Deandrea, N. Gaur, A. Goyal, Phys. Rev. D 75 (2007) 055011, hep-ph/0612327.
- [25] M. Blanke, A.J. Buras, B. Duling, A. Poschenrieder, C. Tarantino, hep-ph/0702136.

- [26] P. Minkowski, Phys. Lett. B 67 (1977) 421;  
M. Gell-Mann, P. Ramond, R. Slansky, in: P. Van Nieuwenhuizen, D. Freedman (Eds.), Proceedings of the Supergravity Stony Brook Workshop, New York, 1979, North-Holland, Amsterdam;  
T. Yanagida, in: A. Sawada, A. Sugamoto (Eds.), Proceedings of the Workshop on Unified Theories and Baryon Number in the Universe, Tsukuba, Japan 1979, KEK Report No. 79-18, Tsukuba;  
R. Mohapatra, G. Senjanovic, Phys. Rev. Lett. 44 (1980) 912.
- [27] E. Ma, M. Raidal, U. Sarkar, Phys. Rev. Lett. 85 (2000) 3769, hep-ph/0006046.
- [28] E. Ma, M. Raidal, U. Sarkar, Nucl. Phys. B 615 (2001) 313, hep-ph/0012101.
- [29] E. Ma, U. Sarkar, Phys. Lett. B 638 (2006) 356, hep-ph/0602116.
- [30] N. Sahu, U. Sarkar, hep-ph/0701062.
- [31] G. Marandella, C. Schappacher, A. Strumia, Phys. Rev. D 72 (2005) 035014, hep-ph/0502096.
- [32] G. Azuelos, et al., Eur. Phys. J. C 39S2 (2005) 13, hep-ph/0402037.
- [33] T. Sjostrand, P. Eden, C. Friberg, L. Lonnblad, G. Miu, S. Mrenna, E. Norrbin, Comput. Phys. Commun. 135 (2001) 238, hep-ph/0010017.
- [34] W.M. Yao, et al., Particle Data Group, J. Phys. G 33 (2006) 1.
- [35] D. Acosta, et al., CMS Collaboration, The CMS Physics Technical Design Report, vol. 1, Section 10.4: Electron reconstruction and selection, CERN/LHCC vols. 2006–001, 2006. CMS TDR 8.1.
- [36] D. Acosta, et al., CDF Collaboration, Phys. Rev. Lett. 93 (2004) 221802, hep-ex/0406073.
- [37] V.M. Abazov, et al., D0 Collaboration, Phys. Rev. Lett. 93 (2004) 141801, hep-ex/0404015.
- [38] E. Boos, et al., CompHEP Collaboration, Nucl. Instrum. Methods A 534 (2004) 250, hep-ph/0403113.
- [39] A.S. Belyaev, et al., hep-ph/0101232.
- [40] D. Acosta, et al., CMS Collaboration, The CMS Physics Technical Design Report, vol. 1, Section 12.2: *b*-tagging tools, CERN/LHCC 2006–001, 2006. CMS TDR 8.1.
- [41] D. Acosta, et al., CMS Collaboration, The CMS Physics Technical Design Report, vol. 2, Physics Performance, J. Phys. G: Nucl. Part. Phys. 34 (2007) 995–1579.
- [42] CMS Collaboration, The Compact Muon Solenoid. Muon Technical Design Report, CERN-LHCC-97-32.
- [43] D. Acosta, et al., CMS Collaboration, The CMS Physics Technical Design Report, vol. 1, Section 11.5: Missing transverse energy, CERN/LHCC vols. 2006–001, 2006, CMS TDR 8.1.
- [44] A.L. Read, Modified frequentist analysis of search results (The CL(s) method), CERN-OPEN-2000-205.
- [45] R. Barate, et al., LEP Working Group for Higgs boson searches, Phys. Lett. B 565 (2003) 61, hep-ex/0306033.
- [46] M. Kadastik, M. Raidal, L. Rebane, in preparation.



---

ARTICLE II

---

The CMS Collaboration, 2006. CMS technical design report, volume II: Physics performance, J.Phys.G34:995-1579,2007.

Authors contribution is Section 12.2.2, "Search for final states with  $\tau$  leptons" which has been reproduced here.

Copyright (2007) IOP Journals.

# CMS Physics Technical Design Report, Volume II: Physics Performance

## The CMS Collaboration

Received 3 January 2007

Published 20 April 2007

Online at [stacks.iop.org/JPhysG/34/995](http://stacks.iop.org/JPhysG/34/995)

### Abstract

CMS is a general purpose experiment, designed to study the physics of pp collisions at 14 TeV at the Large Hadron Collider (LHC). It currently involves more than 2000 physicists from more than 150 institutes and 37 countries. The LHC will provide extraordinary opportunities for particle physics based on its unprecedented collision energy and luminosity when it begins operation in 2007.

The principal aim of this report is to present the strategy of CMS to explore the rich physics programme offered by the LHC. This volume demonstrates the physics capability of the CMS experiment. The prime goals of CMS are to explore physics at the TeV scale and to study the mechanism of electroweak symmetry breaking—through the discovery of the Higgs particle or otherwise. To carry out this task, CMS must be prepared to search for new particles, such as the Higgs boson or supersymmetric partners of the Standard Model particles, from the start-up of the LHC since new physics at the TeV scale may manifest itself with modest data samples of the order of a few  $\text{fb}^{-1}$  or less.

The analysis tools that have been developed are applied to study in great detail and with all the methodology of performing an analysis on CMS data specific benchmark processes upon which to gauge the performance of CMS. These processes cover several Higgs boson decay channels, the production and decay of new particles such as  $Z'$  and supersymmetric particles,  $B_s$  production and processes in heavy ion collisions. The simulation of these benchmark processes includes subtle effects such as possible detector miscalibration and misalignment. Besides these benchmark processes, the physics reach of CMS is studied for a large number of signatures arising in the Standard Model and also in theories beyond the Standard Model for integrated luminosities ranging from  $1 \text{ fb}^{-1}$  to  $30 \text{ fb}^{-1}$ . The Standard Model processes include QCD,  $B$ -physics, diffraction, detailed studies of the top quark properties, and electroweak physics topics such as the  $W$  and  $Z^0$  boson properties. The production and decay of the Higgs particle is studied for many observable decays, and the precision with which the Higgs boson properties can be derived is determined. About ten different supersymmetry benchmark points are analysed using full simulation. The CMS discovery reach is evaluated in the SUSY parameter space covering a large variety of decay signatures.

Furthermore, the discovery reach for a plethora of alternative models for new physics is explored, notably extra dimensions, new vector boson high mass states, little Higgs models, technicolour and others. Methods to discriminate between models have been investigated.

This report is organized as follows. Chapter 1, the Introduction, describes the context of this document. Chapters 2–6 describe examples of full analyses, with photons, electrons, muons, jets, missing  $E_T$ , B-mesons and  $\tau$ 's, and for quarkonia in heavy ion collisions. Chapters 7–15 describe the physics reach for Standard Model processes, Higgs discovery and searches for new physics beyond the Standard Model.

### Acknowledgments

This report is the result of several years of work on the preparation for physics analysis at the LHC with CMS. Subprojects in all areas were involved (Detector, PRS, Software, and Computing) in order to produce the large Monte Carlo simulation samples needed, to develop the software to analyse those samples, to perform the studies reported in this Report, and to write and review our findings.

We wish to thank, for the many useful discussions, our theory and phenomenology colleagues, in particular J Campbell, D Dominici, A Djouadi, S Heinemeyer, W Hollik, V Khoze, T Plehn, M Raidal, M Spira and G Weiglein for their contributions to this Report.

For their constructive comments and guidance, we would like to thank the CPT internal reviewers: J Alexander, J Branson, Y Karyotakis, M Kasemann and R Tenchini.

We would like to thank L Malgeri and R Tenchini for their efficient organisation of the CMS Notes.

For their patience in meeting sometimes impossible demands, we wish to thank the CMS Secretariat: K Aspola, M Azeglio, N Bogolioubova, D Denise, D Hudson, G Martin, and M C Pelloux.

We also would like to thank G Alverson and L Taylor for their invaluable technical assistance in the preparation of this manuscript.

Finally, we wish to thank the CMS management for their strong support and encouragement.

The CMS Collaboration

**The CMS Collaboration****Yerevan Physics Institute, Yerevan, ARMENIA**

G L Bayatian, S Chatrchyan, G Hmayakyan, A M Sirunyan

**Institut für Hochenergiephysik der OeAW, Wien, AUSTRIA**

W Adam, T Bergauer, M Dragicevic, J Erö, M Friedl, R Frühwirth, V Ghete, P Glaser, J Hrubec, M Jeitler, M Krammer, I Magrans, I Mikulec, W Mitaroff, T Noebauer, M Pernicka, P Porth, H Rohringer, J Strauss, A Taurok, W Waltenberger, G Walzel, E Widl, C-E Wulz

**Research Institute for Nuclear Problems, Minsk, BELARUS**

A Fedorov, M Korzhik, O Missevitch, R Zuyeski

**National Centre for Particle and High Energy Physics, Minsk, BELARUS**

V Chekhovsky, O Dvornikov, I Emeliantchik, A Litomin, V Mossolov, N Shumeiko, A Solin, R Stefanovitch, J Suarez Gonzalez, A Tikhonov

**Byelorussian State University, Minsk, BELARUS**

V Petrov

**Vrije Universiteit Brussel, Brussel, BELGIUM**

J D'Hondt, S De Weirtd, R Goorens, J Heyninck, S Lowette, S Tavernier, W Van Doninck<sup>1</sup>, L Van Lancker

**Université Libre de Bruxelles, Bruxelles, BELGIUM**

O Bouhali, B Clerbaux, G De Lentdecker, J P Dewulf, T Mahmoud, P E Marage, L Neukermans, V Sundararajan, C Vander Velde, P Vanlaer, J Wickens

**Université Catholique de Louvain, Louvain-la-Neuve, BELGIUM**

S Assouak, J L Bonnet, G Bruno, J Caudron, B De Callatay, J De Favereau De Jeneret, S De Visscher, C Delaere, P Demin, D Favart, E Feltrin, E Forton, G Grégoire, S Kalinin, D Kcira, T Keutgen, G Leibguth, V Lemaitre, Y Liu, D Michotte, O Militaru, A Ninane, S Oryn, T Pierzchala, K Piotrkowski, V Roberfroid, X Rouby, D Teysier, O Van der Aa, M Vander Donckt

**Université de Mons-Hainaut, Mons, BELGIUM**

E Daubie, P Herquet, A Mollet, A Romeyer

**Universiteit Antwerpen, Wilrijk, BELGIUM**

W Beaumont, M Cardaci, E De Langhe, E A De Wolf, L Rurua

**Centro Brasileiro de Pesquisas Físicas, Rio de Janeiro, RJ, BRAZIL**

M H G Souza

**Universidade do Estado do Rio de Janeiro, Rio de Janeiro, RJ, BRAZIL**

V Oguri, A Santoro, A Sznajder

**Instituto de Física, Universidade Federal do Rio de Janeiro, Rio de Janeiro, RJ, BRAZIL**

M Vaz

**Instituto de Física Teórica, Universidade Estadual Paulista, Sao Paulo, SP, BRAZIL**

E M Gregores, S F Novaes

<sup>1</sup> Also at CERN, European Organization for Nuclear Research, Geneva, Switzerland.

**Institute for Nuclear Research and Nuclear Energy, Sofia, BULGARIA**

T Anguelov, G Antchev, I Atanasov, J Damgov, N Darmenov<sup>1</sup>, L Dimitrov, V Genchev<sup>1</sup>, P Iaydjiev, B Panev, S Piperov, S Stoykova, G Sultanov, I Vankov

**University of Sofia, Sofia, BULGARIA**

A Dimitrov, V Kozuharov, L Litov, M Makariev, A Marinov, E Marinova, S Markov, M Mateev, B Pavlov, P Petkov, C Sabev, S Stoynev, Z Toteva<sup>1</sup>, V Verguilov

**Institute of High Energy Physics, Beijing, CHINA**

G M Chen, H S Chen, K L He, C H Jiang, W G Li, H M Liu, X Meng, X Y Shen, H S Sun, M Yang, W R Zhao, H L Zhuang

**Peking University, Beijing, CHINA**

Y Ban, J Cai, S Liu, S J Qian, Z C Yang, Y L Ye, J Ying

**University for Science and Technology of China, Hefei, Anhui, CHINA**

J Wu, Z P Zhang

**Technical University of Split, Split, CROATIA**

N Godinovic, I Puljak, I Soric

**University of Split, Split, CROATIA**

Z Antunovic, M Dzelalija, K Marasovic

**Institute Rudjer Boskovic, Zagreb, CROATIA**

V Brigljevic, D Ferencek, K Kadija, S Morovic, M Planinic<sup>2</sup>

**University of Cyprus, Nicosia, CYPRUS**

C Nicolaou, A Papadakis, P A Razis, D Tsiakkouri

**National Institute of Chemical Physics and Biophysics, Tallinn, ESTONIA**

A Hektor, M Kadastik, K Kannike, E Lippmaa, M Müntel, M Raidal

**Laboratory of Advanced Energy Systems, Helsinki University of Technology, Espoo, FINLAND**

P A Aarnio

**Helsinki Institute of Physics, Helsinki, FINLAND**

S Czellar, E Haegstroem, A Heikkinen, J Härkönen, V Karimäki, R Kinnunen, T Lampén, K Lassila-Perini, S Lehti, T Lindén, P R Luukka, S Michal<sup>1</sup>, T Mäenpää, J Nysten, M Stettler<sup>1</sup>, E Tuominen, J Tuominiemi, L Wendland

**Lappeenranta University of Technology, Lappeenranta, FINLAND**

T Tuuva

**Laboratoire d'Annecy-le-Vieux de Physique des Particules, IN2P3-CNRS, Annecy-le-Vieux, FRANCE**

J P Guillaud, P Nedelec, D Sillou

**DSM/DAPNIA, CEA/Saclay, Gif-sur-Yvette, FRANCE**

M Anfreville, S Beauceron, E Bougamont, P Bredy, R Chipaux, M Dejardin, D Denegri, J Descamps, B Fabbro, J L Faure, S Ganjour, F X Gentit, A Givernaud, P Gras, G Hamel de Monchenault, P Jarry, F Kircher, M C Lemaire<sup>3</sup>, B Levesy<sup>1</sup>, E Locci, J P Lottin,

<sup>2</sup> Also at University of Zagreb, Zagreb, Croatia.

<sup>3</sup> Also at California Institute of Technology, Pasadena, USA.

I Mandjavidze, M Mur, E Pasquetto, A Payn, J Rander, J M Reymond, F Rondeaux, A Rosowsky, Z H Sun, P Verrecchia

**Laboratoire Leprince-Ringuet, Ecole Polytechnique, IN2P3-CNRS, Palaiseau, FRANCE**  
S Baffioni, F Beaudette, M Bercher, U Berthon, S Bimbot, J Bourotte, P Busson, M Cerutti, D Chamont, C Charlot, C Collard, D Decotigny, E Delmeire, L Dobrzynski, A M Gaillac, Y Geerebaert, J Gilly, M Haguenaer, A Karar, A Mathieu, G Milleret, P Miné, P Paganini, T Romanteau, I Semeniouk, Y Sirois

**Institut Pluridisciplinaire Hubert Curien, IN2P3-CNRS, ULP, UHA Mulhouse, Strasbourg, FRANCE**

J D Berst, J M Brom, F Didierjean, F Drouhin<sup>1</sup>, J C Fontaine<sup>4</sup>, U Goerlach<sup>5</sup>, P Graehling, L Gross, L Houchu, P Juillot, A Lounis<sup>5</sup>, C Maazouzi, D Mangeol, C Olivetto, T Todorov<sup>1</sup>, P Van Hove, D Vintache

**Institut de Physique Nucléaire, IN2P3-CNRS, Université Claude Bernard Lyon 1, Villeurbanne, FRANCE**

M Ageron, J L Agram, G Baulieu, M Bedjidian, J Blaha, A Bonnevaux, G Boudoul<sup>1</sup>, E Chabanat, C Combaret, D Contardo<sup>1</sup>, R Della Negra, P Depasse, T Dupasquier, H El Mamouni, N Estre, J Fay, S Gascon, N Giraud, C Girerd, R Haroutunian, J C Ianigro, B Ille, M Lethuillier, N Lumb<sup>1</sup>, H Mathez, G Maurelli, L Mirabito<sup>1</sup>, S Perries, O Ravat

**Institute of High Energy Physics and Informatization, Tbilisi State University, Tbilisi, GEORGIA**

R Kvatadze

**Institute of Physics Academy of Science, Tbilisi, GEORGIA**

V Roinishvili

**RWTH, I. Physikalisches Institut, Aachen, GERMANY**

R Adolphi, R Brauer, W Braunschweig, H Esser, L Feld, A Heister, W Karpinski, K Klein, C Kukulies, J Olzem, A Ostapchuk, D Pandoulas, G Pierschel, F Raupach, S Schael, G Schwering, M Thomas, M Weber, B Wittmer, M Wlochal

**RWTH, III. Physikalisches Institut A, Aachen, GERMANY**

A Adolf, P Biallass, M Bontenackels, M Erdmann, H Fesefeldt, T Hebbeker, S Hermann, G Hilgers, K Hoepfner<sup>1</sup>, C Hof, S Kappler, M Kirsch, D Lanske, B Philipps, H Reithler, T Rommerskirchen, M Sowa, H Szczesny, M Tonutti, O Tsigenov

**RWTH, III. Physikalisches Institut B, Aachen, GERMANY**

F Beissel, M Davids, M Duda, G Flügge, T Franke, M Giffels, T Hermanns, D Heydhausen, S Kasselmann, G Kaussen, T Kress, A Linn, A Nowack, M Poettgens, O Pooth, A Stahl, D Tornier, M Weber

**Deutsches Elektronen-Synchrotron, Hamburg, GERMANY**

A Flossdorf, B Hegner, J Mnich, C Rosemann

**University of Hamburg, Hamburg, GERMANY**

G Flucke, U Holm, R Klanner, U Pein, N Schirm, P Schleper, G Steinbrück, M Stoye, R Van Staa, K Wick

<sup>4</sup> Also at Université de Haute-Alsace, Mulhouse, France.

<sup>5</sup> Also at Université Louis Pasteur, Strasbourg, France.

**Institut für Experimentelle Kernphysik, Karlsruhe, GERMANY**

P Blüm, V Buege, W De Boer, G Dirkes<sup>1</sup>, M Fahrer, M Feindt, U Felzmann, J Fernandez Menendez<sup>6</sup>, M Frey, A Furgeri, F Hartmann<sup>1</sup>, S Heier, C Jung, B Ledermann, Th. Müller, M Niegel, A Oehler, T Ortega Gomez, C Piasecki, G Quast, K Rabbertz, C Saout, A Scheurer, D Schieferdecker, A Schmidt, H J Simonis, A Theel, A Vest, T Weiler, C Weiser, J Weng<sup>1</sup>, V Zhukov<sup>7</sup>

**University of Athens, Athens, GREECE**

G Karapostoli<sup>1</sup>, P Katsas, P Kreuzer, A Panagiotou, C Papadimitropoulos

**Institute of Nuclear Physics “Demokritos”, Attiki, GREECE**

G Anagnostou, M Barone, T Gerasis, C Kalfas, A Koimas, A Kyriakis, S Kyriazopoulou, D Loukas, A Markou, C Markou, C Mavrommatis, K Theofilatos, G Vermisoglou, A Zachariadou

**University of Ioánnina, Ioánnina, GREECE**

X Aslanoglou, I Evangelou, P Kokkas, N Manthos, I Papadopoulos, G Sidiropoulos, F A Triantis

**KFKI Research Institute for Particle and Nuclear Physics, Budapest, HUNGARY**

G Bencze<sup>1</sup>, L Boldizsar, C Hajdu<sup>1</sup>, D Horvath<sup>8</sup>, A Laszlo, G Odor, F Sikler, N Toth, G Vesztegombi, P Zalan

**Institute of Nuclear Research ATOMKI, Debrecen, HUNGARY**

J Molnar

**University of Debrecen, Debrecen, HUNGARY**

N Beni, A Kapusi, G Marian, P Raics, Z Szabo, Z Szillasi, G Zilizi

**Panjab University, Chandigarh, INDIA**

H S Bawa, S B Beri, V Bhandari, V Bhatnagar, M Kaur, R Kaur, J M Kohli, A Kumar, J B Singh

**University of Delhi, Delhi, INDIA**

A Bhardwaj, S Bhattacharya<sup>9</sup>, S Chatterji, S Chauhan, B C Choudhary, P Gupta, M Jha, K Ranjan, R K Shivpuri, A K Srivastava

**Bhabha Atomic Research Centre, Mumbai, INDIA**

S Borkar, M Dixit, M Ghodgaonkar, S K Kataria, S K Lalwani, V Mishra, A K Mohanty, A Topkar

**Tata Institute of Fundamental Research - EHEP, Mumbai, INDIA**

T Aziz, S Banerjee, S Bose, N Cheere, S Chendvankar, P V Deshpande, M Guhait<sup>10</sup>, A Gurtu, M Maity<sup>11</sup>, G Majumder, K Mazumdar, A Nayak, M R Patil, S Sharma, K Sudhakar, S C Tonwar

<sup>6</sup> Now at Instituto de Física de Cantabria (IFCA), CSIC-Universidad de Cantabria, Santander, Spain.

<sup>7</sup> Also at Moscow State University, Moscow, Russia.

<sup>8</sup> Also at Institute of Nuclear Research ATOMKI, Debrecen, Hungary.

<sup>9</sup> Also at University of California, San Diego, La Jolla, USA.

<sup>10</sup> Also at Tata Institute of Fundamental Research - HECR, Mumbai, India.

<sup>11</sup> Also at University of Visva-Bharati, Santiniketan, India.

**Tata Institute of Fundamental Research - HECR, Mumbai, INDIA**

B S Acharya, S Banerjee, S Bheesette, S Dugad, S D Kalmani, V R Lakkireddi, N K Mondal, N Panyam, P Verma

**Institute for Studies in Theoretical Physics & Mathematics (IPM), Tehran, IRAN**

M Arabgol, H Arfaei, M Hashemi, M Mohammadi, M Mohammadi Najafabadi, A Moshaii, S Paktinat Mehdiabadi

**University College Dublin, Dublin, IRELAND**

M Grunewald

**Università di Bari, Politecnico di Bari e Sezione dell' INFN, Bari, ITALY**

M Abbrescia, L Barbone, A Colaleo<sup>1</sup>, D Creanza, N De Filippis, M De Palma, G Donvito, L Fiore, D Giordano, G Iaselli, F Loddo, G Maggi, M Maggi, N Manna, B Marangelli, M S Mennea, S My, S Natali, S Nuzzo, G Pugliese, V Radicci, A Ranieri, F Romano, G Selvaggi, L Silvestris, P Tempesta, R Trentadue, G Zito

**Università di Bologna e Sezione dell' INFN, Bologna, ITALY**

G Abbiendi, W Bacchi, A Benvenuti, D Bonacorsi, S Braibant-Giacomelli, P Capiluppi, F R Cavallo, C Ciocca, G Codispoti, I D'Antone, G M Dallavalle, F Fabbri, A Fanfani, P Giacomelli<sup>12</sup>, C Grandi, M Guerzoni, L Guiducci, S Marcellini, G Masetti, A Montanari, F Navarra, F Odorici, A Perrotta, A Rossi, T Rovelli, G Siroli, R Travaglini

**Università di Catania e Sezione dell' INFN, Catania, ITALY**

S Albergo, M Chiorboli, S Costa, M Galanti, G Gatto Rotondo, F Noto, R Potenza, G Russo, A Tricomi, C Tuve

**Università di Firenze e Sezione dell' INFN, Firenze, ITALY**

A Bocci, G Ciruolo, V Ciulli, C Civinini, R D'Alessandro, E Focardi, C Genta, P Lenzi, A Macchiolo, N Magini, F Manolescu, C Marchettini, L Masetti, S Mersi, M Meschini, S Paoletti, G Parrini, R Ranieri, M Sani

**Università di Genova e Sezione dell' INFN, Genova, ITALY**

P Fabbriatore, S Farinon, M Greco

**Istituto Nazionale di Fisica Nucleare e Università Degli Studi Milano-Bicocca, Milano, ITALY**

G Cattaneo, A De Min, M Dominoni, F M Farina, F Ferri, A Ghezzi, P Govoni, R Leporini, S Magni, M Malberti, S Malvezzi, S Marelli, D Menasce, L Moroni, P Negri, M Paganoni, D Pedrini, A Pullia, S Ragazzi, N Redaelli, C Rovelli, M Rovere, L Sala, S Sala, R Salerno, T Tabarelli de Fatis, S Vigano<sup>7</sup>

**Istituto Nazionale di Fisica Nucleare de Napoli (INFN), Napoli, ITALY**

G Comunale, F Fabozzi, D Lomidze, S Mele, P Paolucci, D Piccolo, G Polese, C Sciacca

**Università di Padova e Sezione dell' INFN, Padova, ITALY**

P Azzi, N Bacchetta<sup>1</sup>, M Bellato, M Benettoni, D Bisello, E Borsato, A Candelori, P Checchia, E Conti, M De Mattia, T Dorigo, V Drollinger, F Fanzago, F Gasparini, U Gasparini, M Giarin, P Giubilato, F Gonella, A Kaminskiy, S Karaevskii, V Khomenkov, S Lacaprara, I Lippi, M Loreti, O Lytovchenko, M Mazzucato, A T Meneguzzo, M Michelotto, F Montecassiano<sup>1</sup>, M Nigro, M Passaseo, M Pegoraro, G Rampazzo, P Ronchese, E Torassa, S Ventura, M Zanetti, P Zotto, G Zumerle

<sup>12</sup> Also at University of California, Riverside, Riverside, USA.

**Università di Pavia e Sezione dell' INFN, Pavia, ITALY**

G Belli, U Berzano, C De Vecchi, R Guida, M M Necchi, S P Ratti, C Riccardi, G Sani, P Torre, P Vitulo

**Università di Perugia e Sezione dell' INFN, Perugia, ITALY**

F Ambroglini, E Babucci, D Benedetti, M Biasini, G M Bilei<sup>1</sup>, B Caponeri, B Checcucci, L Fanò, P Lariccia, G Mantovani, D Passeri, M Pioppi, P Placidi, V Postolache, D Ricci<sup>1</sup>, A Santocchia, L Servoli, D Spiga

**Università di Pisa, Scuola Normale Superiore e Sezione dell' INFN, Pisa, ITALY**

P Azzurri, G Bagliesi, A Basti, L Benucci, J Bernardini, T Boccali, L Borrello, F Bosi, F Calzolari, R Castaldi, C Cerri, A S Cucoanes, M D'Alfonso, R Dell'Orso, S Dutta, L Foà, S Gennai<sup>13</sup>, A Giammanco, A Giassi, D Kartashov, F Ligabue, S Linari, T Lomtadze, G A Lungu, B Mangano, G Martinelli, M Massa, A Messineo, A Moggi, F Palla, F Palmonari, G Petrucciani, F Raffaelli, A Rizzi, G Sanguinetti, G Segneri, D Sentenac, A T Serban, G Sguazzoni, A Slav, P Spagnolo, R Tenchini, G Tonelli, A Venturi, P G Verdini, M Vos

**Università di Roma I e Sezione dell' INFN, Roma, ITALY**

S Baccaro<sup>14</sup>, L Barone, A Bartoloni, F Cavallari, S Costantini, I Dafinei, D Del Re<sup>9</sup>, M Diemoz, C Gargiulo, E Longo, P Meridiani, G Organtini, S Rahatlou

**Università di Torino e Sezione dell' INFN, Torino, ITALY**

E Accomando, M Arneodo<sup>15</sup>, A Ballestrero, R Bellan, C Biino, S Bolognesi, N Cartiglia, G Cerminara, M Cordero, M Costa, G Dellacasa, N Demaria, E Maina, C Mariotti, S Maselli, P Mereu, E Migliore, V Monaco, M Nervo, M M Obertino, N Pastrone, G Petrillo, A Romero, M Ruspa<sup>15</sup>, R Sacchi, A Staiano, P P Trapani

**Università di Trieste e Sezione dell' INFN, Trieste, ITALY**

S Belforte, F Cossutti, G Della Ricca, A Penzo

**Kyungpook National University, Daegu, KOREA**

K Cho, S W Ham, D Han, D H Kim, G N Kim, J C Kim, W Y Kim, M W Lee, S K Oh, W H Park, S R Ro, D C Son, J S Suh

**Chonnam National University, Kwangju, KOREA**

J Y Kim

**Konkuk University, Seoul, KOREA**

S Y Jung, J T Rhee

**Korea University, Seoul, KOREA**

B S Hong, S J Hong, K S Lee, I Park, S K Park, K S Sim, E Won

**Seoul National University, Seoul, KOREA**

S B Kim

**Universidad Iberoamericana, Mexico City, MEXICO**

S Carrillo Moreno

**Centro de Investigacion y de Estudios Avanzados del IPN, Mexico City, MEXICO**

H Castilla Valdez, A Sanchez Hernandez

<sup>13</sup> Also at Centro Studi Enrico Fermi, Roma, Italy.

<sup>14</sup> Also at ENEA - Casaccia Research Center, S. Maria di Galeria, Italy.

<sup>15</sup> Now at Università del Piemonte Orientale, Novara, Italy.

**Benemerita Universidad Autonoma de Puebla, Puebla, MEXICO**

H A Salazar Iburguen

**Universidad Autonoma de San Luis Potosi, San Luis Potosi, MEXICO**

A Morelos Pineda

**University of Auckland, Auckland, NEW ZEALAND**

R N C Gray, D Krofcheck

**University of Canterbury, Christchurch, NEW ZEALAND**

N Bernardino Rodrigues, P H Butler, J C Williams

**National Centre for Physics, Quaid-I-Azam University, Islamabad, PAKISTAN**

Z Aftab, M Ahmad, U Ahmad, I Ahmed, J Alam Jan, M I Asghar, S Asghar, M Hafeez, H R Hoorani, M Ibrahim, M Iftikhar, M S Khan, N Qaiser, I Rehman, T Solaija, S Toor

**Institute of Nuclear Physics, Polish Academy of Sciences, Cracow, POLAND**J Blocki, A Cyz, E Gladysz-Dziadus, S Mikocki, J Turnau, Z Wlodarczyk<sup>16</sup>, P Zychowski**Institute of Experimental Physics, Warsaw, POLAND**K Bunkowski, H Czyrkowski, R Dabrowski, W Dominik, K Doroba, A Kalinowski, M Konecki, J Krolikowski, I M Kudla, M Pietrusinski, K Pozniak<sup>17</sup>, W Zabolotny<sup>17</sup>, P Zych**Soltan Institute for Nuclear Studies, Warsaw, POLAND**

M Bluj, R Gokiel, L Goscilo, M Górski, K Nawrocki, P Traczyk, G Wrochna, P Zalewski

**Laboratório de Instrumentação Física Experimental de Partículas, Lisboa, PORTUGAL**R Alemany-Fernandez, C Almeida, N Almeida, A Araujo Trindade, P Bordalo, P Da Silva Rodrigues, M Husejko, A Jain, M Kazana, P Musella, S Ramos, J Rasteiro Da Silva, P Q Ribeiro, M Santos, J Semiao, P Silva, I Teixeira, J P Teixeira, J Varela<sup>1</sup>**Joint Institute for Nuclear Research, Dubna, RUSSIA**

S Afanasiev, K Babich, I Belotelov, V Elsha, Y Ershov, I Filozova, A Golunov, I Golutvin, N Gorbounov, I Gramenitski, V Kalagin, A Kamenev, V Karjavin, S Khabarov, V Khabarov, Y Kiryushin, V Konoplyanikov, V Korenkov, G Kozlov, A Kurenkov, A Lanev, V Lysiakov, A Malakhov, I Melnitchenko, V V Mitsyn, K Moisenz, P Moisenz, S Movchan, E Nikonov, D Oleynik, V Palichik, V Perelygin, A Petrosyan, E Rogalev, V Samsonov, M Savina, R Semenov, S Shmatov, S Shulha, V Smirnov, D Smolin, A Tcheremoukhine, O Teryaev, E Tikhonenko, S Vassiliev, A Vishnevskiy, A Volodko, N Zamiatin, A Zarubin, P Zarubin, E Zubarev

**Petersburg Nuclear Physics Institute, Gatchina (St Petersburg), RUSSIA**

N Bondar, V Golovtsov, A Golyash, Y Ivanov, V Kim, V Kozlov, V Lebedev, G Makarenkov, E Orishchin, A Shevel, V Sknar, I Smirnov, V Sulimov, V Tarakanov, L Uvarov, G Velichko, S Volkov, A Vorobyev

**Institute for Nuclear Research, Moscow, RUSSIA**

Yu Andreev, A Anisimov, S Gninenko, N Golubev, D Gorbunov, M Kirsanov, A Kovzelev, N Krasnikov, V Matveev, A Pashenkov, V E Postoev, A Sadovski, A Solovey, A Solovey, D Soloviev, L Stepanova, A Toropin

<sup>16</sup> Also at Institute of Physics, Swietokrzyska Academy, Kielce, Poland.<sup>17</sup> Also at Warsaw University of Technology, Institute of Electronic Systems, Warsaw, Poland.

**Institute for Theoretical and Experimental Physics, Moscow, RUSSIA**

V Gavrilov, N Ilina, V Kaftanov<sup>1</sup>, I Kiselevich, V Kolosov, M Kossov<sup>1</sup>, A Krokhotin, S Kuleshov, A Oulianov, G Safronov, S Semenov, V Stolin, E Vlasov<sup>1</sup>, V Zaytsev

**P N Lebedev Physical Institute, Moscow, RUSSIA**

A M Fomenko, N Konovalova, V Kozlov, A I Lebedev, N Lvova, S V Rusakov, A Terkulov

**Moscow State University, Moscow, RUSSIA**

E Boos, M Dubinin<sup>3</sup>, L Dudko, A Ershov, A Gribushin, V Ilyin, V Klyukhin<sup>1</sup>, O Kodolova, I Lokhtin, S Petrushanko, L Sarycheva, V Savrin, A Sherstnev, A Snigirev, K Teplov, I Vardanyan

**State Research Center of Russian Federation - Institute for High Energy Physics, Protvino, RUSSIA**

V Abramov, I Azhguirei, S Bitioukov, K Datsko, A Filine, P Goncharov, V Grishin, A Inyakin, V Kachanov, A Khmelnikov, D Konstantinov, A Korablev, V Krychkine, A Levine, I Lobov, V Petrov, V Pikalov, R Ryutin, S Slabospitsky, A Sourkov<sup>1</sup>, A Sytine, L Tourtchanovitch, S Troshin, N Tyurin, A Uzunian, A Volkov, S Zelepoukine<sup>18</sup>

**Vinca Institute of Nuclear Sciences, Belgrade, SERBIA**

P Adzic, D Krpic<sup>19</sup>, D Maletic, P Milenovic, J Puzovic<sup>19</sup>, N Smiljkovic<sup>1</sup>, M Zupan

**Centro de Investigaciones Energeticas Medioambientales y Tecnologicas, Madrid, SPAIN**

M Aguilar-Benitez, J Alberdi, J Alcaraz Maestre, M Aldaya Martin, P Arce<sup>1</sup>, J M Barcala, C Burgos Lazaro, J Caballero Bejar, E Calvo, M Cardenas Montes, M Cerrada, M Chamizo Llatas, N Colino, M Daniel, B De La Cruz, C Fernandez Bedoya, A Ferrando, M C Fouz, P Garcia-Abia, J M Hernandez, M I Josa, J M Luque, J Marin, G Merino, A Molinero, J J Navarrete, J C Oller, E Perez Calle, L Romero, J Salicio, C Villanueva Munoz, C Willmott, C Yuste

**Universidad Autónoma de Madrid, Madrid, SPAIN**

C Albajar, J F de Trocóniz, M Fernandez, I Jimenez, R F Teixeira

**Universidad de Oviedo, Oviedo, SPAIN**

J Cuevas, J M Lopez, H Naves Sordo, J M Vizan Garcia

**Instituto de Física de Cantabria (IFCA), CSIC-Universidad de Cantabria, Santander, SPAIN**

A Calderon, D Cano Fernandez, I Diaz Merino, L A Garcia Moral, G Gomez, I Gonzalez Cabellero, J Gonzalez Sanchez, A Lopez Virto, J Marco, R Marco, C Martinez Rivero, P Martinez Ruiz del Arbol, F Matorras, A Patino Revuelta<sup>1</sup>, T Rodrigo, D Rodriguez Gonzalez, A Ruiz Jimeno, M Sobron Sanudo, I Vila, R Vilar Cortabitarte

**CERN, European Organization for Nuclear Research, Geneva, SWITZERLAND**

D Abbaneo, S M Abbas, L Agostino, I Ahmed, S Akhtar, N Amapane, B Araujo Meleiro, S Argiro<sup>20</sup>, S Ashby, P Aspell, E Auffray, M Axer, A Ball, N Bangert, D Barney, C Bernet, W Bialas, C Bloch, P Bloch, S Bonacini, M Bosteels, V Boyer, A Branson, A M Brett,

<sup>18</sup> Also at Institute for Particle Physics, ETH Zurich, Zurich, Switzerland.

<sup>19</sup> Also at Faculty of Physics of University of Belgrade, Belgrade, Serbia.

<sup>20</sup> Also at INFN-CNAF, Bologna, Italy.

H Breuker, R Bruneliere, O Buchmuller, D Campi, T Camporesi, E Cano, E Carrone, A Cattai, R Chierici, T Christiansen, S Cittolin, E Corrin, M Corvo, S Cucciarelli, B Curé, A De Roeck, D Delikaris, M Della Negra, D D'Enterria, A Dierlamm, A Elliott-Peisert, M Eppard, H Foeth, R Folch, S Fratianni, W Funk, A Gaddi, M Gastal, J C Gayde, H Gerwig, K Gill, A S Giolo-Nicollerat, F Glege, R Gomez-Reino Garrido, R Goudard, J Gutleber, M Hansen, J Hartert, A Hervé, H F Hoffmann, A Honma, M Huhtinen, G Iles, V Innocente, W Jank, P Janot, K Kloukinas, C Lasseur, M Lebeau, P Lecoq, C Leonidopoulos, M Letheren, C Ljuslin, R Loos, G Magazu, L Malgeri, M Mannelli, A Marchioro, F Meijers, E Meschi, R Moser, M Mulders, J Nash, R A Ofierzynski, A Oh, P Olbrechts, A Onnela, L Orsini, I Pal, G Papotti, R Paramatti, G Passardi, B Perea Solano, G Perinic, P Petagna, A Petrilli, A Pfeiffer, M Pimiä, R Pintus, H Postema, R Principe, J Puerta Pelayo, A Racz, J Rehn, S Reynaud, M Risoldi, P Rodrigues Simoes Moreira, G Rolandi, P Rosinsky, P Rumerio, H Sakulin, D Samyn, F P Schilling, C Schwick, C Schäfer, I Segoni, A Sharma, P Siegrist, N Sinanis, P Sphicas<sup>21</sup>, M Spiropulu, F Szoncsó, O Teller, D Treille, J Troska, E Tsesmelis, D Tsirigkas, A Tsirou, D Ungaro, F Vasey, M Vazquez Acosta, L Veillet, P Vichoudis, P Wertelaers, A Wijnant, M Wilhelmsson, I M Willers

**Paul Scherrer Institut, Villigen, SWITZERLAND**

W Bertl, K Deiters, W Erdmann, K Gabathuler, S Heising, R Horisberger, Q Ingram, H C Kaestli, D Kotlinski, S König, D Renker, T Rohe, M Spira

**Institute for Particle Physics, ETH Zurich, Zurich, SWITZERLAND**

B Betev, G Davatz, G Dissertori, M Dittmar, L Djambazov, J Ehlers, R Eichler, G Faber, K Freudenreich, J F Fuchs<sup>1</sup>, C Grab, A Holzner, P Ingenito, U Langenegger, P Lecomte, G Leshev, A Lister<sup>22</sup>, P D Luckey, W Lustermann, J D Maillefaud<sup>1</sup>, F Moortgat, A Nardulli, F Nessi-Tedaldi, L Pape, F Pauss, H Rykaczewski<sup>23</sup>, U Röser, D Schinzel, A Starodumov<sup>24</sup>, F Stöckli, H Suter, L Tauscher, P Trüb<sup>25</sup>, H P von Gunten, M Wensveen<sup>1</sup>

**Universität Zürich, Zürich, SWITZERLAND**

E Alagoz, C Amsler, V Chiochia, C Hoermann, K Prokofiev, C Regenfus, P Robmann, T Speer, S Steiner, L Wilke

**National Central University, Chung-Li, TAIWAN**

S Blyth, Y H Chang, E A Chen, A Go, C C Hung, C M Kuo, W Lin

**National Taiwan University (NTU), Taipei, TAIWAN**

P Chang, Y Chao, K F Chen, Z Gao<sup>1</sup>, Y Hsiung, Y J Lei, J Schümann, J G Shiu, K Ueno, Y Velikzhanin, P Yeh

**Cukurova University, Adana, TURKEY**

S Aydin, M N Bakirci, S Cerci, I Dumanoglu, S Erturk, S Esen, E Eskut, A Kayis Topaksu, P Kurt, H Ozkurt, A Polatöz, K Sogut, H Topakli, M Vergili, T Yetkin, G Önengüt

<sup>21</sup> Also at University of Athens, Athens, Greece.

<sup>22</sup> Now at University of California, Davis, Davis, USA.

<sup>23</sup> Now at ESO, Munich-Garching, Germany.

<sup>24</sup> Also at Institute for Theoretical and Experimental Physics, Moscow, Russia.

<sup>25</sup> Also at Paul Scherrer Institut, Villigen, Switzerland.

**Middle East Technical University, Physics Department, Ankara, TURKEY**

H Gamsizkan, C Ozkan, S Sekmen, M Serin-Zeyrek, R Sever, E Yazgan, M Zeyrek

**Bogaziçi University, Department of Physics, Istanbul, TURKEY**

A Cakir<sup>26</sup>, K Cankocak<sup>27</sup>, M Deliomeroğlu, D Demir<sup>26</sup>, K Dindar, E Gülmez, E Isiksal<sup>28</sup>, M Kaya<sup>29</sup>, O Kaya, S Ozkorucuklu<sup>30</sup>, N Sonmez<sup>31</sup>

**Institute of Single Crystals of National Academy of Science, Kharkov, UKRAINE**

B Grinev, V Lyubynskiy, V Senchyshyn

**National Scientific Center, Kharkov Institute of Physics and Technology, Kharkov, UKRAINE**

L Levchuk, P Sorokin

**University of Bristol, Bristol, UNITED KINGDOM**

D S Bailey, T Barrass, J J Brooke, R Croft, D Cussans, D Evans, R Frazier, N Grant, M Hansen, G P Heath, H F Heath, B Huckvale, C Lynch, C K Mackay, S Metson, D M Newbold<sup>32</sup>, V J Smith, R J Tapper

**Rutherford Appleton Laboratory, Didcot, UNITED KINGDOM**

S A Baird, K W Bell, R M Brown, D J A Cockerill, J A Coughlan, P S Flower, V B Francis, M French, J Greenhalgh, R Halsall, J Hill, L Jones, B W Kennedy, L Lintern, A B Lodge, J Maddox, Q Morrissey, P Murray, M Pearson, S Quinton, J Salisbury, A Shah, C Shepherd-Themistocleous, B Smith, M Sproston, R Stephenson, S Taghvirad, I R Tomalin, J H Williams

**Imperial College, University of London, London, UNITED KINGDOM**

F Arteché<sup>1</sup>, R Bainbridge, G Barber, P Barrillon, R Beuselinck, F Blekman, D Britton, D Colling, G Daskalakis, G Dewhurst, S Dris<sup>1</sup>, C Foudas, J Fulcher, S Greder, G Hall, J Jones, J Leaver, B C MacEvoy, O Maroney, A Nikitenko<sup>24</sup>, A Papageorgiou, D M Raymond, M J Ryan, C Seez, P Sharp<sup>1</sup>, M Takahashi, C Timlin, T Virdee<sup>1</sup>, S Wakefield, M Wingham, A Zabi, Y Zhang, O Zorba

**Brunel University, Uxbridge, UNITED KINGDOM**

C Da Via, I Goitom, P R Hobson, P Kyberd, C Munro, J Nebrensky, I Reid, O Sharif, R Taylor, L Teodorescu, S J Watts, I Yaselli

**Boston University, Boston, Massachusetts, USA**

E Hazen, A H Heering, D Lazic, E Machado, D Osborne, J Rohlf, L Sulak, F Varela Rodriguez, S Wu

**Brown University, Providence, Rhode Island, USA**

D Cutts, R Hooper, G Landsberg, R Partridge, S Vanini<sup>33</sup>

<sup>26</sup> Also at Izmir Institute of Technology (IYTE), Izmir, Turkey.

<sup>27</sup> Also at Mugla University, Mugla, Turkey.

<sup>28</sup> Also at Marmara University, Istanbul, Turkey.

<sup>29</sup> Also at Kafkas University, Kars, Turkey.

<sup>30</sup> Also at Suleyman Demirel University, Isparta, Turkey.

<sup>31</sup> Also at Ege University, Izmir, Turkey.

<sup>32</sup> Also at Rutherford Appleton Laboratory, Didcot, United Kingdom.

<sup>33</sup> Also at Università di Padova e Sezione dell' INFN, Padova, Italy.

**University of California, Davis, Davis, California, USA**

R Breedon, M Case, M Chertok, J Conway, P T Cox, R Erbacher, J Gunion, B Holbrook, W Ko, R Lander, D Pellett, J Smith, A Soha, M Tripathi, R Vogt

**University of California, Los Angeles, Los Angeles, California, USA**

V Andreev, K Arisaka, D Cline, R Cousins, S Erhan<sup>1</sup>, M Felcini<sup>1</sup>, J Hauser, M Ignatenko, B Lisowski, D Matlock, C Matthey, B Mohr, J Mumford, S Otwinowski, G Rakness, P Schlein, Y Shi, J Tucker, V Valuev, R Wallny, H G Wang, X Yang, Y Zheng

**University of California, Riverside, Riverside, California, USA**

R Clare, D Fortin, D Fuyan<sup>1</sup>, J W Gary, M Giunta<sup>1</sup>, G Hanson, G Y Jeng, S C Kao, H Liu, G Pasztor<sup>34</sup>, A Satpathy, B C Shen, R Stringer, V Sytnik, R Wilken, D Zer-Zion

**University of California, San Diego, La Jolla, California, USA**

J G Branson, E Dusinberre, J Letts, T Martin, M Mojaver, H P Paar, H Pi, M Pieri, A Rana, V Sharma, A White, F Würthwein

**University of California, Santa Barbara, Santa Barbara, California, USA**

A Affolder, C Campagnari, C Hill, J Incandela, S Kyre, J Lamb, J Richman, D Stuart, D White

**California Institute of Technology, Pasadena, California, USA**

J Albert, A Bornheim, J Bunn, J Chen, G Denis, P Galvez, M Gataullin, I Legrand, V Litvine, Y Ma, D Nae, H B Newman, S Ravot, S Shevchenko, S Singh, C Steenberg, X Su, M Thomas, V Timciuc, F van Lingen, J Veverka, B R Voicu<sup>1</sup>, A Weinstein, R Wilkinson, X Yang, Y Yang, L Y Zhang, K Zhu, R Y Zhu

**Carnegie Mellon University, Pittsburgh, Pennsylvania, USA**

T Ferguson, M Paulini, J Russ, N Terentyev, H Vogel, I Vorobiev

**University of Colorado at Boulder, Boulder, Colorado, USA**

J P Cumalat, W T Ford, D Johnson, U Nauenberg, K Stenson, S R Wagner

**Cornell University, Ithaca, NY, USA**

J Alexander, D Cassel, K Ecklund, B Heltsley, C D Jones, V Kuznetsov, J R Patterson, A Ryd, J Thom, P Wittich

**Fairfield University, Fairfield, Connecticut, USA**

C P Beetz, G Cirino, V Podrasky, C Sanzeni, D Winn

**Fermi National Accelerator Laboratory, Batavia, Illinois, USA**

S Abdullin<sup>24</sup>, M A Afaq<sup>1</sup>, M Albrow, J Amundson, G Apollinari, M Atac, W Badgett, J A Bakken, B Baldin, L A T Bauerdick, A Baumbaugh, U Baur, P C Bhat, F Borcherding, K Burkett, J N Butler, H Cheung, I Churin, S Cihangir, M Demarteau, D P Eartly, J E Elias, V D Elvira, D Evans, I Fisk, J Freeman, P Gartung, F J M Geurts, D A Glenzinski, E Gottschalk, G Graham, D Green, G M Guglielmo, Y Guo, O Gutsche, A Hahn, J Hanlon, S Hansen, R M Harris, T Hesselroth, S L Holm, B Holzman, S Iqbal, E James, M Johnson, U Joshi, B Klima, J Kowalkowski, T Kramer, S Kwan, E La Vallie, M Larwill, S Los, L Lueking, G Lukhanin, S Lusin<sup>1</sup>, K Maeshima, P McBride, S J Murray, V O'Dell, M Paterno, J Patrick, D Petravick, R Pordes, O Prokofyev, V Rasmislovich, N Ratnikova, A Ronzhin, V Sekhri, E Sexton-Kennedy, T Shaw, D Skow, R P Smith, W J Spalding, L Spiegel, M Stavrianakou, G Stiehr, I Suzuki, P Tan, W Tanenbaum, S Tkaczyk, S Veseli, R Vidal, H Wenzel, J Whitmore, W J Womersley, W M Wu, Y Wu, A Yagil, J Yarba, J C Yun

<sup>34</sup> Also at KFKI Research Institute for Particle and Nuclear Physics, Budapest, Hungary.

**University of Florida, Gainesville, Florida, USA**

D Acosta, P Avery, V Barashko, P Bartalini, D Bourilkov, R Cavanaugh, A Drozdetskiy, R D Field, Y Fu, L Gray, D Holmes, B J Kim, S Klimentko, J Konigsberg, A Korytov, K Kotov, P Levchenko, A Madorsky, K Matchev, G Mitselmakher, Y Pakhotin, C Prescott, P Ramond, J L Rodriguez, M Schmitt, B Scurlock, H Stoeck, J Yelton

**Florida International University, Miami, Florida, USA**

W Boeglin, V Gaultney, L Kramer, S Linn, P Markowitz, G Martinez, B Raue, J Reinhold

**Florida State University, Tallahassee, Florida, USA**

A Askew, M Bertoldi, W G D Dharmaratna, Y Gershtein, S Hagopian, V Hagopian, M Jenkins, K F Johnson, H Prosper, H Wahl

**Florida Institute of Technology, Melbourne, Florida, USA**

M Baarmand, L Baksay<sup>35</sup>, S Guragain, M Hohlmann, H Mermerkaya, R Ralich, I Vodopyanov

**University of Illinois at Chicago (UIC), Chicago, Illinois, USA**

M R Adams, R R Betts, C E Gerber, E Shabalina, C Smith, T Ten

**The University of Iowa, Iowa City, Iowa, USA**

U Akgun, A S Ayan, A Cooper, P Debbins, F Duru, M Fountain, N George, E McCliment, J P Merlo, A Mestvirishvili, M J Miller, C R Newsom, E Norbeck, Y Onel, I Schmidt, S Wang

**Iowa State University, Ames, Iowa, USA**

E W Anderson, O Atramentov, J M Hauptman, J Lamsa

**Johns Hopkins University, Baltimore, Maryland, USA**

B A Barnett, B Blumenfeld, C Y Chien, D W Kim, P Maksimovic, S Spangler, M Swartz

**The University of Kansas, Lawrence, Kansas, USA**

P Baringer, A Bean, D Coppage, O Grachov, E J Kim, M Murray

**Kansas State University, Manhattan, Kansas, USA**

D Bandurin, T Bolton, A Khanov<sup>24</sup>, Y Maravin, D Onoprienko, F Rizatdinova, R Sidwell, N Stanton, E Von Toerne

**University of Maryland, College Park, Maryland, USA**

D Baden, R Bard, S C Eno, T Grassi, N J Hadley, R G Kellogg, S Kunori, F Ratnikov, A Skuja

**Massachusetts Institute of Technology, Cambridge, Massachusetts, USA**

R Arcidiacono, M Ballintijn, G Bauer, P Harris, I Kravchenko, C Loizides, S Nahn, C Paus, S Pavlon, C Roland, G Roland, K Sumorok, S Vaurynovich, G Veres, B Wyslouch

**University of Minnesota, Minneapolis, Minnesota, USA**

D Bailleux, S Corum, P Cushman, A De Benedetti, A Dolgoplov, R Egeland, G Franzoni, W J Gilbert, J Grahl, J Haupt, Y Kubota, J Mans, N Pearson, R Rusack, A Singovsky

**University of Mississippi, University, Mississippi, USA**

L M Cremaldi, R Godang, R Kroeger, D A Sanders, D Summers

**University of Nebraska-Lincoln, Lincoln, Nebraska, USA**

K Bloom, D R Claes, A Dominguez, M Eads, C Lundstedt, S Malik, G R Snow, A Sobol

<sup>35</sup> Also at University of Debrecen, Debrecen, Hungary.

**State University of New York at Buffalo, Buffalo, New York, USA**

I Iashvili, A Kharchilava

**Northeastern University, Boston, Massachusetts, USA**

G Alverson, E Barberis, O Boeriu, G Eulisse, Y Musienko<sup>36</sup>, S Muzaffar, I Osborne, S Reucroft, J Swain, L Taylor, L Tuura, D Wood

**Northwestern University, Evanston, Illinois, USA**

B Gobbi, M Kubantsev, H Schellman, M Schmitt, E Spencer, M Velasco

**University of Notre Dame, Notre Dame, Indiana, USA**

B Baumbaugh, N M Cason, M Hildreth, D J Karmgard, N Marinelli<sup>21</sup>, R Ruchti, J Warchol, M Wayne

**The Ohio State University, Columbus, Ohio, USA**

B Bylsma, L S Durkin, J Gilmore, J Gu, D Herman, P Killewald, K Knobbe, T Y Ling

**Princeton University, Princeton, New Jersey, USA**

P Elmer, D Marlow, P Piroué, D Stickland, C Tully, T Wildish, S Wynhoff, Z Xie

**Purdue University, West Lafayette, Indiana, USA**

A Apresyan, K Arndt, K Banicz, V E Barnes, G Bolla, D Bortoletto, A Bujak, A F Garfinkel, O Gonzalez Lopez, L Gutay, N Ippolito, Y Kozhevnikov<sup>1</sup>, A T Laasanen, C Liu, V Marousov, P Merkel, D H Miller, J Miyamoto, N Neumeister, C Rott, A Roy, A Sedov, I Shipsey

**Purdue University Calumet, Hammond, Indiana, USA**

N Parashar

**Rice University, Houston, Texas, USA**

G Eppley, S J Lee, J Liu, M Matveev, T Nussbaum, B P Padley, J Roberts, A Tumanov, P Yepes

**University of Rochester, Rochester, New York, USA**

A Bodek, H Budd, Y S Chung, P De Barbaro<sup>1</sup>, R Demina, R Eusebi, G Ginther, Y Gotra, A Hocker, U Husemann, S Korjenevski, W Sakumoto, P Slattery, P Tipton, M Zielinski

**Rutgers, the State University of New Jersey, Piscataway, New Jersey, USA**

E Bartz, J Doroshenko, E Halkiadakis, P F Jacques, M S Kalelkar, D Khits, A Lath, A Macpherson<sup>1</sup>, L Perera, R Plano, K Rose, S Schnetzer, S Somalwar, R Stone, G Thomson, T L Watts

**Texas Tech University, Lubbock, Texas, USA**

N Akchurin, K W Carrell, K Gumus, C Jeong, H Kim, V Papadimitriou, A Sill, M Spezziga, E Washington, R Wigmans, L Zhang

**Vanderbilt University, Nashville, Tennessee, USA**

T Bapty, D Engh, W Johns, T Keskinpala, E Luiggi Lopez, S Neema, S Nordstrom, S Pathak, P Sheldon, E W Vaandering, M Webster

<sup>36</sup> Also at Institute for Nuclear Research, Moscow, Russia.

**University of Virginia, Charlottesville, Virginia, USA**

M W Arenton, S Conetti, B Cox, R Hirosky, R Imlay, A Ledovskoy, D Phillips II, H Powell, M Ronquest, D Smith

**University of Wisconsin, Madison, Wisconsin, USA**

Y W Baek, J N Bellinger, D Bradley, D Carlsmith, I Crotty<sup>1</sup>, S Dasu, F Feyzi, T Gorski, M Grothe<sup>37</sup>, W Hogg, M Jaworski, P Klabbers, A Lanaro, R Loveless, M Magrans de Abril, D Reeder, W H Smith, D Wenman

**Yale University, New Haven, Connecticut, USA**

G S Atoyan<sup>36</sup>, S Dhawan, V Issakov, H Neal, A Poblaguev, M E Zeller

**Institute of Nuclear Physics of the Uzbekistan Academy of Sciences, Ulugbek, Tashkent, UZBEKISTAN**

B S Yuldashev

<sup>37</sup> Also at Università di Torino e Sezione dell' INFN, Torino, Italy.

**Table 12.3.** The NLO background processes cross sections used (in fb).

background	$t\bar{t} \rightarrow 4l$	$Z b\bar{b}$	$ZZ$	$t\bar{t} Z$
Cross section times BR	$88.4 \cdot 10^3$	$52.4 \cdot 10^3$	229.5	650

section is 1% to 6%. The uncertainty on signal cross section is 10% to 15%. The uncertainty on the luminosity  $\mathcal{L}$  is  $\sim 5\%$  for an integrated luminosity of  $10 \text{ fb}^{-1}$ .

Using a background cross section uncertainty of 6%, a signal cross section uncertainty of 10% and a luminosity uncertainty of 5% the approximated uncertainties on the exclusion mass limit and on the discovery mass limit are:

$$\text{Exclusion Limit} = (760_{-2}^{+0.5}(\text{bkg}) \pm 10(\text{signal}) \pm 4(\text{lumi})) \text{ GeV}/c^2 \quad (12.3)$$

$$\text{Discovery Limit} = (650_{-0.3}^{+0.4}(\text{bkg})_{-0.4}^{+3}(\text{signal}) \pm 0.2(\text{lumi})) \text{ GeV}/c^2. \quad (12.4)$$

### 12.2.2. Search for the final states with $\tau$ leptons

**12.2.2.1. Introduction.** In this section, we discuss the doubly charged Higgs boson pair-production via a Drell–Yan process and investigate decays which involve taus and muons. The branching ratios are assumed to be  $1/3$  for the following three channels:  $\Delta^{\pm\pm} \rightarrow 2\mu^{\pm}$ ,  $\Delta^{\pm\pm} \rightarrow \mu^{\pm}\tau^{\pm}$  and  $\Delta^{\pm\pm} \rightarrow 2\tau^{\pm}$ . The reasoning comes from recent neutrino mixing measurements. As the neutrino mixing matrix and doubly charged Higgs boson decays are directly related then the appropriate branchings can be determined.

**12.2.2.2. Event generation.** The doubly charged Higgs boson pair-production via Drell–Yan process is generated using PYTHIA. Datasets are produced with Higgs boson mass from  $200 \text{ GeV}/c^2$  to  $600 \text{ GeV}/c^2$ . The taus from Higgs boson decays can decay both leptonically and hadronically while in analysis we only consider hadronic decays.

The backgrounds which were considered for this analysis are as follows:

- $t\bar{t} \rightarrow W^+W b\bar{b}$  generated by PYTHIA, COMPHEP, ALPGEN, TOPREX and MADGRAPH with W boson decay  $W \rightarrow \ell\nu$  ( $\ell = e, \mu, \tau$ ) forced.
- $t\bar{t} Z \rightarrow W^+W^-Z b\bar{b}$  generated with COMPHEP. The W and Z bosons are allowed to decay arbitrarily.
- $Zb\bar{b}$  where the Z boson decays to muons and  $\tau$  leptons, generated with COMPHEP.
- $ZZ$  generated with PYTHIA, where the Z bosons are forced to decay leptonically ( $e, \mu, \tau$ ). The contribution of  $\gamma^*$  is included with  $m_{\gamma^*} > 12 \text{ GeV}/c^2$ .

The next-to-leading order (NLO) cross sections times branching ratios used for the backgrounds can be found in Table 12.3. The Monte Carlo statistics of the generated background exceed  $30 \text{ fb}^{-1}$  except  $Zb\bar{b}$  background, where it is  $8 \text{ fb}^{-1}$ . Therefore the results will be presented for an integrated luminosity of  $10 \text{ fb}^{-1}$ .

**12.2.2.3. Event selection and reconstruction.** The events are triggered by the single muon trigger at Level 1 and HLT. After HLT the event is only used if it is possible to reconstruct the event primary vertex. If the primary vertex fails to be reconstructed the event is rejected.

The muons are reconstructed using Global Muon Reconstructor. The  $\tau$  leptons are reconstructed using  $\tau$ -jet candidates and missing transverse energy after selection cuts. The doubly charged Higgs boson invariant mass is reconstructed from the same charge lepton pairs after all selection cuts.

The selection cuts used on muons are:

- The transverse momentum must be higher than 50 GeV/c. For background events 80% of muons have  $p_T$  less than 50 GeV/c while for the signal with Higgs boson mass 200 GeV/c<sup>2</sup> it is 27% and for higher masses it reduces to around 10%.
- The distance to primary vertex in z-direction must not exceed 0.03 cm. It does not cut away any muons from the signal events but limits analysis to leptons coming from the same primary vertex.

The selection cuts used on  $\tau$  jets are:

- For  $\tau$  jets we consider  $\tau$  decays which involve 1 or 3 charged tracks. We use  $\tau$ -jet candidates which passed the  $\tau$ -jet filtering algorithms described in [280]. Two isolation criteria are used. Either one or three charged tracks in the signal cone and no charged tracks in the isolation cone or two tracks in signal cone and exactly one charged track in the isolation cone.
- The maximal distance to the primary vertex in the z-direction of any charged track in the  $\tau$  jet must not exceed 0.2 cm.
- The transverse energy of the hottest HCAL tower of the  $\tau$  jet must be higher than 2 GeV. This cut eliminates 86% of all electrons taken as  $\tau$  candidates and only removes 7.5% of real  $\tau$  jets.
- The transverse energy of the  $\tau$  jet candidate must exceed 50 GeV. It has been chosen to be the same as the cut used on muons.
- No muon track should be in a cone with  $\Delta R = 0.3$  constructed around the  $\tau$ -jet candidate. If there is, then the candidate is dropped. This eliminates false  $\tau$ -jet candidates which are generated when a charged muon track passes the same region as photons or hadrons. With this cut only a few real  $\tau$  jets are discarded however most of the false  $\tau$  jets coming from this misidentification are rejected.

Missing transverse energy ( $E_T^{\text{miss}}$ ) is reconstructed using calorimeter Type 1  $E_T^{\text{miss}}$  ( $E_T^{\text{miss}}$  with the jet energy corrections) and  $p_T$  of muons.

Only events with at least four objects, muons or  $\tau$  jets, are accepted. The possible final states are:

- $\Delta^{++}\Delta^{--} \rightarrow 4\mu$ : this channel is investigated in the previous subsection.
- $\Delta^{++}\Delta^{--} \rightarrow 3\mu 1\tau$ : this channel is easily reconstructible as there is only one neutrino and it goes the direction of the  $\tau$  jet.
- $\Delta^{++}\Delta^{--} \rightarrow 2\mu 2\tau$ : this channel can also be reconstructed using the assumption that the neutrinos go in the same directions as the  $\tau$  jets.
- $\Delta^{++}\Delta^{--} \rightarrow 1\mu 3\tau$ : this channel can be reconstructed only with very good  $E_T^{\text{miss}}$  resolution as it requires an additional assumption that the masses of the two reconstructed Higgs bosons are the same. However the reconstruction is very sensitive to  $E_T^{\text{miss}}$  accuracy and often the event has to be dropped due to negative  $\tau$ -lepton energies.
- $\Delta^{++}\Delta^{--} \rightarrow 4\tau$ : this channel can not be reconstructed (and triggered by the single muon trigger).

Once the event leptons are reconstructed, some additional selections are performed:

- Z boson veto: if the odd sign pairing gives an invariant mass of  $91 \pm 5$  GeV/c<sup>2</sup> then these leptons are removed from further use.
- Same charge lepton pairs are reconstructed and only those reconstructed Higgs candidate pairs whose invariant mass difference is within 20% of each other are considered.

The reconstructed mass of doubly charged Higgs boson is shown on Figure 12.7 for the Higgs boson masses 200 and 500 GeV/c<sup>2</sup>.

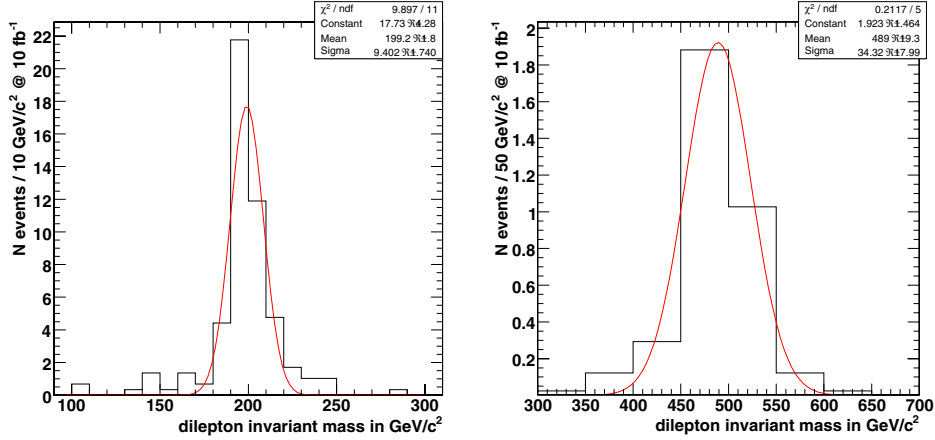


**Figure 12.7.** The reconstructed invariant mass for  $M(\Delta^{\pm\pm}) = 200 \text{ GeV}/c^2$  and  $500 \text{ GeV}/c^2$ .

**Table 12.4.** The signal selection efficiencies for different  $\Delta^{\pm\pm}$  masses. Total efficiency is the product of the single efficiencies.

$m_{\Delta^{\pm\pm}} \text{ (GeV}/c^2)$	200	300	400	500	600
Level 1 and HLT	83.7%	86.0%	86.7%	85.8%	88.3%
Primary vertex	96.9%	98.5%	97.0%	97.5%	98.0%
4 leptons in final state	10.1%	17.2%	23.6%	24.7%	26.7%
two pairs and at least one $\tau$	44.9%	46.1%	41.7%	53.2%	52.9%
Mass difference	62.5%	77.2%	80.4%	74.3%	63.6%
Total signal efficiency	2.3%	5.1%	6.6%	8.1%	7.7%

**12.2.2.4. Selection efficiencies.** The upper limit of the signal selection efficiency is given by the fraction of events with  $3\mu 1\tau$ ,  $2\mu 2\tau$ ,  $1\mu 3\tau$  ( $\tau \rightarrow \text{hadrons}$ ) topology relative to all possible final states with muons and  $\tau$  leptons from decays of two Higgs bosons. Assuming the above mentioned branching ratios the upper limit is  $\simeq 35\%$ . The fraction of every selected topology is given below:

- $\Delta^{++}\Delta^{--} \rightarrow 3\mu 1\tau = 2/9 \text{ events} \times 0.65 = 14.4\%$
- $\Delta^{++}\Delta^{--} \rightarrow 2\mu 2\tau = 3/9 \text{ events} \times 0.65^2 = 14.1\%$
- $\Delta^{++}\Delta^{--} \rightarrow 1\mu 3\tau = 2/9 \text{ events} \times 0.65^3 = 6.1\%$ .

where 0.65 is the branching ratio of  $\tau \rightarrow \text{hadrons}$  decays. Table 12.4 summarises the efficiencies of each selection (relative to the previous one) for the signal of different  $\Delta^{\pm\pm}$  masses. The lepton selection efficiency and purity is shown in Table 12.5. Background efficiencies are shown in Table 12.6.

**12.2.2.5. Systematic errors.** At the integrated luminosity of  $10 \text{ fb}^{-1}$  the cuts implemented above result in an almost background free signal. For datasets with Monte Carlo statistics above  $30 \text{ fb}^{-1}$  giving zero Monte Carlo events after all selections ( $t\bar{t}$ ,  $ZZ^*$ ) we assume the background to be zero. For  $t\bar{t}Z$  background where is one Monte Carlo event passing all cuts, which corresponds to 0.05 expected events when scaled with cross section and luminosity.

**Table 12.5.** Single muon and  $\tau$  selection efficiencies and purity.

$m_{\Delta}^{\pm\pm}$ (GeV/c <sup>2</sup> )	200	300	400	500	600
Single $\mu$ selection efficiency	70.7%	82.0%	86.1%	87.2%	89.2%
1 - purity of accepted muons:	0.1%	0.4%	0.8%	0.7%	1.0%
Single $\tau$ selection efficiency	36.6%	42.3%	50.6%	53.3%	53.3%
1 - purity of accepted $\tau$ jets:	2.2%	2.2%	4.2%	3.6%	3.2%

**Table 12.6.** Selection efficiencies for background. Total efficiency is the product of the single efficiencies.

Process	$t\bar{t}$	$t\bar{t}Z$	$ZZ$	Zbb
Level 1 and HLT trigger	40.7%	20.3%	40.0%	42.1%
Primary vertex	99.3%	99.8%	96.7%	98.2%
4 leptons in final state	0.0015%	0.04 %	3.0%	0.0005%
two pairs and at least one $\tau$	–	0.1%	–	–
Mass difference	–	100%	–	–
Total signal efficiency	–	0.0008%	–	–

For  $Zb\bar{b}$  background where the Monte Carlo statistics corresponds to  $8\text{ fb}^{-1}$  no events passed all cuts. The analysis was repeated with  $p_T$  cut on muon ( $\tau$  jet) of 40 GeV/c, 30 GeV/c and 20 GeV/c, again with no events passing the cuts, which confirms the assumption that leptons coming from  $Zb\bar{b}$  are too soft to produce a background. Considering the smallness of all backgrounds we assume no background at  $10\text{ fb}^{-1}$  for the following analysis.

The systematic uncertainties used for the signal are the following:

- muon misidentification ( $\Delta\mu$ ): 1% per muon;
- muon isolation ( $\Delta\mu_{isol}$ ): 2% per event;
- $\tau$  jets identification ( $\Delta\tau$ ): 9% per  $\tau$  jet;
- luminosity ( $\Delta\mathcal{L}$ ): 5%;
- PDF and scale ( $\Delta\sigma$ ) 10% (theoretical uncertainty, it is not used for the signal cross section measurement with no background).

As the events are a mixture of different decay modes the total selection efficiency uncertainty ( $\Delta\epsilon_S$ ) is calculated per decay channel and then added together with the corresponding weights:

$$\Delta 3\mu 1\tau = \sqrt{3\Delta\mu^2 + \Delta\tau^2} = 8.2\%,$$

$$\Delta 2\mu 2\tau = \sqrt{2\Delta\mu^2 + 2\Delta\tau^2} = 11.4\%,$$

$$\Delta 1\mu 3\tau = \sqrt{\Delta\mu^2 + 3\Delta\tau^2} = 13.9\%,$$

giving

$$\Delta\epsilon_S = \frac{144\Delta 3\mu 1\tau + 141\Delta 2\mu 2\tau + 61\Delta 1\mu 3\tau}{346} = 10.5\%.$$

The total systematic error for cross section measurement is then

$$\frac{\Delta\sigma}{\sigma} = \sqrt{\Delta\mu_{isol}^2 + \Delta\mathcal{L}^2 + \Delta\epsilon_S^2} = 13\%.$$

**Table 12.7.** Expected number of events, NLO cross section with expected statistical and systematic uncertainty of the cross section measurement at  $10 \text{ fb}^{-1}$ , and integrated luminosity needed for exclusion at 95% CL.

$m_{\Delta}^{\pm\pm}$ (GeV)	200	300	400	500
$N_{\text{ev}}$ expected at $10 \text{ fb}^{-1}$	26	10	4	2
$\sigma_{\text{NLO}} \pm \text{stat} \pm \text{syst}$ (fb)	$93.9^{+19.3}_{-17.5} \pm 12.2$	$19.6^{+6.6}_{-5.6} \pm 2.5$	$5.9^{+3.4}_{-2.5} \pm 0.8$	$2.2^{+1.9}_{-1.3} \pm 0.3$
Luminosity for 95% CL exclusion, $\text{fb}^{-1}$	1.3	3.0	7.7	16.8

The statistical errors were evaluated constructing the shortest Bayesian confidence interval for the confidence level of 67% [669].

*12.2.2.6. Results.* The expected number of events at  $10 \text{ fb}^{-1}$  and the NLO cross section with expected statistical and systematic uncertainty of the cross section measurement are given in Table 12.7. Table 12.7 shows also the integrated luminosity needed for exclusion at 95% CL.



---

ARTICLE III

---

Kadastik, M., Raidal, M., Rebane, L., 2008. "Direct determination of neutrino mass parameters at future colliders", Phys.Rev.D77:115023, 2008.

Copyright (2008) by the American Physical Society.

**Direct determination of neutrino mass parameters at future colliders**

M. Kadastik, M. Raidal, and L. Rebane

*National Institute of Chemical Physics and Biophysics, Ravala 10, Tallinn 10143, Estonia*

(Received 19 February 2008; published 26 June 2008)

If the observed light neutrino masses are induced by their Yukawa couplings to singlet right-handed neutrinos, the natural smallness of those makes direct collider tests of the electroweak scale neutrino mass mechanisms difficult in the simplest models. In the triplet Higgs seesaw scenario the smallness of light neutrino masses may come from the smallness of  $B - L$  breaking parameters, allowing sizable Yukawa couplings even for a TeV scale triplet. We show that, in this scenario, measuring the branching fractions of doubly charged Higgs to different same-charged lepton flavors at CERN LHC and/or ILC experiments will allow one to measure the neutrino mass parameters that neutrino oscillation experiments are insensitive to, including the neutrino mass hierarchy, lightest neutrino mass, and Majorana phases.

DOI: [10.1103/PhysRevD.77.115023](https://doi.org/10.1103/PhysRevD.77.115023)

PACS numbers: 14.80.Cp

**I. INTRODUCTION**

In the recent past neutrino oscillation experiments have shown convincingly that at least two light neutrinos have nonzero masses and their mixing is characterized by two large mixing angles [1]. Those facts constitute indisputable evidence of new physics beyond the standard model (SM). However, despite intense experimental and theoretical effort over many years, understanding of the origin of neutrino masses is still missing.

From the experimental point of view the information on neutrino masses coming from oscillation experiments is limited by the fact that these experiments are only able to measure the differences of squared neutrino masses and not their absolute magnitude; neither are they sensitive to the Dirac or Majorana nature of light neutrinos. In particular, the present oscillation experiments cannot distinguish between the two possible mass ordering patterns of light neutrinos, the normal and the inverted ones, and are insensitive to the possible Majorana phases [2] of neutrinos. The observed smallness of the neutrino  $\theta_{13}$  mixing angle makes it very difficult to measure any new parameter, such as the neutrino Dirac  $CP$  phase  $\delta$ , in neutrino oscillation experiments before a distant-future neutrino factory [3]. To learn conceptually new facts about light neutrinos in a shorter time scale likely requires an experimental breakthrough either in low energy neutrino experiments, such as the neutrinoless double beta decay ( $0\nu\beta\beta$ ) decay experiments, or in collider physics.

From the theory side we still do not know why neutrinos are so light compared to charged fermions. It is natural that the  $SU(2)_L$  doublet neutrinos couple to new singlet (right-handed) neutrinos  $N$  and the SM Higgs doublet in a direct analogy with all other SM fermions. If this is the only new physics, the smallness of neutrino masses requires unnaturally small Dirac Yukawa couplings. Alternatively, the singlet neutrinos may have very large Majorana masses which suppress the light neutrino masses to the observed range via the seesaw mechanism of type I [4–8] even for

large values of the Yukawa couplings. Generically neither of those simple scenarios can be directly probed at low energy nor collider experiments.<sup>1</sup> Making the singlet neutrinos as light as 1 TeV to be kinematically accessible at colliders does not help because their only interactions are of Yukawa type, and the seesaw mechanism predicts that the couplings are too small for any observable signal except the neutrino masses. Complicated model building is required to ensure the correct light neutrino masses, 1 TeV heavy neutrinos, and meaningfully large neutrino Yukawa couplings at the same time. Unfortunately the direct tests of singlet neutrino mass mechanism at LHC are experimentally demanding even in those models [12–15]. Brighter prospects for the discovery of TeV scale heavy neutrinos at LHC occur in the context of models with extended gauge sector [16].

However, group theory tells us that generation of non-zero masses for the SM doublet neutrinos does not require the existence of singlets. One of the best motivated and best studied neutrino mass scenario is the triplet Higgs mechanism [17–21], sometimes called seesaw mechanism of type II. From the point of view of direct tests the triplet Higgs neutrino mass mechanism has several advantages over the singlet one. First, the  $SU(2)_L$  triplet multiplet contains a doubly charged scalar which can be pair produced at colliders independently of their Yukawa couplings. Thus tests of this mechanism are limited only by the collision energy. Second, the smallness of neutrino masses does not imply the smallness of triplet Yukawa couplings. As neutrino masses in this scenario are necessarily of Majorana type, they may be different from the

<sup>1</sup>This conclusion may be different if softly broken supersymmetry exists in nature. Flavor violating Yukawa couplings of heavy neutrinos may induce flavor off-diagonal elements in the soft slepton mass matrices via the renormalization effects [9,10] which may lead to observable rates of lepton flavor violating processes. This very complex scenario requires analyses beyond the present one [11].

Dirac fermion masses because of the smallness of  $B - L$  breaking. This is natural by the 't Hooft criterion as  $B - L$  is a conserved quantum number in the SM. Thus the neutrino Yukawa couplings to triplet may be sizable, constrained by unobserved lepton flavor violating interactions, and dominate over the triplet coupling to two gauge bosons. Third, the triplet Yukawa couplings directly induce the neutrino mass matrix up to the small  $B - L$  breaking triplet vacuum expectation value (VEV) which appears in neutrino masses as a common proportionality factor. Altogether those arguments imply that one can study the neutrino mass parameters at CERN Large Hadron Collider (LHC) and/or International Linear Collider (ILC) experiments by just counting flavors of the same-charged lepton pairs originating from the doubly charged Higgs boson decays.

In this work we extend the analysis of our previous paper [22]. While in Ref. [22] we studied the discovery potential of LHC experiments for the process  $pp \rightarrow \Phi^{++}\Phi^{--}$  [22–29] assuming that the subsequent decays of  $\Phi^{\pm\pm}$  are determined by neutrino data, in this analysis we turn the argument around and study what can one learn about neutrino physics if LHC and/or ILC will discover the triplet Higgs bosons. In particular, we concentrate on neutrino parameters which cannot be measured in oscillation experiments, the light neutrino mass ordering, the mass of the lightest neutrino, and the Majorana phases  $\alpha_1$  and  $\alpha_2$ . Neutrino mass hierarchy patterns at colliders have been previously studied in [30]. First we derive analytical expressions for those quantities which are functions of the doubly charged Higgs branching fractions to different flavor combinations of charged lepton pairs,  $\Phi^{\pm\pm} \rightarrow \ell_i \ell_j$ ,  $i, j = e, \mu, \tau$ . Thus neutrino physics at colliders turns out to be just a counting experiment of lepton flavors. This simplifies the life, in particular, at LHC experiments which, in general, have larger measurement errors than at ILC. The analytical results are first derived assuming the tribimaximal mixing for neutrinos, which predicts  $\sin\theta_{13} = 0$ , and extended later to nonzero values of  $\sin\theta_{13}$ . After that we study to what precision those quantities can be measured in realistic experiments. Finally we demonstrate that combining positive collider signals of this scenario with the possible measurement of the neutrino mass matrix entry  $(m_\nu)_{ee}$  would allow one to determine separately the size of triplet Yukawa couplings and the  $B - L$  breaking VEV of the triplet. Thus one can entirely probe the neutrino mass generating mechanism at terrestrial experiments.

We find that there are distinctive flavor signals which indicate certain patterns of neutrino mass matrix. For example, very few electrons in  $\Phi^{--}$  decays definitely points towards normally hierarchical light neutrinos. There is theoretical ambiguity in determination of the Majorana phases and only a combination of them can be measured. However, in the case of a very hierarchical

neutrino mass spectrum one of the Majorana phases is effectively decoupled from physics and one can, in principle, measure the magnitude of the physical phase. Although the experimental errors in determining those quantities may turn out to be quite large in general, we show that there exist scenarios which can already be fully solved at LHC. In the optimistic scenarios the branching fractions of the doubly charged Higgs boson decays can be used to (i) determine the neutrino mass hierarchy; (ii) estimate the mass of the lowest neutrino state; (iii) estimate the Majorana phases of  $CP$  violation; (iv) measure the value of Higgs triplet VEV. We note that those measurements are also sensitive to all other neutrino parameters including the mixing angles and  $CP$  violating phase  $\delta$ . We show that the latter two are, in principle, measurable at collider experiments. However, those quantities can be determined with much higher precision in other experiments, and we do not study their effects in detail in this paper.

The paper is organized as follows. In Sec. II we present the collider phenomenology of the doubly charged Higgs boson and relate the collider observables to the neutrino parameters. In Sec. III we present details of the analysis of neutrino parameter measurements at colliders. In Sec. IV we discuss the possibility of measuring the triplet Higgs VEV and determination of the full neutrino mass matrix. Finally we conclude in Sec. V.

## II. PHENOMENOLOGICAL SETUP

In this work we assume that the SM particle spectrum is extended by a scalar multiplet  $\Phi$  with the  $SU(2)_L \times U(1)_Y$  quantum numbers  $\Phi \sim (3, 2)$ . We also assume that its mass is below  $\mathcal{O}(1)$  TeV and the pair production processes at colliders,

$$pp \rightarrow \Phi^{++}\Phi^{--} \quad \text{and} \quad e^+e^- \rightarrow \Phi^{++}\Phi^{--}, \quad (1)$$

are kinematically allowed. Such a scenario is realized, for example, in the little Higgs models [31–34].

The triplet couples to leptons via the Lagrangian

$$L = i\bar{\ell}_{Li}^c \tau_2 Y_\Phi^{ij} (\tau \cdot \Phi) \ell_{Lj} + \text{H.c.}, \quad (2)$$

where  $(Y_\Phi)_{ij}$  are the Majorana Yukawa couplings of the triplet to the lepton generations  $i, j = e, \mu, \tau$ . If the neutral component of triplet acquires a VEV  $v_\Phi$ , the nonzero neutrino mass matrix is generated via

$$(m_\nu)_{ij} = 2(Y_\Phi)_{ij} v_\Phi. \quad (3)$$

To avoid the existence of phenomenologically unacceptable Majoron the  $B - L$  breaking VEV  $v_\Phi$  cannot occur spontaneously. Instead it should be induced effectively via the coupling of  $\Phi$  to the SM Higgs doublet  $H$  as  $\mu \Phi^0 H^0 H^0$ , where the dimensionful parameter  $\mu$  breaks  $B - L$  explicitly [35]. Because in the limit  $\mu \rightarrow 0$  the symmetry of the model is enhanced, it is natural that  $\mu$

is a small parameter. Model building in this direction [36–38] is beyond the scope of the present analysis. Indeed, the above described scenario is consistent with the observation that neutrino masses are much smaller than the masses of other SM fermions. Thus the smallness of neutrino masses is explained by the smallness of  $v_\Phi$  and the Yukawa couplings  $(Y_\Phi)_{ij}$  can be of order SM Yukawa couplings. The most stringent constraint on them arises from nonobservation of the muon decay  $\mu \rightarrow eee$  which implies  $Y_{ee}Y_{e\mu}^* < 2 \cdot 10^{-5}$  for  $m_\Phi = 1$  TeV [39].

It is important to emphasize that the precise values of  $(Y_\Phi)_{ij}$  are not relevant for the collider physics we consider in this work. The relationship between neutrino parameters and doubly charged Higgs boson decays comes from the fact that the Yukawa coupling matrix of doubly charged Higgs to leptons is proportional to the Majorana mass matrix as given by Eq. (3). Thus, to establish this connection experimentally, observable rates of the leptonic branching fractions must exist.

The decay width of doubly charged Higgs to the corresponding leptonic channel is given by

$$\Gamma_{ij} \equiv \Gamma(\Phi^{\pm\pm} \rightarrow \ell_i^\pm \ell_j^\pm) = \begin{cases} \frac{1}{8\pi} |(Y_\Phi)_{ii}|^2 m_{\Phi^{\pm\pm}} & i = j, \\ \frac{1}{4\pi} |(Y_\Phi)_{ij}|^2 m_{\Phi^{\pm\pm}} & i \neq j, \end{cases} \quad (4)$$

and the decay width to the  $WW$  channel is

$$\begin{aligned} \Gamma_{WW} &\equiv \Gamma(\Phi^{\pm\pm} \rightarrow W_L^\pm W_L^\pm) \\ &= \frac{g_L^4 v_\Phi^2 m_{\Phi^{\pm\pm}}}{16\pi m_{W_L^\pm}^2} \left( \frac{3m_{W_L^\pm}^2}{m_{\Phi^{\pm\pm}}^2} + \frac{m_{\Phi^{\pm\pm}}^2}{4m_{W_L^\pm}^2} - 1 \right) \left( 1 - \frac{4m_{W_L^\pm}^2}{m_{\Phi^{\pm\pm}}^2} \right)^{1/2} \\ &\equiv kv_\Phi^2. \end{aligned} \quad (5)$$

We assume the possible decays  $\Phi^{++} \rightarrow \Phi^+ W^+$  to be kinematically forbidden and neglect them in the following analysis. The branching ratio of  $\Phi^{\pm\pm}$  to a single leptonic channel can be calculated using the decay widths

$$\text{BR}_{ij} \equiv \text{BR}(\Phi^{\pm\pm} \rightarrow \ell_i^\pm \ell_j^\pm) = \frac{\Gamma_{ij}}{\Gamma_{\text{tot}}}, \quad (6)$$

where  $\Gamma_{\text{tot}} = \sum_{i \geq j} \Gamma_{ij} + \Gamma_{WW}$  is the total decay width. Since  $\Gamma_{ij}$  is directly related to neutrino mass matrix, we can derive a relation between the  $\Phi^{++}\Phi^{--}$  branching ratios that can be measured in collider experiments and the neutrino mass matrix, that contains all currently unknown neutrino parameters. The branching ratio to a single decay channel can be found combining Eqs. (3), (4), and (6)

$$\text{BR}(\Phi^{\pm\pm} \rightarrow \ell_i^\pm \ell_j^\pm) = \frac{|(m_\nu)_{ij}|^2}{\sum_{i \geq j} |(m_\nu)_{ij}|^2 + 4kv_\Phi^4}, \quad (7)$$

where  $(m_\nu)_{ij}$  is the neutrino mass matrix in flavor basis.

Equation (7) shows the direct relationship between neutrino parameters and the  $\Phi^{\pm\pm}$  branching ratios.

The neutrino mass matrix can be diagonalized by unitary leptonic mixing matrix  $U$ ,

$$m_\nu = U^* m_\nu^D U^\dagger, \quad (8)$$

where the diagonalized neutrino mass matrix  $m_\nu^D$  is given by

$$m_\nu^D = \begin{pmatrix} m_1 & 0 & 0 \\ 0 & m_2 & 0 \\ 0 & 0 & m_3 \end{pmatrix}.$$

Here  $m_1$ ,  $m_2$ , and  $m_3$  represent the masses of neutrino mass eigenstates  $\nu_1$ ,  $\nu_2$ , and  $\nu_3$ .  $\nu_1$  and  $\nu_2$  masses differ by  $\Delta m_{\text{sol}}^2 = 7.92(1 \pm 0.09) \times 10^{-5}$  eV<sup>2</sup> measured by solar oscillation experiments [40] and  $m_1 < m_2$ . The third eigenstate  $\nu_3$  is separated from the first two by splitting  $\Delta m_{\text{atm}}^2 = 2.6(1_{-0.15}^{+0.14}) \times 10^{-3}$  eV<sup>2</sup> [41] and can be heavier or lighter than the solar pair. The two possibilities are called normal and inverted spectrum, respectively. The third possibility—nearly degenerate masses—appears when the lowest neutrino mass is large compared to the measured mass differences and  $m_1 \approx m_2 \approx m_3$ . Cosmology implies that neutrinos are lighter than about 0.2 eV [42].

Since we have assumed that there are only three Majorana neutrinos,  $U$  is a  $3 \times 3$  mixing matrix that depends on three mixing angles and three phases and can be parametrized as

$$\begin{aligned} U &= \begin{pmatrix} 1 & 0 & 0 \\ 0 & c_{23} & s_{23} \\ 0 & -s_{23} & c_{23} \end{pmatrix} \begin{pmatrix} c_{13} & 0 & s_{13}e^{-i\delta} \\ 0 & 1 & 0 \\ -s_{13}e^{i\delta} & 0 & c_{13} \end{pmatrix} \\ &\times \begin{pmatrix} c_{12} & s_{12} & 0 \\ -s_{12} & c_{12} & 0 \\ 0 & 0 & 1 \end{pmatrix} \begin{pmatrix} e^{i\alpha_1} & 0 & 0 \\ 0 & e^{i\alpha_2} & 0 \\ 0 & 0 & 1 \end{pmatrix}, \end{aligned} \quad (9)$$

where  $c_{ij} \equiv \cos\theta_{ij}$ ,  $s_{ij} \equiv \sin\theta_{ij}$ , and  $\theta_{ij}$  denote the mixing angles. The quantities  $\delta$ ,  $\alpha_1$ , and  $\alpha_2$  are  $CP$  violating phases.  $\delta$  is the Dirac phase and characterizes  $CP$  violation regardless of the character of neutrinos.  $\alpha_1$  and  $\alpha_2$  are called Majorana phases and are physical only if neutrinos are Majorana particles. If the neutrinos were Dirac fermions, both Majorana phases could be absorbed by appropriately redefining the neutrino fields, and the only observable  $CP$  violation parameter would be the Dirac phase  $\delta$ . Also note that  $\delta$  appears in the mixing matrix only as  $\sin\theta_{13}e^{i\delta}$ —so the influence of  $\delta$  crucially depends on the value of  $\theta_{13}$  and has physical consequences only if  $\theta_{13}$  is nonzero.

The mixing matrix contains six independent parameters: three mixing angles ( $\theta_{13}$ ,  $\theta_{23}$ , and  $\theta_{12}$ ) and three phases ( $\alpha_1$ ,  $\alpha_2$ , and  $\delta$ ). Mixing angles are known from the global fit to neutrino oscillation data and are given by ( $2\sigma$  errors) [40,41]

$$\begin{aligned}\sin^2\theta_{12} &= 0.314(1_{-0.15}^{+0.18}), & \sin^2\theta_{23} &= 0.45(1_{-0.20}^{+0.35}), \\ \sin^2\theta_{13} &= 0.8_{-0.8}^{+2.3} \times 10^{-2}.\end{aligned}\quad (10)$$

Up to now no experiment has been able to determine the values of phases so that

$$\delta, \alpha_1, \alpha_2 \in [0, 2\pi], \quad (11)$$

remain unconstrained.

So far we have shown that doubly charged Higgs boson branching ratios are directly related to neutrino parameters as given by Eq. (7) and depend on neutrino mass matrix  $m_\nu^D$  and mixing matrix  $U$ . Additional information can be acquired from the neutrinoless double beta decay experiments, which independently probe the absolute value of the  $(m_\nu)_{ee}$  entry in the neutrino Majorana mass matrix. Such relations allow direct measurements of neutrino parameters in particle collider experiments.

### III. MEASURING NEUTRINO PARAMETERS AT COLLIDERS

We assume that the doubly charged Higgs in this scenario has been produced and discovered as shown in Ref. [22]. The produced doubly charged Higgs bosons have 6 different leptonic decay channels. Branching ratios to these channels are functions of neutrino parameters according to Eq. (7). We have fixed the values of mass differences  $\Delta m_{\text{atm}}^2$  and  $\Delta m_{\text{sol}}^2$  in the subsequent calculations, as they have been measured with a good precision in neutrino oscillation experiments. With such an assumption we can write an equation system of six independent equations that relates branching ratios of six different  $\Phi^{\pm\pm}$  leptonic decay channels with unknown neutrino parameters,

$$\text{BR}_{ij} = f_k(m_0, \text{sign}(\Delta m_{\text{atm}}), \theta_{13}, \theta_{23}, \theta_{12}, \delta, \alpha_1, \alpha_2), \quad (12)$$

where  $m_0$  represents the mass of the lowest neutrino mass eigenstate ( $m_1$  or  $m_3$  for normal or inverted mass spectrum, respectively),  $k = 1, \dots, 6$  and  $i, j = e, \mu, \tau$ . Notice that leptonic tau decays provide extra background to the doubly charged Higgs decay modes with primary electrons and muons. Detection of taus and discriminating this background from the signal has been studied in [22] and we assume that such an analysis provides us with the physical branching ratios. In the subsequent analysis we have used relations between the leptonic branching ratios instead of their absolute values. This method is independent of the possible  $\Phi^{\pm\pm}$  decay to  $WW$  channel, which is more complicated to measure accurately at LHC. In such an approach we simply count the events of  $\Phi^{\pm\pm}$  decays to different channels and calculate their relative differences. As a result we have five independent equations. In order to solve this equation system with respect to unknown neutrino parameters, we have to fix at least some of them.

Consequently we can solve the equation system (12) for different neutrino parameters and obtain them as functions of the  $\Phi^{\pm\pm}$  leptonic branching ratios  $\text{BR}_{ij}$ .

#### A. Results for the tribimaximal mixing

Since approximate values of neutrino mixing angles are known from oscillation experiments and the precision of measurements is expected to be increased in upcoming years [43], we fix their values in most of our analysis. We have chosen to follow the tribimaximal model [44]. It has been proposed that the combined existing data from neutrino oscillations point to a specific form of the lepton mixing matrix with effective bimaximal mixing of  $\nu_\mu$  and  $\nu_\tau$  at the atmospheric scale and effective trimaximal mixing at the solar scale—hence denoted as tribimaximal mixing. The tribimaximal mixing predicts

$$\sin^2\theta_{12} = \frac{1}{3}, \quad \sin^2\theta_{23} = \frac{1}{2}, \quad \sin^2\theta_{13} = 0, \quad (13)$$

which are perfectly compatible with the present experimental uncertainties given by Eq. (10). The main aim of this paper is to provide information about the Majorana phases and absolute values of neutrino masses. In the tribimaximal model the  $CP$  violating phase  $\delta$  is not physical due to the zero value of  $\theta_{13}$  and the only remaining unknown variables are the lowest neutrino mass  $m_0$ , neutrino hierarchy, i.e.,  $\text{sign}(\Delta m_{\text{atm}})$ , and Majorana phases  $\alpha_1$  and  $\alpha_2$ .

Having fixed the mixing angles according to Eq. (13), we end up with four independent equations for branching ratios, since  $\text{BR}_{e\mu} = \text{BR}_{e\tau}$  and  $\text{BR}_{\mu\mu} = \text{BR}_{\tau\tau}$ . If a measurement would show that these branching ratios are not equal, this is a clear indication that the tribimaximal model has to be modified. As we are using the relations between branching ratios for the calculations, the number of independent equations is reduced to three. Such an equation system can be solved with respect to three unknown parameters: the lowest neutrino mass  $m_0$  and Majorana phases  $\alpha_1$  and  $\alpha_2$ . We show how the mass of the lowest neutrino mass eigenstate, neutrino mass hierarchy, and the difference of two Majorana phases  $|\Delta\alpha|$  can be uniquely determined from the relation (7). Unique solutions for  $\alpha_1$  and  $\alpha_2$  are not determined by the  $\Phi^{++}\Phi^{--}$  branching ratios, and two sets of degenerate solutions are found.

#### 1. Neutrino hierarchy and the lowest neutrino mass

First we consider the equation system given by Eq. (12) with the fixed tribimaximal mixing angles. For the neutrino mass hierarchy and lowest neutrino mass determination we combine the branching ratios of  $\mu\mu$ ,  $\mu\tau$ ,  $ee$ , and  $e\mu$  channels. After some simple algebra we find a relation between these branching ratios that depends only on neutrino masses and is independent of the Majorana phases,

$$C_1 \equiv \frac{2\text{BR}_{\mu\mu} + \text{BR}_{\mu\tau} - \text{BR}_{ee}}{\text{BR}_{ee} + \text{BR}_{e\mu}} = \frac{-m_1^2 + m_2^2 + 3m_3^2}{2m_1^2 + m_2^2}. \quad (14)$$

Here and onwards in this paper  $C_x$  denote constant dimensionless parameters which can be measured in experiments.

The mass hierarchy can be easily determined by simply measuring the value of  $C_1$  that is independent of the values of  $\alpha_1$  and  $\alpha_2$ . It can be found that  $C_1$  uniquely determines the mass hierarchy as follows:

- (i)  $C_1 > 1$ —normal mass hierarchy,
- (ii)  $C_1 < 1$ —inverted mass hierarchy,
- (iii)  $C_1 \approx 1$ —degenerate masses.

After the mass hierarchy measurement we can solve Eq. (14) for either normal or inverted mass hierarchy. For the normal mass hierarchy  $m_1$  is the lowest mass state,  $m_2^2 = m_1^2 + \Delta m_{\text{sol}}^2$  and  $m_3^2 = m_1^2 + \Delta m_{\text{sol}}^2 + \Delta m_{\text{atm}}^2$ . After substituting  $m_2$  and  $m_3$ , we get the following equation that can be solved with respect to  $m_1$ ,

$$m_1^2 = \frac{\Delta m_{\text{sol}}^2(4 - C_1) + 3\Delta m_{\text{atm}}^2}{3(C_1 - 1)}. \quad (15)$$

Alternatively, for the inverted mass hierarchy  $m_3$  is the lowest mass state,  $m_2^2 = m_3^2 + \Delta m_{\text{atm}}^2$  and  $m_1^2 = m_3^2 + \Delta m_{\text{atm}}^2 - \Delta m_{\text{sol}}^2$ . After the substitutions, Eq. (14) can be solved with respect to  $m_3$  as follows:

$$m_3^2 = \frac{\Delta m_{\text{sol}}^2(1 + 2C_1) - 3C_1\Delta m_{\text{atm}}^2}{3(C_1 - 1)}. \quad (16)$$

For nearly degenerate masses ( $m_1 > 0.1$  eV) accurate measurement of the lowest neutrino mass requires very

good experimental precision (which is not likely to be achieved at LHC) because the branching ratios are increasingly less mass dependent for larger mass values. This is demonstrated in Fig. 1, which presents the dependency of doubly charged Higgs branching ratios on the lightest neutrino mass for the normal and inverted mass hierarchies. We have assumed a real mixing matrix, i.e., fixed Majorana phases to zero. The  $e\mu$  and  $e\tau$  channels have only vanishingly small contributions for  $\alpha_1 = \alpha_2 = 0$ , but are increased for nonzero values of the Majorana phases. The branching ratio to  $ee$  channel is a especially good characteristic for mass hierarchy determination that varies greatly depending on the hierarchy and the neutrino mass. This branching ratio is negligible for the normal mass hierarchy with very small mass while it is the dominant decay channel for the inverted mass hierarchy. If the mass of the lightest state increases, both the normal and inverted hierarchies have almost the same distribution of branching ratios,  $\Phi^{\pm\pm}$  decay to  $ee$ ,  $\mu\mu$ , and  $\tau\tau$  with nearly equal probabilities while the decays to other channels are negligible. This indicates the degenerate masses.

## 2. Majorana phases

If the neutrino masses are measured as shown in the previous section, we can determine the values of Majorana phases in a similar way. Once again we use the tribimaximal values for all mixing angles and combine expressions from the equation system (12). We first determine the difference between the Majorana phases  $\Delta\alpha = |\alpha_1 - \alpha_2|$ . Using a relation between the  $ee$  and  $e\mu$  decays channels we obtain

$$C_2 \equiv \frac{\text{BR}_{e\mu}}{\text{BR}_{ee}} = \frac{2(m_1^2 + m_2^2 - 2m_1m_2 \cos\Delta\alpha)}{4m_1^2 + m_2^2 + 4m_1m_2 \cos\Delta\alpha}. \quad (17)$$

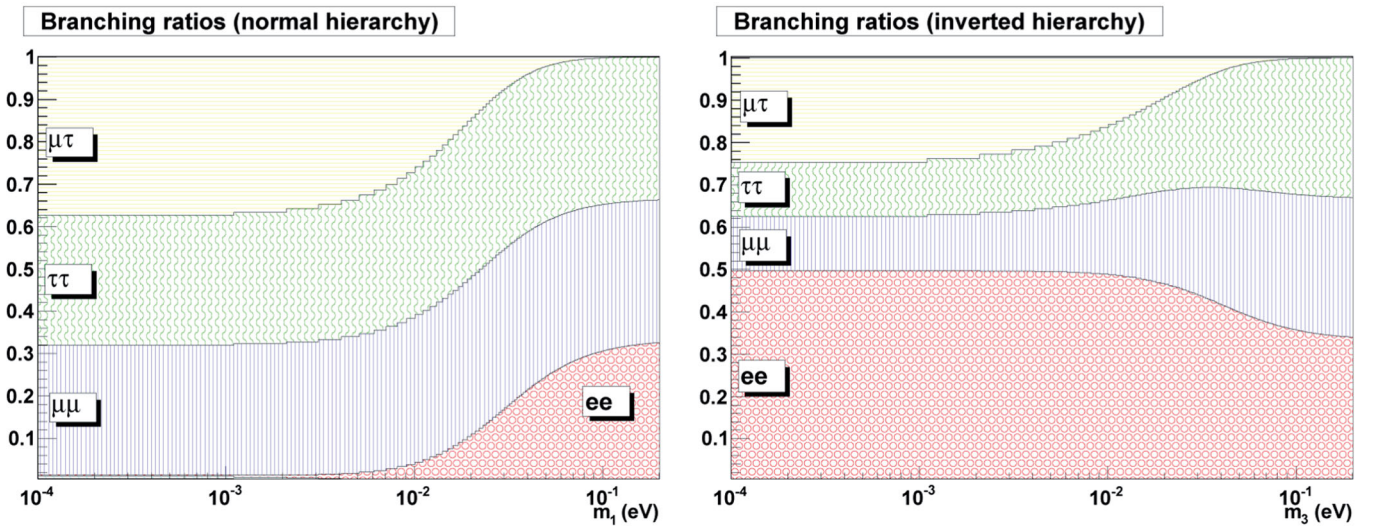


FIG. 1 (color online). Distribution of the  $\Phi^{++}$  leptonic branching ratios as a function of the lightest neutrino mass. The left (right) panel corresponds to the normal (inverted) mass hierarchy. For nearly degenerate masses the two possibilities imply almost the same result.

From this expression we can find separate solutions for the different mass hierarchies. For the normal hierarchy  $\Delta\alpha$  can be found to be

$$\Delta\alpha = \arccos\left(\frac{(4 - 5C_2)m_1^2 + (2 - C_2)\Delta m_{\text{sol}}^2}{4(1 + C_2)m_1\sqrt{m_1^2 + \Delta m_{\text{sol}}^2}}\right), \quad (18)$$

while for the inverted hierarchy we find

$$\Delta\alpha = \arccos\left(\frac{2(2C_2 - 1)\Delta m_{\text{sol}}^2 + (4 - 5C_2)(\Delta m_{\text{atm}}^2 + m_3^2)}{4(1 + C_2)\sqrt{(\Delta m_{\text{atm}}^2 + m_3^2)(m_3^2 + \Delta m_{\text{atm}}^2 - \Delta m_{\text{sol}}^2)}}\right), \quad (19)$$

which can be approximated as

$$\Delta\alpha = \arccos\left(\frac{4 - 5C_2}{4(1 + C_2)}\right) + \mathcal{O}\left(\frac{\Delta m_{\text{sol}}^2}{\Delta m_{\text{atm}}^2}\right). \quad (20)$$

For the inverted hierarchy, up to small corrections, the equation for  $\Delta\alpha$  is independent of the value of  $m_3$ . This means that Eq. (20) is valid both for the inverted hierarchy and degenerate mass spectrum. The solution for the normal hierarchy given by Eq. (18) contains the lowest neutrino mass which must be measured previously with an acceptable precision.

We found that  $|\Delta\alpha|$  can be uniquely determined up to a sign uncertainty  $\text{sgn}(\alpha_1 - \alpha_2)$  since cosine is an even function. In order to find a solution that separately determines  $\alpha_1$  and  $\alpha_2$ , we use the expression for  $\Delta\alpha$  given either by Eq. (18) or Eq. (20) together with the definition of cosine of the difference of angles and construct the equation system of two independent equations,

$$C_3 \equiv \frac{2\text{BR}_{\mu\mu} - \text{BR}_{\mu\tau}}{\text{BR}_{ee} + \text{BR}_{e\mu}} = \frac{2m_3(\cos\alpha_1 m_1 + 2\cos\alpha_2 m_2)}{2m_1^2 + m_2^2},$$

$$\cos\Delta\alpha = \cos\alpha_1 \cos\alpha_2 + \sin\alpha_1 \sin\alpha_2. \quad (21)$$

Unfortunately such an equation system does not have a unique solution due to the uncertainty in  $\text{sgn}(\alpha_1 - \alpha_2)$ , and two sets of degenerate solutions for  $\alpha_1$  and  $\alpha_2$  are found, one of which is correct for  $\alpha_1 > \alpha_2$  and the other corresponding to  $\alpha_2 > \alpha_1$ . It is not possible to tell only from the collider data which angle is bigger and which of

the solutions is correct. In the following we present the effect of the Majorana phases to branching ratios for three different mass hierarchies and discuss the consequences of nonvanishing  $\theta_{13}$ .

## B. Measuring Majorana phases for different mass hierarchies

In this section we study some well motivated particular cases of neutrino mass parameters which can be well measured at LHC. Those are:

- (i) Normal mass hierarchy,  $m_1 = 0$ . Branching ratios are independent of  $\alpha_1$ ;  $\alpha_2$  can be determined.
- (ii) Inverted mass hierarchy,  $m_3 = 0$ . Branching ratios are independent of absolute values of Majorana phases;  $\Delta\alpha = |\alpha_1 - \alpha_2|$  can be determined.
- (iii) Nearly degenerate masses,  $m_1 \approx m_2 \approx m_3 = m$ . Expressions for branching ratios become independent of  $m$ .

We have kept the mixing angles fixed to tribimaximal values unless stated otherwise.

### 1. Normal hierarchy, $m_1 = 0$

In this case the doubly charged Higgs branching ratios are independent of  $\alpha_1$  and we can determine  $\alpha_2$ . Branching ratios to the decay channels that involve electrons can be neglected and, for expressing the solutions, we use the branching ratios to  $\mu\mu$  and  $\mu\tau$  channels. The relation between these channels gives the following equation with  $\alpha_2$  as the only unknown parameter:

$$C_4 \equiv \frac{\text{BR}_{\mu\mu}}{\text{BR}_{\mu\tau}} = \frac{13\Delta m_{\text{sol}}^2 + 9\Delta m_{\text{atm}}^2 + 12\cos\alpha_2\sqrt{\Delta m_{\text{sol}}^2}\sqrt{\Delta m_{\text{sol}}^2 + \Delta m_{\text{atm}}^2}}{2(13\Delta m_{\text{sol}}^2 + 9\Delta m_{\text{atm}}^2 - 12\cos\alpha_2\sqrt{\Delta m_{\text{sol}}^2}\sqrt{\Delta m_{\text{sol}}^2 + \Delta m_{\text{atm}}^2})}. \quad (22)$$

This can be solved uniquely for  $\alpha_2$  as

$$\alpha_2 = \arccos\left(\frac{(2C_4 - 1)(13\Delta m_{\text{sol}}^2 + 9\Delta m_{\text{atm}}^2)}{12(1 + 2C_4)\sqrt{\Delta m_{\text{sol}}^2}\sqrt{\Delta m_{\text{sol}}^2 + \Delta m_{\text{atm}}^2}}\right). \quad (23)$$

The distribution of branching ratios for the tribimaximal mixing angles is shown in the left panel of Fig. 2. The dominant decay channels are  $\mu\mu$ ,  $\tau\tau$ , and  $\mu\tau$ . Decays including electrons can be neglected, since the branching ratios to the  $ee$ ,  $e\mu$ , and  $e\tau$  channels are suppressed by  $\Delta m_{\text{sol}}^2/\Delta m_{\text{atm}}^2$ , which is small compared to the relevant terms in other decay channels. Nonzero  $\alpha_2$  causes a small

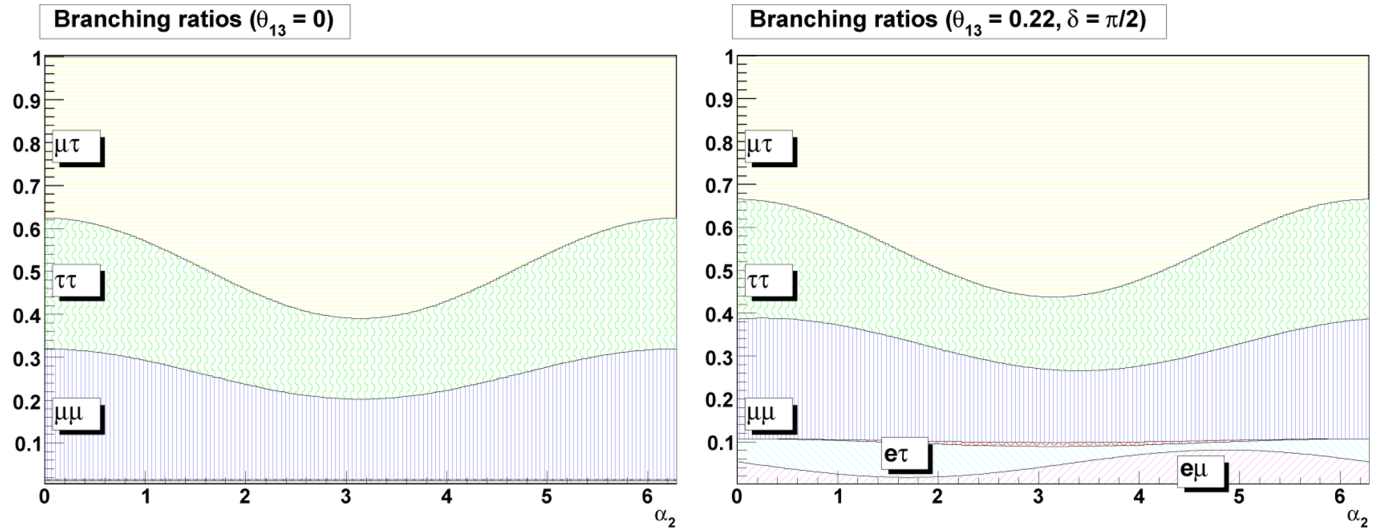


FIG. 2 (color online). Distributions of the branching ratios as a function of  $\alpha_2$ . The left panel corresponds to  $\theta_{13} = 0$  with the  $ee$ ,  $e\mu$ , and  $e\tau$  channels giving nearly negligible contributions. When  $\theta_{13}$  is nonzero (the right panel), small branching ratios to  $e\mu$  and  $e\tau$  channels can be measured. Nonzero  $\delta$  in the right panel causes the slight asymmetry with respect to  $\alpha_2 = \pi$ .

variation in branching ratios; the  $\mu\tau$  channel is increased while the  $\tau\tau$  and  $\mu\mu$  channels are reduced proportionally. The right panel shows the effect of nonzero  $\theta_{13}$  and  $\delta$  that create small nonzero contributions to the  $e\mu$  and  $e\tau$  channels. In this case nonzero  $\theta_{13}$  could be clearly detected. However, those can comprise only about 10% of all the decays and require high statistics to be adequately measured at colliders. We also emphasize that the asymmetry of distributions in this case is  $CP$ -violation effect due to nonvanishing Dirac phase  $\delta$ .

In conclusion, if we have identified the normal mass hierarchy with nearly zero value of  $m_1$ , which is being described by  $\mu\mu$ ,  $\mu\tau$ , and  $\tau\tau$  as the dominant decay channels, we can measure  $\alpha_2$  from the ratio between  $\mu\mu$  and  $\mu\tau$  channels. We note that the changes in branching ratios are symmetrical with respect to  $\alpha_2 = \pi$  and we always have two possible solutions. The nonzero  $\theta_{13}$  and  $\delta$  can create a slight asymmetry in the solutions due to the  $CP$ -violation and thus provide a possibility of unique determination of  $\alpha_2$ . However, this is a very small effect that requires a precision measurement and most likely can not be detected at the LHC.

## 2. Inverted hierarchy, $m_3 = 0$

In this case the branching ratios do not depend on absolute values of Majorana phases and only their relative difference  $\Delta\alpha$  can be measured. We still can use Eq. (20) to determine the value of  $\Delta\alpha$ . The distribution of all  $\Phi^{\pm\pm}$  branching ratios as functions of  $\Delta\alpha$  is presented in Fig. 3. One can see that the changes in branching ratios caused by nonzero  $\Delta\alpha$  are much more prominent than the changes caused by  $\alpha_2$  for normal hierarchy. When  $\Delta\alpha = 0$ ,  $ee$  is the dominant decay channel and the  $e\mu$  and  $e\tau$  channels can have only very small contributions resulting from

small nonzero  $\theta_{13}$ . If  $\theta_{13} = 0$  is assumed, any nonzero contribution to the  $e\mu$  or  $e\tau$  channels would indicate nonzero value of  $\Delta\alpha$ . Nonzero  $\Delta\alpha$  suppresses the  $ee$  channel considerably, and the branching ratios to  $e\mu$  and  $e\tau$  channels can occupy more than 80% of all leptonic decays. The branching ratio to the  $ee$  channel remains nonzero in this case. The effect of nonzero  $\theta_{13}$  and  $CP$  violation angle  $\delta$  is presented in the right panel of Fig. 3. The nonzero  $\theta_{13}$  causes small changes in branching ratios. For  $\Delta\alpha = 0$ , it causes an increase of the branching ratios to  $e\mu$  and  $e\tau$  channels while the number of decays to the  $ee$  channel is decreased. For  $\Delta\alpha \approx \pi$ , the branching ratios to the  $\mu\mu$  and  $\tau\tau$  channels are increased. The nonzero Dirac phase  $\delta$  is responsible for the small asymmetry of the plot with respect to  $\Delta\alpha = \pi$ . As in the previous case, the asymmetry is a signal of  $CP$ -violation. Such a small deviations are, however, very difficult to measure at colliders in practice.

## 3. Degenerate masses

When neutrino masses are large compared to the mass differences  $\Delta m_{\text{sol}}$  and  $\Delta m_{\text{atm}}$ , all three mass states are approximately equal and we can use the model of nearly degenerate neutrino masses:  $m_1 \approx m_2 \approx m_3 = m$ . As shown before, the exact value of neutrino mass can not be determined by  $\Phi^{\pm\pm}$  decay statistics, since  $m$  becomes independent of branching ratios in the degenerate limit. This means that  $m$  is canceled from the expressions for branching ratios and the calculation of the Majorana phases is significantly simplified. To obtain general predictions we first assume a small value of  $\theta_{13}$ , so that higher order terms of the expansion can be neglected, and do not fix other parameters.

First we can check whether any of the Majorana phases has a nonzero value. When  $\alpha_1 = \alpha_2 = 0$ , we would ob-

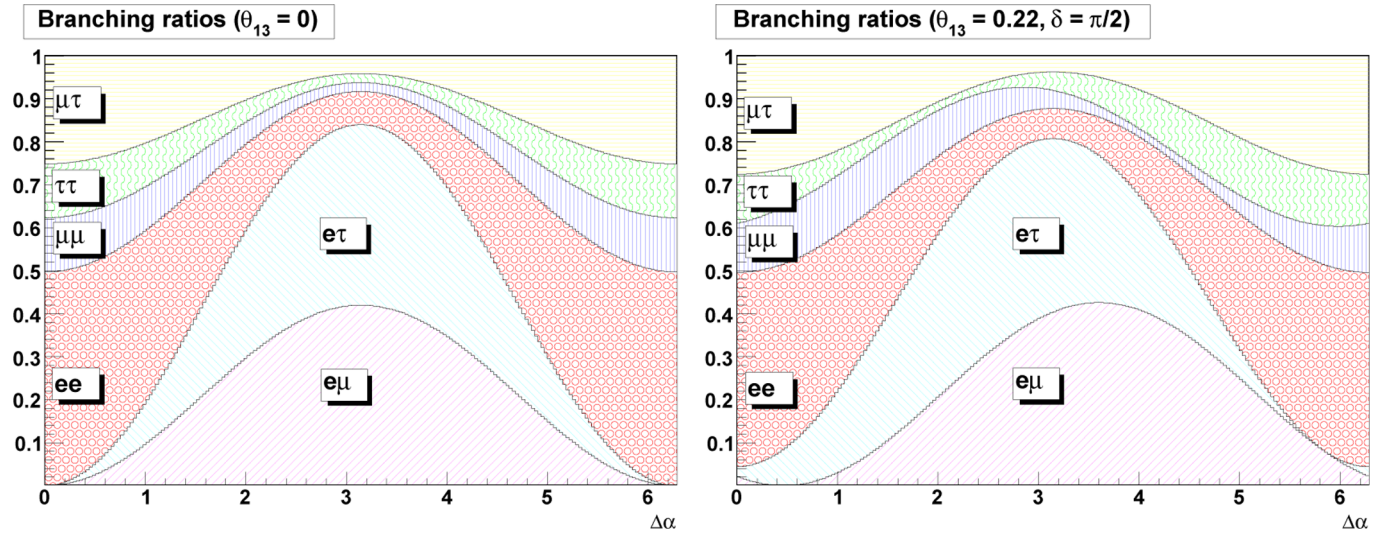


FIG. 3 (color online). Distribution of the  $\Phi^{\pm\pm}$  branching ratios as a function of  $\Delta\alpha$  for  $\theta_{13} = 0$  (left panel), and  $\theta_{13} = 0.22$ ,  $\delta = \pi/2$  (right panel). The asymmetry of the latter plot signals nonvanishing  $CP$ -violation.

serve nearly equal amount of decays to  $ee$ ,  $\mu\mu$ , and  $\tau\tau$  channels, while all other decay channels would be suppressed:

$$\text{BR}_{ee} \approx \text{BR}_{\mu\mu} = \text{BR}_{\tau\tau} = \frac{1}{3}, \quad (24)$$

$$\text{BR}_{e\mu} = \text{BR}_{e\tau} = \text{BR}_{\mu\tau} = 0. \quad (25)$$

Nonvanishing branching ratios to  $e\mu$  and  $e\tau$  channels are clear indicators for nonzero  $\Delta\alpha$ . When  $\alpha_1 = \alpha_2 = \alpha$  branching ratios to both  $e\mu$  and  $e\tau$  channels are very close to zero  $\text{BR}_{e\mu} = \text{BR}_{e\tau} \approx 0$ . A small nonzero contribution can be added when  $\theta_{13}$  has a value that is close to its upper limit and higher order effects (nonzero  $\sin^2\theta_{13}$ ) become influential.

A very clearly recognizable signature appears when both Majorana phases are maximal ( $\alpha_{1,2} = \pi$ ). If we also assume  $\theta_{23} = \pi/4$  (the best fit value), then  $\Phi^{\pm\pm}$  has only two possible decay channels predicting  $\text{BR}_{ee} = 0.34$  and  $\text{BR}_{\mu\tau} = 0.66$ , while all other channels are completely suppressed. Small deviations in  $\theta_{23}$  cause small contributions to the  $\mu\mu$  and  $\tau\tau$  channels while the branching ratio to  $\mu\tau$  channel is decreased by the same amount.

The behavior of branching ratios is plotted in Figs. 4 and 5, which present the dependence of branching ratios on  $\Delta\alpha$ . The case for  $\alpha_2 = 0$  is shown in the left panel and the one for  $\alpha_1 = 0$  in the right panel. Figure 5 shows the branching ratios for different values of Majorana phases when  $\Delta\alpha = 0$ . If we have identified the degeneracy of neutrino masses, we can analyze the values of Majorana

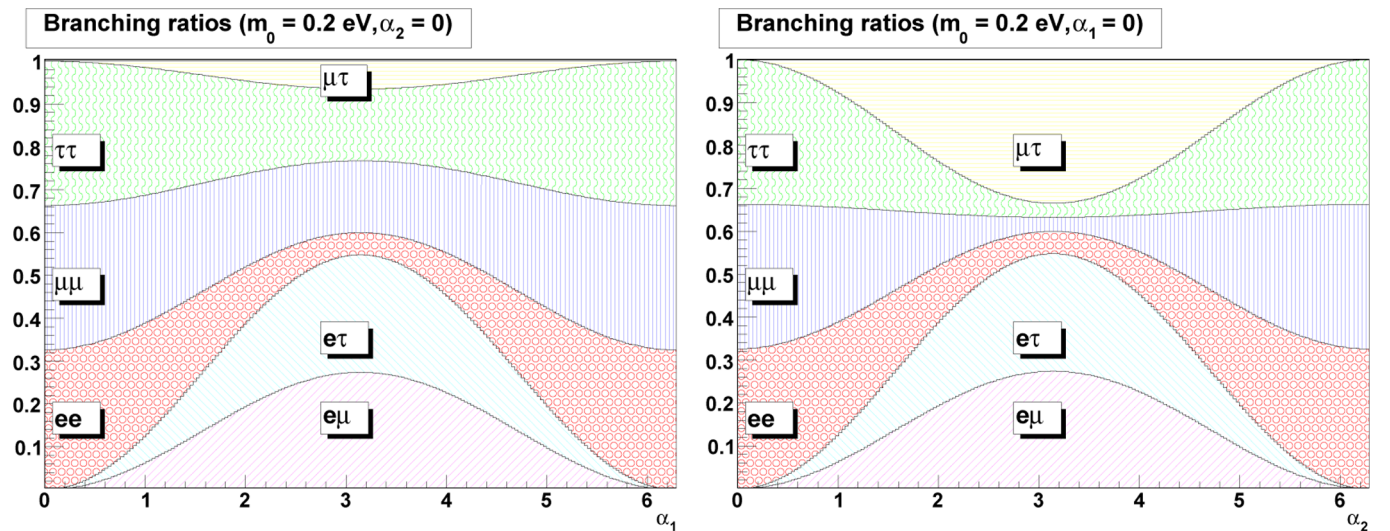


FIG. 4 (color online). Distributions of the  $\Phi^{\pm\pm}$  branching ratios for nonzero  $\Delta\alpha$ . The left figure presents the case for fixed  $\alpha_2 = 0$ , and the right figure for fixed  $\alpha_1 = 0$ .

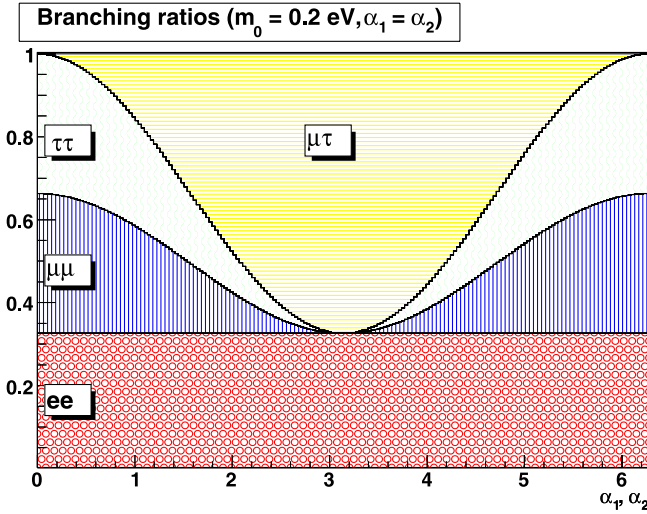


FIG. 5 (color online). Distributions of the  $\Phi^{\pm\pm}$  branching ratios for different values of  $\alpha_1$  and  $\alpha_2$ , assuming  $\Delta\alpha = 0$ .

phases without making any assumption about the values of mixing angles.

- (i) Equal branching ratios to the  $ee$ ,  $\mu\mu$ , and  $\tau\tau$  channels with all other channels being suppressed indicates that  $\alpha_1 = \alpha_2 = 0$ .
- (ii) Nonzero branching ratio to the  $\mu\tau$  channel means that at least one of the Majorana phases has to be nonzero.
- (iii) Nonzero branching ratios to the  $e\mu$  and  $e\tau$  channels and the deviation from the result  $\text{BR}_{ee} = 0.34$  can be generated only by nonzero  $\Delta\alpha$ . Small nonzero contribution to the  $e\mu$  and  $e\tau$  channels can be alternatively caused by a large value of  $\theta_{13}$ .

To give exact solutions for the Majorana phases, we fix the values of mixing angles according to the tribimaximal model.  $|\Delta\alpha|$  can be found from Eq. (20) which is valid both for the inverted mass hierarchy and the degenerate spectrum. Separate values for  $\alpha_1$  and  $\alpha_2$  can be determined from the equation system

$$C_5 \equiv \frac{2\text{BR}_{\mu\tau} - \text{BR}_{ee}}{2\text{BR}_{\mu\mu} + \text{BR}_{\mu\tau} + \text{BR}_{e\mu}} = \frac{1}{6}(3 - 2\cos\alpha_1 - 4\cos\alpha_2), \quad (26)$$

$$\cos\Delta\alpha = \cos\alpha_1 \cos\alpha_2 + \sin\alpha_1 \sin\alpha_2 = \frac{4 - 5C_2}{4(1 + C_2)}.$$

Again, two possible sets of solutions are found for the Majorana phases and the  $\Phi^{\pm\pm}$  branching ratios do not provide the information to decide which of the solutions is correct.

### C. Effects of nonzero $\theta_{13}$

If our assumption about the exact tribimaximal neutrino mixing should not be valid, the form of previously obtained

solutions would also be changed. However, the results and methodology would generally remain the same. Hopefully new upcoming neutrino oscillation experiments will measure the mixing angles with improved precision in the near future [43]. Small changes in  $\theta_{23}$  or  $\theta_{12}$  would not affect the structure of the found solutions, and we would only need to substitute different values for the mixing angles. Qualitative changes in the analytical expressions appear if  $\theta_{13}$  is taken to be nonvanishing. This influences the structure of the solutions and makes the  $CP$ -violating angle  $\delta$  a physically measurable quantity. We note, however, that, due to the smallness of  $\sin\theta_{13}$ , the effect of  $\theta_{13}$  and  $\delta$  would enter to the branching ratios as a small correction, and extremely precise measurements would be required to detect it. The goal of this section is to analyze the effect of nonzero  $\theta_{13}$  to the previously found solutions for Majorana phases and neutrino masses.

In the following we have still assumed  $\theta_{13}$  to be a small parameter and considered only the leading terms in the expansion with respect to it. We can find the lowest neutrino mass from the same equation as for  $\theta_{13} = 0$  (see Eq. (14)), only the measured parameter  $C_1$  is replaced by  $C'_1$ . The calculation of parameter  $C'_1$  involves more decay channels than  $C_1$  as the relations  $\text{BR}_{e\mu} = \text{BR}_{e\tau}$  and  $\text{BR}_{\mu\mu} = \text{BR}_{\tau\tau}$  no longer hold:

$$C'_1 \equiv \frac{2\text{BR}_{\mu\mu} + 2\text{BR}_{\tau\tau} + 2\text{BR}_{\mu\tau} - 2\text{BR}_{ee}}{2\text{BR}_{ee} + \text{BR}_{e\mu} + \text{BR}_{e\tau}} = \frac{-m_1^2 + m_2^2 + 3m_3^2}{2m_1^2 + m_2^2} + \mathcal{O}(\sin^2\theta_{13}). \quad (27)$$

Similarly the determination of Majorana phases has exactly the same structure as earlier.  $\Delta\alpha$  can be determined uniquely and two possible sets of solutions are found for  $\alpha_1$  and  $\alpha_2$  when we attempt to determine the absolute values of Majorana phases. All solutions remain valid for  $\theta_{13} = 0$  and can be used for calculations in case  $\theta_{13}$  remains to be unknown.

In conclusion, assuming small but nonzero  $\theta_{13}$  does not significantly complicate the determination of neutrino parameters at colliders. The solutions would only be more complex and involve more decay channels. There is a theoretical possibility to find solutions also for  $\theta_{13}$  and  $\delta$ , but such solutions are very sensitive to experimental errors and, in practice, cannot be used at the LHC.

### D. Estimation of the impact of experimental uncertainties

In this section we consider the effects of experimental uncertainties to the determination of  $\Phi^{\pm\pm}$  leptonic branching ratios at colliders and, consequently, to the determination of neutrino parameters in collider experiments. The sources of the uncertainties under consideration are

- (i) *Statistical errors* that are relevant for a small number of reconstructed events. In this case the number of

events observed in particle colliders follows the Poisson statistics with theoretically expected average number of events as a mean value.

- (ii) *Random measurement errors* that dominate in the case of large statistical samples and result from the errors in the measurements of particle energies and momentas in the detector and in the event reconstruction. Those errors vary greatly for different decay channels and their values are strongly experiment and detector specific.
- (iii) *Systematical measurement errors* in the measurements of particle parameters and event reconstruction.

For the numerical simulation of experimental uncertainties we have first modified the theoretically expected number of doubly charged Higgs production events  $N^{\text{theor}}$  with the Poisson distribution, then calculated and normalized the corresponding branching ratios and finally modified them with Gaussian distortion functions to account for random measurement errors. Possible systematical errors have been neglected. Note that for  $\Phi^{\pm\pm}$  pair production each detected event comprises two doubly charged Higgs decays and  $N^{\text{theor}} = 2N^{\text{events}}$ .

In reality the measurement errors are different for different decay channels and their values depend on the specific detector. As full detector-specific error analysis is out of the scope of this paper, we have used uniform uncertainties for all branching ratios for the rough estimation of the effect. In particular, we have assumed Gaussian distortion functions with  $\sigma_{\text{BR}} = 0.1\text{BR}_{ij}^{\text{theor}}$ , where  $\text{BR}_{ij}^{\text{theor}}$  is the theoretically expected branching ratio into the corresponding decay channel and  $i, j = e, \mu, \tau$ . Finally we have run the simulation with randomly distorted branching ratios for 50 000 times, calculating each time the neutrino parameter

of interest. As a result we get the distribution function of particular neutrino parameter which measures the stability of previously found analytical solutions.

### 1. Mass hierarchy determination

We remind that the neutrino mass hierarchy is identified by the parameter  $C_1$ , defined in Eq. (14), as follows:  $C_1 > 1$  corresponds to the normal hierarchy,  $C_1 < 1$  to the inverted hierarchy, and  $C_1 \approx 1$  to the nearly degenerate mass spectrum. In general, if the lowest neutrino mass is close to zero, the mass hierarchy is very well determined. When the mass increases, the distribution of branching ratios is reaching the nearly degenerate limit and the mass hierarchy or  $\text{sign}(\Delta m_{\text{atm}})$  is increasingly more difficult to measure.

As an example we have analyzed the behavior of  $C_1$  for three different cases: the normal hierarchy for  $m_0 = 0.02$  eV, the inverted hierarchy for  $m_0 = 0.02$  eV, and the nearly degenerate limit for  $m_0 = 0.2$  eV. The results are presented in Fig. 6 which shows the simulated experimental distribution of  $C_1$  for two cases with different statistical samples of events. Those imply the following  $1\sigma$  errors.

- (1) Normal hierarchy ( $m_0 = 0.02$  eV)
  - (a) 1000  $\Phi^{\pm\pm}$  decays:  $C_1 = 6.6 \pm 1.1 \gg 1$ ,
  - (b) 100  $\Phi^{\pm\pm}$  decays:  $C_1 = 6.6 \pm 2.1 \gg 1$ .
- (2) Degenerate limit ( $m_0 = 0.2$  eV)
  - (a) 1000  $\Phi^{\pm\pm}$  decays:  $C_1 = 1.0 \pm 0.3$ ,
  - (b) 100  $\Phi^{\pm\pm}$  decays:  $C_1 = 1.0 \pm 0.5$ .
- (3) Inverted hierarchy ( $m_0 = 0.02$  eV)
  - (a) 1000  $\Phi^{\pm\pm}$  decays:  $C_1 = 0.06 \pm 0.15 \ll 1$ ,
  - (b) 100  $\Phi^{\pm\pm}$  decays:  $C_1 = 0.06 \pm 0.28 \ll 1$ .

The results show that sufficiently good hierarchy detection accuracy is achieved for small lightest neutrino masses

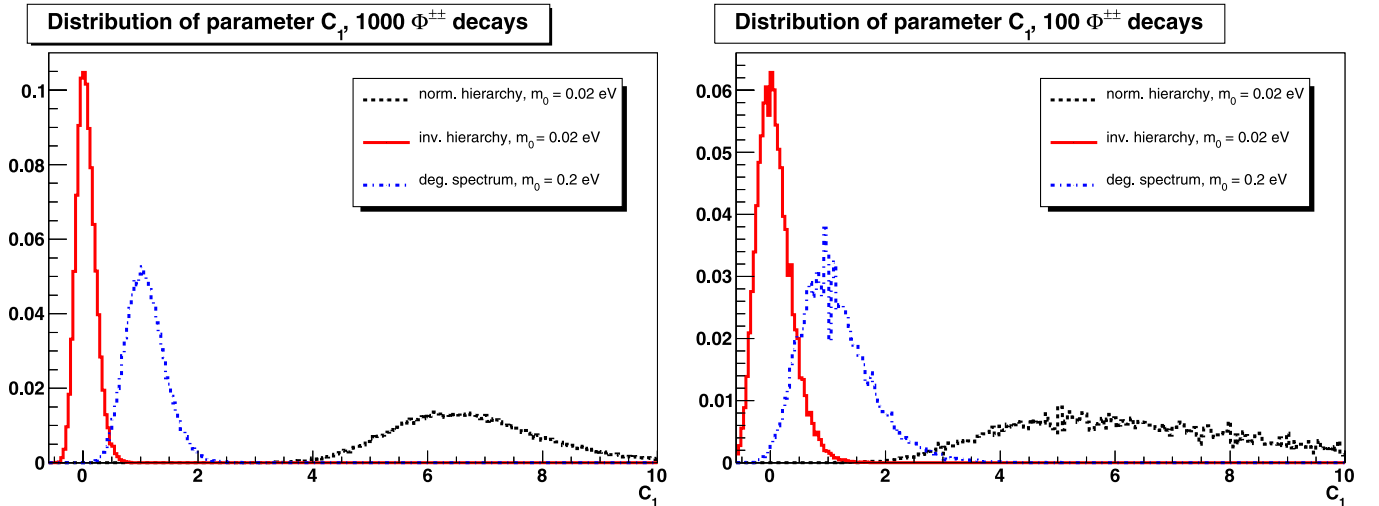


FIG. 6 (color online). Simulated distributions of the parameter  $C_1$  due to experimental errors for statistical samples of 1000 and 100  $\Phi^{\pm\pm}$  decays in the left and right panel, respectively. We have assumed  $\sigma_{\text{BR}} = 0.1\text{BR}_{ij}^{\text{theor}}$  for the branching ratio measurement errors. The solid line represents the inverted hierarchy with  $m_0 = 0.02$  eV, the dot-dashed line the degenerate spectrum with  $m_0 = 0.2$  eV, and the dashed line the normal hierarchy with  $m_0 = 0.02$  eV.

in both the normal and the inverted hierarchy cases. The accuracy decreases when the mass  $m_0$  increases and  $C_1 \rightarrow 1$ . Such tendency can be understood by comparing the normal and the inverted hierarchy plots in Fig. 1 where the distribution of branching ratios clearly differs for small mass values and becomes very similar to each other when the mass is increased. Figure 6 shows that the normal hierarchy is very well determined by the parameter  $C_1$  even for small statistics, while at  $3\sigma$  level the inverted hierarchy can be confused with the degenerate mass spectrum for small statistics. The main factor that clearly distinguishes the normal mass hierarchy with small  $m_0$  is the negligible value of  $\text{BR}_{ee}$  that can not occur for the inverted or degenerate spectra.

## 2. $m_0$ measurement

After the neutrino mass hierarchy has been determined, we can use either Eq. (15) (for the normal hierarchy) or Eq. (16) (for the inverted hierarchy) to estimate the value of the lowest neutrino mass. In the following we analyze the achievable precision for these parameters. Again, for small values of  $m_0$  the measurement precision is sufficiently high and decreases when  $m_0$  approaches the degenerate values.

As already verified by the hierarchy determination accuracy, the normal hierarchy provides a distinguishable signature and could thus be easily identified, while the inverted hierarchy can be confused with the degenerate spectrum. Such a tendency is also notable in the measurement of lowest neutrino mass. For the normal hierarchy not only hierarchy but also the actual value of the lowest neutrino mass can be measured with relatively good precision. Turning back to our earlier example we assume the true value of the lowest neutrino mass to be  $m_1 = 0.02$  eV,  $\sigma_{\text{BR}} = 0.1\text{BR}_{ij}^{\text{theor}}$  to be the branching ratio measurement errors at collider experiments, and find that the  $1\sigma$  experimental errors for the lightest neutrino masses are  $\delta m_1 = 2 \cdot 10^{-3}$  eV and  $\delta m_1 = 5 \cdot 10^{-3}$  eV for the statistical samples of 1000 and 100  $\Phi^{\pm\pm}$  decays, respectively. In order to measure  $m_3$  from Eq. (16) for the inverted mass hierarchy with comparable precision, a very good statistical basis (more than 5000 events) and the measurement errors smaller than  $\sigma_{\text{BR}} = 0.01\text{BR}_{ij}^{\text{theor}}$  are required. The data of such quality would not be obtainable from the LHC experiments but only from the future colliders (possibly ILC).

## 3. Measurement of Majorana phases

Determination of Majorana phases is discussed in detail in Sec. III B. It depends on the neutrino mass hierarchy. For the normal mass hierarchy with small  $m_1$  it is very difficult to estimate the Majorana phases with realistic measurement errors. This is due to the fact that the only observable  $\alpha_2$  does not significantly influence the distribution of branching ratios (see Fig. 2). To the contrary, for the degenerate spectrum or inverted hierarchy the Majorana

phases strongly influence the distribution of branching ratios which, in principle, can be measured in realistic experimental conditions. As an example we estimate the measurement error for  $\Delta\alpha$  for the inverted hierarchy. As we have shown earlier in Eq. (20), to high accuracy such a calculation does not depend on the value of  $m_3$ . We find that the  $1\sigma$  errors for  $\Delta\alpha$  are  $0.06\pi$  and  $0.03\pi$  for 100 and 1000  $\Phi^{\pm\pm}$  decays, respectively. Similar precision is achieved assuming the degenerate spectrum. This result is general and does not depend considerably on the particular value of  $\Delta\alpha$ .

Full detector-specific analysis for the measurement errors of branching ratios requires separate analyses. The error estimations that are found in this section are only approximate, but still emphasize the promising nature of our method for determining neutrino parameters in particle collider experiments.

## IV. DETERMINATION OF TRIPLET HIGGS VEV

In our scenario the neutrino mass matrix is directly related to the doubly charged Higgs leptonic branching fractions according to Eq. (3), and the overall normalization factor is the triplet Higgs VEV  $v_\Phi$ . Therefore, one needs additional experimental measurements for determination of  $v_\Phi$ , and thus the entire low energy neutrino mass matrix. Those measurements can come either from collider physics, from the low energy neutrino mass measurements, or from cosmology.

Let us first assume that  $v_\Phi$  is large enough to imply, according to Eq. (5), observable fraction of the decays  $\Phi^{++} \rightarrow W^+W^+$ , and the collider experiments are sensitive enough to measure not just the branching fractions but also the partial widths of the triplet, namely,  $\Gamma_{ij}$  and  $\Gamma_{WW}$ . The latter may not be possible at LHC but could be possible at ILC experiments [45] if the collision energy is sufficient for the  $\Phi^{++}$  production. In such a case one gets from Eq. (4) and (5),

$$\begin{aligned} \frac{\text{BR}_{ll}}{\text{BR}_{WW}} &= \frac{\Gamma_{ll}}{\Gamma_{WW}} = \frac{\Gamma_{ll}}{kv_\Phi^2} \Rightarrow v_\Phi = \sqrt{\frac{\Gamma_{ll}\text{BR}_{WW}}{k\text{BR}_{ll}}} \\ &= \sqrt{\frac{\Gamma_{\text{tot}}\text{BR}_{WW}}{k}}, \end{aligned} \quad (28)$$

and the determination of  $v_\Phi$  from collider experiments is possible.

If the collider experiments are not able to measure the partial widths of the triplet, one needs additional information on the neutrino mass matrix. Assuming that the branching ratio to  $WW$  channel is measured at any accelerator experiment and  $|(m_\nu)_{ee}|$  is probed from  $0\nu\beta\beta$  experiment one gets

$$\frac{\text{BR}_{ee}}{\text{BR}_{WW}} = \frac{\Gamma_{ee}}{\Gamma_{WW}} = \frac{1}{32\pi} \frac{|(m_\nu)_{ee}|^2 m_{\Phi^{\pm\pm}}}{kv_\Phi^4}. \quad (29)$$

Now  $v_\Phi$  can be directly found as

$$v_\Phi = \left( \frac{|(m_\nu)_{ee}|^2 m_{\Phi^{\pm\pm}} \text{BR}_{WW}}{32\pi k \text{BR}_{ee}} \right)^{1/4}. \quad (30)$$

Finally, if  $v_\Phi$  is too small to imply observable  $\Phi \rightarrow WW$  decay rates at colliders, one has to rely entirely on leptonic data. If one of the leptonic Yukawa couplings is directly measured in the accelerator experiments and  $|(m_\nu)_{ee}|$  is probed from the  $0\nu\beta\beta$  experiments, one is able to derive the VEV from data. As the simplest example, when  $\Gamma_{ee}$  is measured, perhaps from the resonance at  $e^-e^-$  collider [46], the VEV can be directly found from

$$\Gamma_{ee} = \frac{|(m_\nu)_{ee}|^2 m_{\Phi^{\pm\pm}}}{32\pi v_\Phi^2} \Rightarrow v_\Phi = \sqrt{\frac{|(m_\nu)_{ee}|^2 m_{\Phi^{\pm\pm}}}{32\pi\Gamma_{ee}}}. \quad (31)$$

As shown, direct measurement of the VEV is possible. However it does require additional information which cannot be obtained from the LHC alone. Should the  $0\nu\beta\beta$  yield positive results or some of the triplet Yukawa coupling be measured at ILC, we can also give estimates on the magnitude of the VEV of the Higgs triplet.

## V. CONCLUSIONS

The main motivation for the present paper is to study how to test the TeV scale triplet Higgs neutrino mass mechanism directly at collider experiments. From the collider physics point of view this mechanism has several advantages over the singlet neutrino mass mechanism. As the triplet has gauge quantum numbers, its production at colliders is limited only by the mass reach not by tiny Yukawa couplings as is the case for singlets. Thus several hundred of those particles can be produced at LHC and ILC experiments.

The branching ratios of doubly charged Higgs decays to two same-charged leptons directly probe the corresponding element of the neutrino mass matrix. This allows us to study what one can learn about the light neutrino parameters from collider experiments. We have shown that the neutrino mass ordering, the lightest neutrino mass, and the Majorana phases can be measured at colliders by just counting the lepton flavors. We emphasize that those are

exactly these neutrino parameters which present neutrino oscillation experiments are not sensitive to. Therefore collider tests of the neutrino mass mechanism may provide a major breakthrough in neutrino physics.

We find that there are some flavor combinations of the doubly charged Higgs decay products which definitely point towards certain solutions. For example, should LHC see only doubly charged Higgs decays to muons and taus, light neutrinos must have strong normal hierarchy, and the lightest neutrino mass can be measured. In particular, the observation or nonobservation of  $ee$  final states is a clear discriminator between the mass hierarchies. Similarly, in the optimistic scenarios discussed in Sec. III, one can estimate the magnitude of the Majorana phase(s) of light neutrinos. In less clear cases, however, the experimental errors of the collider experiments may jeopardize the neutrino parameter measurements and no definite conclusion can be drawn.

We have also shown that one can actually fully determine the light neutrino mass matrix from collider experiments and/or from the measurement of neutrinoless double beta decay parameters. This requires determination of the triplet Higgs partial widths to leptons and to gauge bosons which could be possible at ILC experiments if the collision energy allows its production. If the triplet Higgs turns out to be light enough to be produced at colliders, neutrino physics may get an unexpected contribution from collider experiments.

## ACKNOWLEDGMENTS

We thank A. Hektor and M. Müntel for discussions and J. Garayoa for pointing out an error in the first version of this paper. This work is partially supported by ESF Grant No. 6140, by EC I3 Contract No. 026715 and by the Estonian Ministry of Education and Research.

*Note added.*—When the research presented in this paper was completed, an e-print [47] appeared in the arXive addressing the same topic. Our numerical results are in agreement with theirs. However, our results on neutrino parameters are also obtained in an analytical form which is not the case in [47].

- 
- [1] M.C. Gonzalez-Garcia and Y. Nir, *Rev. Mod. Phys.* **75**, 345 (2003).
  - [2] J. Schechter and J. Valle, *Phys. Rev. D* **23**, 1666 (1981).
  - [3] P. Huber, M. Lindner, M. Rolinec, T. Schwetz, and W. Winter, *Phys. Rev. D* **70**, 073014 (2004).
  - [4] P. Minkowski, *Phys. Lett.* **67B**, 421 (1977).
  - [5] T. Yanagida, “Horizontal Symmetry and Masses of Neutrinos,” in *Proceedings of the Workshop on the Baryon Number of the Universe and Unified Theories*, Tsukuba, Japan, 13–14 Feb. 1979.
  - [6] M. Gell-Mann, P. Ramond, and R. Slansky, in *Supergravity*, edited by P. van Nieuwenhuizen and D. Z. Freedman (North Holland, Amsterdam, 1979).
  - [7] S.L. Glashow, *NATO Adv. Study Inst. Ser. B Phys.* **59**, 687 (1979).
  - [8] R.N. Mohapatra and G. Senjanovic, *Phys. Rev. Lett.* **44**,

- 912 (1980).
- [9] F. Borzumati and A. Masiero, *Phys. Rev. Lett.* **57**, 961 (1986).
- [10] L.J. Hall, V.A. Kostelecky, and S. Raby, *Nucl. Phys.* **B267**, 415 (1986).
- [11] For an extensive review see, M. Raidal *et al.*, arXiv:0801.1826.
- [12] A. Ali, A.V. Borisov, and N.B. Zamorin, *Eur. Phys. J. C* **21**, 123 (2001).
- [13] T. Han and B. Zhang, *Phys. Rev. Lett.* **97**, 171804 (2006).
- [14] S. Bray, J.S. Lee, and A. Pilaftsis, *Nucl. Phys.* **B786**, 95 (2007).
- [15] F. del Aguila, J.A. Aguilar-Saavedra, and R. Pittau, *J. High Energy Phys.* 10 (2007) 047.
- [16] F. del Aguila *et al.*, arXiv:0801.1800.
- [17] M. Magg and C. Wetterich, *Phys. Lett.* **94B**, 61 (1980).
- [18] J. Schechter and J.W.F. Valle, *Phys. Rev. D* **22**, 2227 (1980).
- [19] G. Lazarides, Q. Shafi, and C. Wetterich, *Nucl. Phys.* **B181**, 287 (1981).
- [20] R.N. Mohapatra and G. Senjanovic, *Phys. Rev. D* **23**, 165 (1981).
- [21] G.B. Gelmini and M. Roncadelli, *Phys. Lett.* **99B**, 411 (1981).
- [22] A. Hektor, M. Kadastik, M. Muntel, M. Raidal, and L. Rebane, *Nucl. Phys.* **B787**, 198 (2007).
- [23] J.F. Gunion, J. Grifols, A. Mendez, B. Kayser, and F.I. Olness, *Phys. Rev. D* **40**, 1546 (1989).
- [24] K. Huitu, J. Maalampi, A. Pietila, and M. Raidal, *Nucl. Phys.* **B487**, 27 (1997).
- [25] J.F. Gunion, C. Loomis, and K.T. Pitts, in Proceedings of 1996 DPF/DPB Summer Study on New Directions for High-Energy Physics (Snowmass 96), Snowmass, Colorado, 1996, p. LTH096, arXiv:hep-ph/9610237.
- [26] B. Dion, T. Gregoire, D. London, L. Marleau, and H. Nadeau, *Phys. Rev. D* **59**, 075006 (1999).
- [27] M. Muhlleitner and M. Spira, *Phys. Rev. D* **68**, 117701 (2003).
- [28] A.G. Akeroyd and M. Aoki, *Phys. Rev. D* **72**, 035011 (2005).
- [29] T. Han, B. Mukhopadhyaya, Z. Si, and K. Wang, *Phys. Rev. D* **76**, 075013 (2007).
- [30] E.J. Chun, K.Y. Lee, and S.C. Park, *Phys. Lett. B* **566**, 142 (2003).
- [31] N. Arkani-Hamed, A.G. Cohen, and H. Georgi, *Phys. Rev. Lett.* **86**, 4757 (2001).
- [32] H.C. Cheng, C.T. Hill, S. Pokorski, and J. Wang, *Phys. Rev. D* **64**, 065007 (2001).
- [33] N. Arkani-Hamed, A.G. Cohen, and H. Georgi, *Phys. Lett. B* **513**, 232 (2001).
- [34] N. Arkani-Hamed, A.G. Cohen, E. Katz, and A.E. Nelson, *J. High Energy Phys.* 07 (2002) 034.
- [35] E. Ma and U. Sarkar, *Phys. Rev. Lett.* **80**, 5716 (1998).
- [36] E. Ma, M. Raidal, and U. Sarkar, *Phys. Rev. Lett.* **85**, 3769 (2000).
- [37] E. Ma, M. Raidal, and U. Sarkar, *Nucl. Phys.* **B615**, 313 (2001).
- [38] N. Sahu and U. Sarkar, *Phys. Rev. D* **76**, 045014 (2007).
- [39] C.X. Yue and S. Zhao, *Eur. Phys. J. C* **50**, 897 (2007).
- [40] G.L. Fogli *et al.*, *Phys. Rev. D* **75**, 053001 (2007).
- [41] G.L. Fogli, E. Lisi, A. Marrone, A. Palazzo, and A.M. Rotunno, *Prog. Part. Nucl. Phys.* **57**, 71 (2006).
- [42] J. Lesgourgues and S. Pastor, *Phys. Rep.* **429**, 307 (2006).
- [43] T. Schwetz, *Phys. Rev. D* **75**, 053001 (2007).
- [44] P.F. Harrison, D.H. Perkins, and W.G. Scott, *Phys. Lett. B* **458**, 79 (1999).
- [45] G. Barenboim, K. Huitu, J. Maalampi, and M. Raidal, *Phys. Lett. B* **394**, 132 (1997).
- [46] M. Raidal, *Phys. Rev. D* **57**, 2013 (1998).
- [47] J. Garayoa and T. Schwetz, *J. High Energy Phys.* 03 (2008) 009.

## Curriculum Vitae

Name: Mario Kadastik  
Date of birth: 05.11.1981  
Phone: (+372) 6466670  
E-mail: mario.kadastik@cern.ch

### Career:

2000 – 2003 Eesti Telefon IP Teenused  
2003 – 2005 MicroLink Eesti AS  
2004 - ... NICPB; Engineer  
2005 – 2006 National Institute of Chemical Physics and Biophysics;  
Extraordinary Researcher  
2006 - ... National Institute of Chemical Physics and Biophysics;  
Researcher

### Education:

2000 - 2004 Tallinn University of Technology, bachelor study  
2004 - 2005 Tallinn University of Technology, master study  
2005 - 2008 Tallinn University of Technology, PhD student

### Administrative responsibilities:

2004 - ... Participation in CMS experiment at CERN  
2005 - 2010 BalticGrid project Operations Director  
2007 - ... WLCG collaboration board

### Degree:

Mario Kadastik, Master's Degree, 2005, (sup) Martti Raidal, Doubly charged Higgs boson decay to muons at the LHC (Topeltlaetud Higgsi bosoni lagunemine müüoniteks LHC juures), TTÜ

### Honors and awards:

2003, TUT development fund Hansapank stipendium  
2004, Jaan Poska stipendium

### Current grants and projects:

- EURATOM Association European Fusion Development Agreement
- BalticGrid
- BalticGrid-II
- Modern methods of statistical physics: applications to diffusion processes in complex systems
- Leptogenesis, Supersymmetry and LHC Physics

### Publications:

- Kadastik, Mario; Raidal, Martti; Rebane, Liis (2008). Direct determination of neutrino mass parameters at future colliders. *Physical Review D* 77, 115023 (2008)
- del Aguila, F.; Hektor, A.; Kadastik, M.; Müntel, M.; Raidal, M.; Rebane, L. (2008). Collider aspects of flavour physics at high Q. *European Physical Journal C*, ilmumas
- Raidal, M.; Hektor, A.; Kadastik, M.; Müntel, M.; Rebane, L. (2008). Flavour physics of leptons and dipole moments. *European Physical Journal C*, ilmumas
- CMS Collaboration (2007). CMS Physics Technical Design Report: Addendum on High Density QCD with Heavy Ions. *Journal of Physics G: Nuclear and Particle Physics*, 34(11), 2307 - 2455.
- Hektor, A.; Kadastik, M.; Müntel, M.; Raidal, M.; Rebane, L. (2007). Testing neutrino masses in little Higgs models via discovery of doubly charged Higgs at LHC. *Nuclear Physics B*, 787, 198 - 210.
- CMS Collaboration (2007). CMS Physics Technical Design Report, Volume II: Physics Performance. *Journal of Physics G: Nuclear and Particle Physics*, 34(6), 995 - 1579.
- Ellis, J.; Hektor, A.; Kadastik, M.; Kannike, K.; Raidal, M. (2005). Running of low-energy neutrino masses, mixing angles and CP violation. *Physics Letters B*, 631(1-2), 32 - 41
- Hektor, Andi; Kadastik, Mario; Kannike, Kristjan; Müntel, Mait; Raidal, Martti (2006). Studying doubly charged Higgs pair production at the LHC. *Eesti Teaduste Akadeemia Toimetised. Füüsika. Matemaatika*, 55(2), 128 - 136.
- Hektor, A.; Anton, L.; Kadastik, M.; Skaburskas, K.; Teder, H. (2005). First scientific results from the Estonian Grid. *Proceedings of the Estonian Academy of Sciences. Physics. Mathematics*, 54(2), 111 - 127.
- Allanach, B.C. et al. Les Houches physics at TeV colliders 2005 beyond the standard model working group: Summary report (191 - 196). Stanford University Press

## Curriculum Vitae

Nimi: Mario Kadastik  
Sünd: 05.11.1981  
Telefon: (+372) 6466670  
E-mail: mario.kadastik@cern.ch

### Töökogemus:

2000 – 2003 Eesti Telefon IP Teenused  
2003 – 2005 MicroLink Eesti AS  
2004 - ... KBFi; Insener  
2005 – 2006 KBFi; Erakorraline teadur  
2006 - ... KBFi; Teadur

### Haridus:

2000 - 2004 Tallinn Tehnikaülikool, bakalaureuseõpe  
2004 - 2005 Tallinn Tehnikaülikool, magistriõpe  
2005 - 2008 Tallinn tehnikaülikool, doktoriõpe

### Administratiivsed kohustused:

2004 - ... Osalemine CMS eksperimendis CERN-s  
2005 - 2010 BalticGrid projekti operatsioonidirektor  
2007 - ... WLCG kollaboratsiooni juhatus

### Kraad:

Mario Kadastik, magistrikraad, 2005, (sup) Martti Raidal, Doubly charged Higgs boson decay to muons at the LHC (Topeltlaetud Higgsi bosoni lagunemine müüoniteks LHC juures), TTÜ

### Tunnustused ja auhinnad:

2003, TTÜ arengufondi Hansapanga stipendium  
2004, Jaan Poska stipendium

## Grandid ja projektid:

- EURATOM Association European Fusion Development Agreement
- BalticGrid
- BalticGrid-II
- Modern methods of statistical physics: applications to diffusion processes in complex systems
- Leptogenesis, Supersymmetry and LHC Physics

## Publikatsioonid:

- Kadastik, Mario; Raidal, Martti; Rebane, Liis (2008). Direct determination of neutrino mass parameters at future colliders. *Physical Review D* 77, 115023 (2008)
- del Aguila, F.; Hektor, A.; Kadastik, M.; Müntel, M.; Raidal, M.; Rebane, L. (2008). Collider aspects of flavour physics at high Q. *European Physical Journal C*, ilmumas
- Raidal, M.; Hektor, A.; Kadastik, M.; Müntel, M.; Rebane, L. (2008). Flavour physics of leptons and dipole moments. *European Physical Journal C*, ilmumas
- CMS Collaboration (2007). CMS Physics Technical Design Report: Addendum on High Density QCD with Heavy Ions. *Journal of Physics G: Nuclear and Particle Physics*, 34(11), 2307 - 2455.
- Hektor, A.; Kadastik, M.; Müntel, M.; Raidal, M.; Rebane, L. (2007). Testing neutrino masses in little Higgs models via discovery of doubly charged Higgs at LHC. *Nuclear Physics B*, 787, 198 - 210.
- CMS Collaboration (2007). CMS Physics Technical Design Report, Volume II: Physics Performance. *Journal of Physics G: Nuclear and Particle Physics*, 34(6), 995 - 1579.
- Ellis, J.; Hektor, A.; Kadastik, M.; Kannike, K.; Raidal, M. (2005). Running of low-energy neutrino masses, mixing angles and CP violation. *Physics Letters B*, 631(1-2), 32 - 41
- Hektor, Andi; Kadastik, Mario; Kannike, Kristjan; Müntel, Mait; Raidal, Martti (2006). Studying doubly charged Higgs pair production at the LHC. *Eesti Teaduste Akadeemia Toimetised. Füüsika. Matemaatika*, 55(2), 128 - 136.
- Hektor, A.; Anton, L.; Kadastik, M.; Skaburskas, K.; Teder, H. (2005). First scientific results from the Estonian Grid. *Proceedings of the Estonian Academy of Sciences. Physics. Mathematics*, 54(2), 111 - 127.
- Allanach, B.C. et al. Les Houches physics at TeV colliders 2005 beyond the standard model working group: Summary report (191 - 196). Stanford University Press

---

ABSTRACT

Standard Model, which describes the strong, weak and electromagnetic force has been in very good accordance with the experimental results. The parts which have shown contradictory results involve the mass of particles. In SM the mass of all particles is generated through interactions with the Higgs field, which is mediated by the Higgs boson which so far has not been observed. In the neutrino sector the discovery of non-zero neutrino masses as well as definite mixing between the mass and flavor states is a clear indication of physics beyond the SM. The model we use to extend the SM is based on the addition of a scalar triplet which has interactions with the electroweak and lepton sector of SM. The triplet contains neutral, singly charged and doubly charged components. Through the interaction with this scalar field the neutrinos obtain a non-zero mass and as the interaction strength between the field and neutrinos is also the same for the field and charged leptons, we can use these relations to give estimates on the model parameters.

The main topic of this thesis is the application of the above mentioned model in HEP experiments. The first application is the prediction of experimental signatures to confirm the validity of this model. In this thesis we give predictions on the possible experimental signatures through the relations that exist between the neutrino sector and the scalar triplet. The best possible signature in current and future experiments is the doubly charged component which provides a channel with very small contamination from similar SM backgrounds. Taking into account the current results in neutrino experiments we can also estimate the actual final state statistics and hence provide better search strategies.

Once the scalar triplet has been found and the respective experimental statistics have been measured we can reverse the process and use these results to give in turn predictions and more precise measurements of the various parameters in the neutrino sector including some parameters which have not been observable so far like the Majorana phases. If additional measurements are done for example at neutrinoless double beta decay experiments, then the full model parameters could be measured.

The search algorithms as well as the utilization of connection between  $\Phi^{\pm\pm}$  and neutrino mixing matrix to estimate the  $\Phi^{\pm\pm}$  branching ratios as well as the use of the actual experimentally measured ratios to estimate the neutrino sector parameters are the original work of the author and further described in the attached three articles.

---

## RESÜMEE

Standardmudel (SM), mis kirjeldab elektromagneetilist, nõrka ja tugevat interaktsiooni, on praegu kehtivatest teooriatest kõige edukam. Lisaks sisaldab antud teooria Higgsi välja, mis võimaldab läbi sümmeetria spontaanse lagunemise seletada osakeste massi. SM teooria ei seleta aga viimaste eksperimentide poolt kinnitust leidnud neutriinode nullist erinevat seisumassi. On vaja uusi teooriaid ning nendest üks lihtsamaid on SM täiendamine skalaarse tripletiga. Antud triplet on oma olemuselt sarnane SM-i Higgsi dupletiga, andes osakestele massi, kuid kuna ta omab vastasmõju vaid leptonite ja elektronõrga sektoriga, on tulemuseks neutriinode masside muutumine SM-i suhtes.

Käesoleva töö eesmärk on kirjeldada kahekordselt laetud Higgsi bosoni otsimise meetodikat kõrge energiaga kiirendi eksperimentide juures. Samuti on kirjeldatud võimalikke lõppolekuid ning nende omavahelisi suhteid kasutades neutriino sektori teadaolevaid parameetreid läbi skalaarvälja suhte leptonitega. Teades, millised on võimalikud lagunemise lõppolekud, on võimalik suurendada eksperimentide efektiivsust ning seeläbi avastamise tõenäosust.

Kui mõnes kiirendi eksperimentis õnnestub leida  $\Phi^{\pm\pm}$  ning määrata tema lõppolekute statistika, siis saame panna lisakitsendusi neutriinosektori tundmatutele parameetritele. Lihtsaimal juhul on võimalik määrata neutriino masside hierarhia, kergeima neutriino mass ning juba suurema koguse ja täpsemate tulemuste olemasolul ka potentsiaalselt Majoraana faasid ning kontrollida mudeli eelduste kehtimist  $\theta_{13}$  nurga kaudse määramise kaudu.

Kui on olemas piisav kogus statistikat ning lisaks leptonilistele lagunemistele õnnestub mõõta ka neutriinota topelt beeta lagunemisest elektron-neutriino mass, siis on võimalik määrata ka viimane tundmatu parameeter tripleti mudelis, tema vaakum-keskväärtus.

Antud töös kirjeldatud  $\Phi^{\pm\pm}$  otsimise algoritmid ja neutriino massidega seoste kasutamine nii  $\Phi^{\pm\pm}$  lagunemiste ennustamiseks kui eksperimentaalselt mõõdetavate lagunemiste kaudu neutriino parameetrite määramine on originaalne autori töö ning pikemalt lahti seletatud tööga kaasas olevas kolmes artiklis.